Dysregulated NF-κB – dependent ICOSL Expression in Human Dendritic Cell Vaccines Impairs T Cell Responses in Melanoma Patients

by

Deena Marie Maurer

Bachelor of Science, Marywood University, 2014

Master of Science, Johns Hopkins University, 2015

Submitted to the Graduate Faculty of the

School of Medicine in partial fulfillment

of the requirements for the degree of

Doctor of Philosophy

University of Pittsburgh

2020

UNIVERSITY OF PITTSBURGH

SCHOOL OF MEDICINE

This dissertation was presented

by

Deena Marie Maurer

It was defended on

September 30, 2020

and approved by

Olivera J. Finn, Distinguished Professor, Immunology and Surgery

Hassane M. Zarour, Professor of Immunology, Medicine, and Dermatology, Co-leader of the Melanoma Program and the Cancer Immunology and Immunotherapy Program

Michael R. Shurin, Professor of Pathology and Immunology, Director, Division of Clinical Immunopathology

Dissertation Director: Walter J. Storkus, Professor of Dermatology, Immunology, Pathology, and Bioengineering

Dissertation Director: Lisa H. Butterfield, Adjunct Professor of Microbiology and Immunology, University California San Francisco, Vice President, PICI Research and Development, Parker Institute for Cancer Immunotherapy

Dysregulated NF-κB – dependent ICOSL Expression in Human Dendritic Cell Vaccines Impairs T Cell Responses in Melanoma Patients

Deena Marie Maurer, PhD

University of Pittsburgh, 2020

FDA approved treatments for advanced melanoma have shown clinical efficiency in a subset of patients. Combinational therapy using checkpoint blockade has shown the most success, but many patients do not respond. The patients that do respond often have a pre-existing antitumor immunity. Dendritic cell (DC)-based vaccination can be used to help mount pre-existing immune responses. Although shown to be safe and immunogenic, the clinical response rate of DC vaccination remains low. We have profiled autologous DC vaccines used to treat 35 patients with advanced melanoma to identify potential biomarkers and signaling pathways that correlate with clinical outcomes. We show that DC expression of checkpoint molecules induced by *ex vivo* maturation of this therapeutic cell product correlates with *in vivo* vaccine activity. Importantly, melanoma patient DC were observed to express reduced levels of cell surface ICOSL and to be defective in intrinsic NF-κB signaling. ChIP assays revealed NF-κB-dependent transcriptional regulation of ICOSL expression. Blockade of ICOSL on DC reduced their capacity to prime antigen-specific $CD8^+$ and $CD4^+$ T cells *in vitro*. Additionally, levels of extracellular/soluble ICOSL released from vaccine DC positively correlated with clinical outcomes, which we have shown to be partially regulated by intrinsic ADAM10/17 sheddase activity. These data point to the critical role of canonical NF-κB signaling, the regulation of metalloproteinases, and DC-expressed/shed ICOSL in antigen-specific priming of T cell responses. In Appendix A, we used transcriptional profiling of patient and HD DC to identify disease-associated transcriptional differences. We observed that metabolic

signaling pathways were dysregulated in patient mature DC (mDC). Functional assays showed that reduced activation of oxidative phosphorylation and fatty-acid β-oxidation in patient mDC correlated with immune responses and favorable outcomes. In Appendix B, another recent autologous DC vaccine (n=16) for the treatment of advanced melanoma is highlighted. We identified gene targets in patient DC that correlate with overall survival and immune response. These biomarkers are expected to serve as key biologic indices in defining therapeutic DC release criteria and endpoints for targeted interventional approaches designed to optimize the therapeutic anti-tumor efficacy of DC-based modalities or the intrinsic anti-tumor activities of DC *in situ* in cancer patients.

Table of Contents

List of Tables

List of Figures

Preface

"I was taught that the way of progress was neither swift nor easy." – Marie Curie.

This dissertation is dedicated to my loving grandmother, Susan Marie Alfiero (September 29th, 1932 – November 22nd, 2018), who believed in my ability and passion to become a scientist before I even knew that was the career path I wanted to follow. She always said, "Deena Marie, one day, you will be my Madame Marie Curie". Well, I do not think that the work outlined in this dissertation pales in comparison to the work set forth by Marie Curie, but I sure do hope it makes my grandmother proud.

I would like to take this opportunity to thank my graduate school mentors, Dr. Lisa H. Butterfield and Dr. Walter J. Storkus. Dr. Butterfield, I was honored to be your first and only graduate student during your time at the University of Pittsburgh. You have been an outstanding mentor to me throughout my career and always pushed me to ask the hard questions and really listen to what my data was telling me. You have been a role model for me as a woman in science and taught me to never settle and believe in my abilities as a scientist. Thank you. Dr. Storkus, you have been a blessing in disguise. When I first transferred into your lab, I didn't know what to expect. Throughout the last year and a half, you have become an exceptional mentor to me. You door was always open to talk about science and/or life in general. You were always willing to help me in whatever way you could to help me succeed. I am grateful that I had the chance to be a part of your lab and contribute to your work. I am in constant awe of your scientific knowledge and

goodwill towards others. Dr. Butterfield and Dr. Storkus you have both been the best mentors and I hope that we continue our mentee-mentor relationship throughout my scientific career.

I would also like to also thank the members of my thesis committee: Dr. Olivera J. Finn, Dr. Hassane M. Zarour, and Dr. Michael R. Shurin. Thank you all for your helpful conversations during each of my committee meetings and for extending yourselves outside of my committee meetings to discuss science and career advice.

One of the most important lessons that I have learned throughout graduate school is that science is indeed a collaborative effort. The work outlined in this dissertation would not have been possible without the helpful conversations, support, and experimental guidance given to me by my professional colleagues. I would personally like to thank Dr. Patricia Santos, Dr. Lazar Vujanović, Dr. Jian Shi, Dr. Jennifer Taylor, Dr. Ronald Fecek, Dr. Juraj Adamik, Dr. Paul Munson, Manoj Chelvanambi, and Jessica Filderman. Whether you have taught me a new experimental technique, talked out experimental hypotheses, helped me plan future experiments, or just listen to me ramble about the trials and tribulations as life of a science graduate student, your support never went unnoticed. Thank you all for what you have taught me and for challenging me to always ask more questions.

Lastly, I would like to thank my personal support system. To my husband, my parents, my sister & brother-in-law, and my brother: Thank you for your unwavering support throughout my educational career. I could not have been as successful as I am today or have gotten through graduate school without you. I love each and every one of you.

1.0 Introduction

1.1 Foreword

Portions of this chapter were adapted from the previous published research review in *Melanoma Research:* Maurer, D.M., Butterfield, L.H., and Vujanovic, L. Melanoma Vaccines: Clinical Status and Immune Endpoints. *Melanoma Research,* 2018.

1.2 Hallmarks of Cancer

Cancer is the second leading cause of death in the United States(1). It is estimated that approximately 606,520 deaths with occur from the disease this year alone(1). Historically, cancer has been defined as rapid, dynamic changes in the genome. These changes are based on genetic mutations that often result in an over expression or a loss of expression in genetic material(2). This can cause the rapid proliferation of cells, which often results in tumorigenesis.

Bishop and Weinberg were the first to define tumorigenesis in humans as a multi-step process governed by genetic alterations(2). Bishop and Weinberg's work revealed that cells require six essential traits, coined "hallmarks", that control malignant growth. The original six hallmarks of cancer included the following: 1) self-sufficient in growth signals, 2) evasion of apoptosis, 3) limitless replication capacity, 4) sustained angiogenesis, 5) insensitivity to anti-growth signals, and 6) tissue invasion and metastasis(2). Cells require all of the above six genetic alterations in order to transition from a normal to a malignant state (Figure 1).

1.2.1 The Hallmarks of Cancer: The Next Generation

Soon after the original hallmarks of cancer was published, novel research discoveries suggested that the immune system plays a critical role in the development of cancer. Yet, the first evidence of the importance of the immune system in tumorigenesis occurred many years prior. Sir Frank Burnet coined the "Immune Surveillance Theory" in 1970 and was one of the first scientists to identify the ability of tumor cell neoantigens to induce immune responses(3). Then, in 1971, Thomas Starzl, along with others, reported the occurrence of *de novo* tumors in individuals with immunological deficiencies(4). Additionally, early studies with Bacillus Calmette-Guerin (BCG) for the treatment of cutaneous neoplasms showed promising results in animal and human models(5). Fifteen years later, in 1986, Dvorak et al. showed tumors were infiltrated by innate and adaptive immune cells(6). However, it was not until the early 2000s that immunotherapy for the treatment of cancer was widely accepted by the scientific community.

Early studies revealed that immunodeficient mice had more frequent and rapidly growing tumors, compared to immunocompetent hosts(7,8). Additionally, studies suggested cancer cells transplanted from immunodeficient mice were not capable of generating secondary tumors in mice with competent immune systems, yet, tumors from immunocompetent animals were able to generate secondary tumor responses in immunosuppressed mice(7,8). Additionally, human studies on renal transplant recipients showed evidence of rapid cancer development in these individuals, suggesting the induced immunosuppression enabled cancer cell growth(9). Additionally, immunocompromised transplant recipients often developed donor derived cancers(10). Moreover, studies revealed that ovarian, colon, and melanoma human tumors infiltrated with immune cells, such as cytotoxic T cells and natural killer cells, had a better prognosis, compared to tumors that lacked infiltrating lymphocytes(11-14). All of the above studies indicated tumorigenesis is often

kept “in check” by a functional immune system. In 2011, Bishop and Weinberg updated the original hallmarks of cancer to include to include the following two emerging hallmarks: 1) deregulated metabolism and 2) evasion of the immune system. In addition, Bishop and Weinberg defined two “enabling characteristics”: 1) genome instability and 2) inflammation (Figure 1). It was hypothesized that the development of the “enabling characteristics” would lead to the acquisition of the hypothesized hallmarks(15).

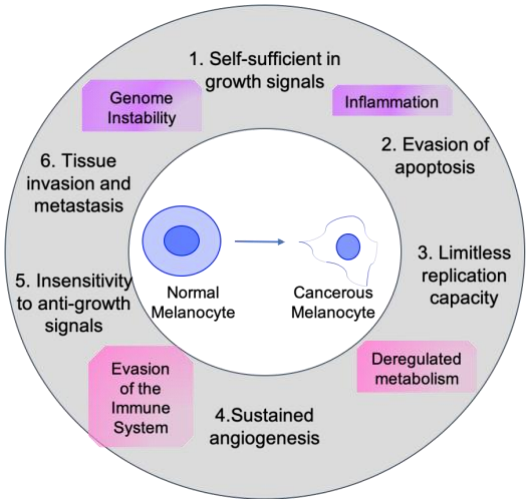

Figure 1. The Hallmarks of Cancer. This figure was modified from the orginal published figure by by Bishop and Weinberg(15). The emerging hallmarks are highlighted in pink and the enabling characteristics are highlighted in purple.

The growing evidence of the involvement of the immune system in cancer development led to a more complex concept known as the “Cancer Immunoediting Model”. This model was first developed by Ikeda, Old, and Schreiber, and has is defined by three essential elements: 1) Elimination of tumors, 2) Equilibrium between the immune system and tumor development, and 3) Tumor Escape(16). The elimination phase is often referred to “Immunosurveillance” in which cancer cells are detected and eliminated by the immune system(17). The equilibrium phase is a balance between immune recognition and tumorigenesis. During this phase, characteristics of the immune system and tumor are shaped by each other(17). Often, “immunoediting” occurs in the

equilibrium phase, in which highly immunogenic cancer cell clones are eliminated. The final phase, Tumor Escape, involves the development of an immunosuppressive tumor microenvironment and enables the tumor to escape the generated immune response and progression occurs(17).

1.3 Dendritic Cell Biology

Dendritic cells (DC) are derived from the bone marrow and are localized in the peripheral blood, epithelial tissues, and lymph tissues(18). DC were first identified by Ralph Steinman in the 1970's as accessory cells that can activate an adaptive immune response by the priming of lymphocytes(19). These cells have physiological sensors, and antigen processing machinery that enable them to recognize and internally process foreign pathogens and then present antigen peptides via MHC class molecules to adaptive immune cells(19).

In the periphery, DC are usually in their immature, phagocytic state. They express low levels of MHCII and co-stimulation molecules, and secrete low levels of cytokines, such as IL-12(20). Immature DC can present self-antigens to T cells and induce tolerance by the expansion of regulatory T cells(20). Upon interaction with a foreign antigen, DC will undergo maturation, and migrate towards the lymph nodes(20).

Matured DC will upregulate MHCII and costimulation molecules (e.g. CD80, CD86) on their cell surface, and secrete inflammatory cytokines(20). Naive T cells in the lymph nodes will bind to the MHC/antigen peptide complex presented by DC via their TCR. In order for the T cell to become fully activated, the following three events need to occur: 1) binding of MHCI or MHCII molecules to the TCR, 2) a co-stimulation event, and 3) secretion of cytokines by the DC(21). The

above three signals will result in the full activation and proliferation of antigen-specific T cells. This schema is depicted in Figure 2. In the absence of one or more of these signals in antigen-presenting DC, T cell “responders” will often become anergic.

DC have the capacity to skew the immune response depending on the cytokines secreted. T helper type 1 (Th1) polarized T cells are known to produce inflammatory cytokines and attack intracellular pathogens. A Th1 response will often be generated from inflammatory cytokines, such as IL-12, IL-23, IL-27, and type I interferons being secreted from DC(18). Likewise, a Th2 generated immune response often is a result of an allergic reaction and is reported to be stimulated by the cytokines IL-4, IL-5, and IL-13(22,23). On the other hand, a regulatory response can be generated by the presence of regulatory or immunosuppressive cytokines, such as IL-10 and TGF-β(18).

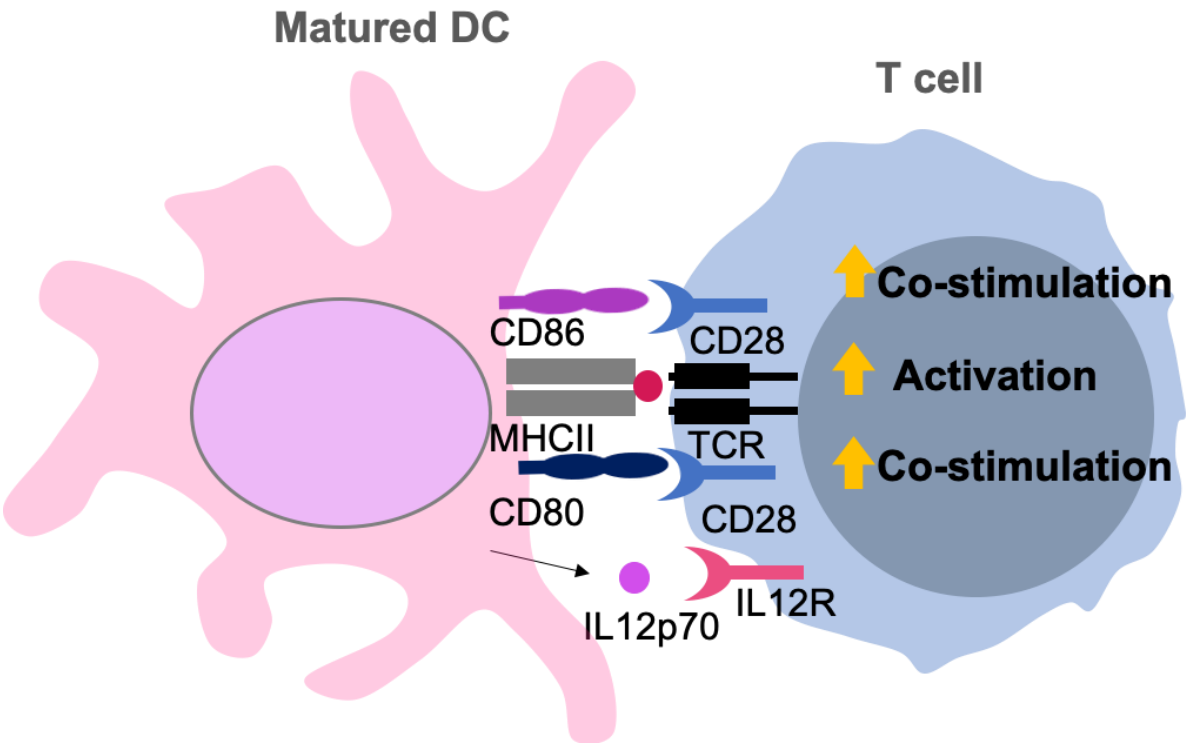

Figure 2. Immunological Synapse.
In order to become fully activated, T cells need to recieve three signals from a dendritic cell. The first event that has to occur is binding of the MHC molecule to the TCR. This is followed by a co-stimulation event, which is usually CD28 on the T cell binding to CD80/CD86 on the DC. Lastly, DC will secrete cytokines to the T cell that impacts T cell functional polarization. As shown, the DC is secreting IL-12, skewing the immune response towards a pro-inflammatory Th1 response. Preferential DC production of alternate cytokines may result in alternate T cell functionality, including Th2, Th17 or Treg. All three of these signals are required for full activation and proliferation of responder T cells.

1.3.1 Antigen Processing and Presentation

Self and foreign antigens are processed and presented by APC to adaptive immune cells in order to regulate immune responses. Presentation of antigens occurs within the context of MHC I and MHC II molecules expressed on the surface of APC, such as DC. MHC I molecules have a constrained peptide presenting groove capable of bind peptide fragments of between 8-15 amino acid (a.a.) in length, with most presented peptides averaging 9 a.a. in length(24-26). MHC II molecules have an open binding groove, and therefore, can accommodate larger peptide fragments

between the sizes of 11-30 a.a. in length, with extended portions of the peptide "dangling" from the ends of the peptide binding groove(27).

MHC I molecules process and present endogenous antigens to $CD8^+$ T cells. Class I molecules are assembled in the endoplasmic reticulum (ER) and consist of two chains: 1) polymorphic heavy chain and 2) β2 – macroglobulin (β_2m)(28). Class I molecules are normally stabilized in the ER by the chaperone proteins, calreticulin, Erp57, tapasin, and protein disulfide isomerase(28). In the cytosol, foreign and/or self-antigens will be degraded into small fragments. The Transporter Associated with Antigen Presentation (TAP) translocates the resultant protein fragments from the cytosol into the ER, where they have access to, and may bind to nascent MHC I molecules. Upon binding of peptides to MHC I and β_2m, chaperone proteins are released, and "mature" MHC I/peptide complexes are translocated to the cell surface.(28)

MHC II molecules present peptide derived from both intrinsic and exogenous proteins to $CD4^+$ T cells, with exogenous proteins acquired via endocytosis in APC(21). Class II molecules are comprised of α and β proteins, which are stabilized by an invariant chain(29). Due to the acidic pH in endocytic vesicles, the invariant chain will become digested by cathepsin S and cathepsin L. When the invariant chain becomes digested, a fragment known as the Class II associated invariant chain peptide (CLIP) remains bound to the binding groove of the MHC II molecule, preventing access to free peptides(29). The chaperon protein, HLA-DM aids in the binding of protein fragments to the MHC II molecules endocytic compartments. Upon binding with the antigen fragment, CLIP is released and the MHC II/peptide complex is translocated to the cell surface for interaction with $CD4^+$ T cells(29).

MHC I molecules remain at the cell surface for variable periods of time, after which peptide and β_2m may dissociate from the MHC I heavy chain, with the MHC I heavy chain then

internalized. When MHC I molecules are internalized, they can potentially enter the MHC II antigen-processing pathway, where cross-presentation of MHC I (and other internalized) peptides in MHC II complexes can occur. Cross-presentation is a process in which exogenous peptides can be presented by MHC I molecules to $CD8^+$ T cells(30). This process has been shown to critical in the processing and presentation of many tumor antigens. Foreign antigens have been shown to be taken up by pinocytosis, phagocytosis, or receptor-mediated endocytosis(30). Two different pathways of cross presentation have been reported: 1) the cytosolic pathway, which occurs in the cytosol and 2) the vacuolar pathway, which occurs in endocytic compartments(31). Cells that are capable of cross presentation have specialized antigen processing machinery. Human DC subtypes that are able to cross-present antigens are known as conventional DC 1 (cDC1). The differentiation of cDC1 is regulated by IRF8 and is associated with production of the chemokine, XCR1, and expression of the surface molecule, CD141(31).

1.3.2 DC Subtypes

All DC express high levels of MHC class II (HLA-DR) molecules and lack the lineage markers, CD3 (expressed by T cells), CD19/20 (expressed by B cells), and CD56 (expressed by NK cells)(32,33). DC, including those in blood, can be separated into two categories: myeloid and plasmacytoid DC. Human myeloid DC are positive for expression of CD11c, CD13, CD33, and CD11b, and fail to express the monocyte markers CD14 and CD16(32,33). $CD11c^+$ DC can be further separated into $CD1c^+$ and $CD141^+$ fractions. These subtypes of DC are homologous with the mouse $CD11b^+$ and $CD8/CD103^+$ DC, respectively(34,35). Plasmacytoid DC express CD123, CD303, and CD304 on their surface and express high levels of TLR7 and TLR9. Plasmacytoid DC usually respond to viral infections and secrete high amounts of type I interferons(32,33,35).

Additionally, there is a unique self-renewing subset of DC known as Langerhans cells, which are localized to the stratified squamous epithelium of the skin(32,33). Inflammatory DC can be generated from $CD14^+$ blood monocytes by culturing them in the presence of GM-CSF and IL-4. Such DC can activate $CD8^+$ and $CD4^+$ T cells by cross presentation of antigens. These DC secrete pro-inflammatory cytokines, such as IL-1β and IL-12(32,33).

1.4 Crosstalk Between DC and T Cells

As stated above, post-thymic activation of T cells typically occurs in the lymph nodes via an interaction with antigens presented by matured DC that have emigrated from peripheral tissue sites. The physical interaction structure between naïve T cells and matured DC is often referred to as the "Immunological Synapse"(36). Mempel et al showed that T cell priming occurs in three distinct phases. After naïve T cells reach the lymph nodes, they undergo short encounters with matured DC. These interactions reduce T cell motility, leading to T cell expression of activation markers. In the following 12hrs, T cells make long lasting interactions with the matured DC. At this time, T cells will begin to secrete IL-2 and IFN-γ. By the second day, cognate T cells may down-regulate expression of their T cell receptor (TCR) and initiate proliferative/differentiative programming to become functional, mature T cells (36).

1.5 Co-stimulatory & Checkpoint Molecules

The immune system is kept in balance by the presence of numerous checkpoint inhibitory and co-stimulation molecules. In healthy cells, checkpoint inhibitory molecules are upregulated after activation of immune cells. Checkpoint molecules will down regulate the immune response in order to prevent autoimmunity(37). Likewise, co-stimulation molecules will be upregulated on cells when an infection occurs in the milieu of activating pathogen signals. Co-stimulation molecules are known to help induce activation signals from antigen presenting cells (APC), such as DC, to stimulate and activate antigen-specific T cell responses(38).

PD-1/PD-L1 and CTLA-4 are well-known inhibitory molecules. Both PD-1 and CTLA-4 are expressed on T cells during early activation events(39,40). Studies have also indicated that PD-1, PD-L1, and CTLA-4 are expressed on APC(41). PD-1 has a cytoplasmic domain that contains immunoreceptor tyrosine based inhibitory/switch motifs (ITIM and ITSM). Upon interacting with PD-L1, PD-1 will recruit phosphatases containing SH2 domains that will prevent the phosphorylation of ITAMS on the TCR(42,43). This will result in the inhibition of T cell activation. CTLA-4 binds to CD80 and CD86 on APC with greater affinity, compared to CD28. When T cells express CTLA-4 it will outcompete CD28 for the binding of CD80/CD86. Upon binding to CD80/CD86, CTLA-4 will send inhibitory signals to the T cell, preventing activation(44-46).

In cancer, these molecules are often upregulated on immune cells and tumor cells as a means of immune escape(41). Studies have shown that PD-1 and PD-L1 expression inhibits $CD4^+$ and $CD8^+$ T cell-specific responses(47). Studies have suggested that PD-1 upregulation on T cells inhibits CD28 co-stimulation(48). Moreover, soluble PD-1 and PD-L1 can act as neutralizing antibodies which block the PD-1/PD-L1 pathway to promote antigen-specific T cell responses(47).

The PD-1/PD-L1 pathway is regulated by NF-κB and JAK/STAT signaling in DC(49,50). CTLA-4 is expressed on activated T cells. Prior to T cell activation, CTLA-4 is maintained intracellularly. Upon activation, CTLA-4 is translocated to the cell surface and is regulated by TRIM, PLD, ARF-1, and TIR-7(51,52). Some studies suggest expression of surface CTLA-4 on mature DC with its expression regulated by JAK2 and STAT1 through IFN-γ signaling(53). However, not much is known about possible roles of CTLA-4 in dendritic cells. Tumor cells also upregulate CTLA-4 and clinical studies have proven anti-CTLA-4 antibodies are associated with overall survival rates and clinical outcomes.

ICOSL is commonly expressed on matured APC and its receptor (ICOS) is commonly expressed on T cells. ICOSL can provide co-stimulation for the activation of antigen-specific T cells. Specifically, in the cancer setting, ICOS signaling has been reported to mediate both immunoregulatory and immunostimulatory roles, suggesting the importance of context. Some studies have shown that increased expression of ICOSL on tumor cells is associated with disease progression and poor clinical outcome(54), and high levels of ICOSL on cancer cells facilitates development of immunosuppressive $CD4^+$ T cells(55). Conversely, studies in colon cancer have shown that high ICOS expression on infiltrating leukocytes is associated with better overall survival(56). In patients previously treated with α-CTLA-4, high ICOS expression on T cells was associated with better prognosis(57). Furthermore, treatment with vaccines engineered to express ICOSL along with co-administered CTLA-4 blockade increased the magnitude of specific T cell responses in prostate and melanoma mouse models(58), suggesting an important role of ICOS signaling in the optimal development of anti-tumor immunity.

1.6 Environmental Influence on DC Priming Abilities

The tumor microenvironment has the ability to negatively impact immune responses. Studies have shown that infiltrating immune cells will quickly become suppressed upon entering the tumor microenvironment. Tumor cells secrete the immunosuppressive cytokines, IL-10 and TGF- β, that can prohibit an anti-tumor immune response(59). Tumor cells can also upregulate the expression of checkpoint molecules that bind to activated immune cells and provide an inhibitory signal(60). In addition, tumor cells secrete high levels of VEGF and the chemokines, CXCL1 and CXCL5, which have been shown to prohibit DC maturation(61). Tumor-conditioned immune cells are suggested to induce tolerance among infiltrating immune cells. Studies have further shown that melanoma-derived DC have express lower levels of CD86 on their cell surface, and secrete higher levels of IL-10, leading to anergy in $CD4^+$ T cells and promotion of tumor progression/metastasis in patients(62).

1.7 Melanoma

Melanoma is classified as a solid tumor that develops from the melanocytes in the skin. It accounts for 1% of all skin cancers and, if caught early, is highly-treatable(1). The overall survival rate for melanoma is 98%. However, the incidence rate of melanoma continues to rise yearly. It is projected that 100,000 new cases of the disease will be diagnosed this year. Moreover, melanoma is the leading cause of skin cancer-related deaths in the United States(1). The advanced stage of this disease has a 10-year survival rate of only 15%. It is estimated in 2020, 6,850 patients will die of this disease(1).

To date, there are no successful standard care of treatments yielding general benefit for patients with advanced stage disease. However, there are several FDA approved therapies that reproducibly result in clinical benefit in a minority of patients. Systemic cytokine treatments such as, IL-2 and IFN-α, have been used as a therapeutic for tumor regression. These treatments have shown favorable clinical responses, but only in 10-20% of patients(63). Additionally, high doses of IL-2 and IFN-α can produce toxic side effects(64-66). Likewise, T-Vec, an approved oncolytic virus for the treatment of melanoma, has been reported to shrink tumors localized in the skin and lymph tissues(67). However, it is unknown if the virus can aid in regression of metastatic sites in other parts of the body, or if the virus helps increase the quality of life of the patient. In addition, molecular targeted therapies have been used for the treatment of melanoma. Targeted therapies against mutations in the BRAF or MEK genes, that serve as oncogene drivers in melanoma, have shown clinical success. However, patients often develop resistance to these drugs or they may develop a secondary cancer, such as squamous cell skin cancer(68). Immune checkpoint blockade therapies, such as anti-CTLA-4 and anti-PD1, have shown success in the clinic(69). Clinical trials have shown that in combination these two therapies yield a clinical response rate of approximately 70%(69,70). However, only a subset of patients exhibit durable treatment benefit, and these patients typically exhibit baseline immune response to tumor.

1.8 Cancer Vaccines for the Treatment of Melanoma

It has been known for decades that the immune system can be spontaneously activated against melanoma. The presence of tumor infiltrating lymphocytes (TIL) in tumor deposits is a positive prognostic factor(71). Cancer vaccination includes approaches to generate, amplify, or

skew antitumor immunity for clinical benefit. To accomplish this goal, tested approaches involve administration of tumor antigens, APC or other immune modulators, or direct modulation of the tumor. Since the success of checkpoint blockade may depend in part on an existing antitumor response, "booster" cancer vaccination may play an important role in future combination therapies.

1.8.1 Historical Perspective of Cancer Vaccination

Active immunotherapies are not a novel concept. Over a century ago, William B. Coley injected live streptococci into sarcoma patients to promote erysipelas and induce immune system-mediated tumor rejection. While therapies such as these have shown limited clinical benefit and high degree of systemic toxicity, they did usher in an era of onco-immunology(72). Some of the first melanoma cancer vaccine trials occurred in the 1970s. These included testing tumor lysate injections and use of pathogen-derived adjuvants like Bacillus Calmette-Guerin (BCG)(73,74); vaccinia virus oncolysate(75) or Corynebacterium parvum(76). The results were promising, with some patients displaying clinical responses that were often transient. In the 1980s, there were studies focused on vaccines based on injection of irradiated allogeneic melanoma cells(77). The injection of irradiated tumor cells, especially those genetically engineered to secrete GM-CSF, revealed high infiltration of immune cells into the tumor. In the early 1990s, gangloside (GM2, GD3)-based vaccines with adjuvants and immunogenic conjugates were investigated as treatment modalities(78). The use of gangloside-based vaccines were proven to safe and immunogenic within the clinical setting. Application of recombinant cytokines was also tested at this time, both as systemically delivered agents (IL-2, IFN-α) or as cytokine-secreting genetically modified tumor cell vaccines (especially GM-CSF)(79,80). Studies using vaccines encoding IL-2 and GM-CSF indicated immunological benefits, as vaccine-induced immune responses were observed in a

subset of participants. During the 1990s, the molecular identification of the tumor antigens expressed by melanomas which were recognized by the cytotoxic T cells (CTL) infiltrating tumors were beginning to be published which had a major impact on the field, since specific melanoma-associated antigens could now be targeted in vaccine formulations (81-83).These studies suggested that vaccines encoding shared tumor antigens could generate anti-tumor immune responses.

The most common approach to cancer vaccination in the last two decades involves immunization with shared tumor antigens expressed by many different patients' tumors. The earliest tumor associated antigens (TAAs) identified were proteins that were overexpressed in tumor cells but minimally expressed in untransformed normal tissues(81,82,84,85). TAAs were also identified after cloning the genes that encoded proteins that included epitopes recognized by tumor reactive TILs. Other types of TAA tested in melanoma include cancer testis antigens and mutated antigens (tumor specific or private neoantigens).

1.9 Melanoma Antigens

Melanoma antigens can be segregated into four major categories: overexpressed antigens, cancer testis antigens, mutated oncogenes and mutated neoantigens. Overexpressed antigens include melanoma lineage antigens such as MART-1/Melan-A, tyrosinase, and gp100. Overexpression of the above antigens have resulted in the activation of antigen-specific T cells *in vitro* and in murine models, and have been tested in clinical trials with some objective RECIST (response evaluation criteria in solid tumors) clinical responses(86-88). A concern about targeting such TAAs is that the highest avidity T cells specific to these normal "self" antigens may have

been deleted or exhausted by chronic antigen stimulation, leaving only less effective, lower avidity T cells to be activated.

Cancer testis antigens are expressed in a proportion of most tumor tissue types and in germ cells that, because of their physiologic location in so-called “immune privileged sites”, are generally ignored by the immune system. Such antigens include the large MAGE-A, MAGE-B, and MAGE-C families, and NY-ESO-1. These antigens have been tested in human clinical trials and implicated in therapeutic responses amongst patients with melanoma(89).

Tumor specific mutations have been known for decades, and commonly occurring mutations in the RAS family of oncogenes (NRAS is mutated in 15% of melanomas) have been identified. However, earlier it was thought unlikely that such single amino acid mutations would translate into commonly-expressed altered peptides presented by MHC class I or II molecules for T cell recognition, making shared mutations unattractive for target in vaccine clinical trials(90). Neoantigens are those antigens that arise from random somatic mutations in individual tumors(91). These antigens have been assessed in many personalized DC vaccine clinical trials and have been shown to be immunogenic and increase Progression Free Survival (PFS) rates in melanoma patients(92-95).

1.10 Cancer Vaccine Platforms

Most cancer vaccines are designed to activate tumor specific $CD8^+$ CTL because studies in mice reproducibly support the key therapeutic role played by these cells. The most common vaccination strategies used have been based on MHC class I restricted peptide epitopes from TAAs. These have been delivered in a variety of adjuvant formulations (including cytokines and

toll-like receptor (TLR) ligands) to promote *in vivo* presentation by endogenous APC. Peptide based vaccines take advantage of the existing data on MHC class I peptide binding motifs for the most common HLA types, and the algorithms which can screen protein amino acid sequences for peptide epitopes derived from TAAs. Data from animal models support the potential for such vaccines to have a substantial therapeutic effect(96-98).

1.10.1 Peptide Based Strategies

Peptides formulated in adjuvants (such as Montanide, which is analogous to incomplete Freund's adjuvant (IFA)), with or without cytokines, such as GM-CSF and interferon γ (IFN-γ), or TLR agonists, have shown clinical benefit (partial responses, complete responses, and durable disease stabilization) in small- and large-scale clinical trials(99-102). In smaller trials, peptides loaded onto APCs, such as DCs, have also resulted in positive immune and clinical effects(103-105). DC cancer vaccine trials are discussed in greater detail below.

As peptide-based vaccines are tested, optimal adjuvants and formulations of these vaccines are still being identified. Clinical trials of peptide-based vaccines were recently reviewed(106). A benefit of peptide-based approaches is that 9 to 10 a.a long peptides are simple and inexpensive to manufacture. Large scale manufacture is possible and the peptides are stable when stored and shipped between treatment sites.

Because of the HLA restricted nature of T cell recognition, individuals who do not express common HLA types are logistically more difficult to treated with general peptide-based vaccines. In addition, the usual MHC class I binding short peptides do not activate $CD4^+$ helper T cells, which may limit the expansion/functionality of vaccine-induced $CD8^+$ cytotoxic T cells. In some cases, this limitation has been overcome by the inclusion of non-tumor specific help (inclusion of

keyhole limpet hemocyanin (KLH), tetanus, or (pan-DR binding synthetic helper (PADRE) peptides), although data are limited over the nature of the "help" provided by these heterologous helper peptides. Shared melanoma antigen-derived helper peptides have been tested in several trials, with data suggesting improved survival in vaccinated patients(107).

Another strategy that has shown significant clinical efficacy in the setting of cervical cancer is the use of synthetic peptides that are long enough to include multiple MHC class I and II epitopes(108,109). These 23-45 a.a. long peptides, delivered subcutaneously, have been shown to be especially effective, possibly because of a more efficient processing and presentation pathway, which leads to superior T cell activation(110). We have observed *in vitro* that a 16 a.a. long MAGE-A6-derived peptide, MAGE-A6$_{172\text{-}187}$, that has been reported to be promiscuously presented by multiple HLA-DR alleles, can also induce HLA-A2-restricted $CD8^+$ T cell responses against the MAGE-A6$_{176–185}$ epitope(111,112). These results indicate that long peptides derived from melanoma antigens could also be implemented in future melanoma vaccine modalities.

Multiple peptides can be given at the same time, coordinately targeting T cell clones reactive against a range of tumor antigens(113-115). Combination trials using vaccines and other therapies, such as cyclophosphamide, have resulted in a broader immune response and a reduction of regulatory cells. For example, a trial combining pre-vaccine cyclophosphamide with multiple peptides and GM-CSF showed that improved survival was associated with antigenic breadth of response and reduced suppressive circulating regulatory T cells (Tregs) and myeloid derived suppressor cells (MDSCs)(113). The Slingluff group has previously generated a cocktail of 6 MHC class II-restricted peptides (6MHP; derived from MAGE, MART-1, gp100, and tyrosinase (TAAs)) which has been tested in two phase I/II vaccine trials. Survival outcomes of patients

treated with the 6MHP vaccine were observed to be superior to those of matched institutional controls(116,117).

To enhance the efficacy of cancer vaccines, "wild type" (non-mutated) tumor antigen-derived epitopes can be modified in order to activate cross-reactive T cell clones, resulting in activation of higher avidity T cell clones capable of superior tumor recognition and killing. One or two a.a. substitutions, normally within the predicted epitope anchor residues, have been shown to lead to higher binding affinity that resulted in induction of higher avidity, tumor-specific T cells(118,119). The design of heteroclitic peptides (aka altered peptide ligands) can be difficult and labor-intensive. Recently, Cristian Capasso et al. have developed The Epitope Discovery and Improvement System (EDIS), an automated algorithm-driven platform to accelerate the design and application of heteroclitic peptides in the vaccine setting(120).

Another potential strategy to enhance tumor antigen-derived epitope immunogenicity is to utilize highly homologous and cross-reactive "mimicking" peptides derived from proteins found in common microbial pathogens to which many individuals have pre-existing immunity. We have shown that a peptide derived from the *Mycoplasma penetrans* HF-2 permease protein, HF-$2_{216–229}$, shares a high degree of structural and functional homology with the aforementioned MAGE-$A6_{172-187}$ epitope. The functional avidities of $CD4^+$ and $CD8^+$ T cells primed with HF-$2_{216–229}$ are 100 and 1000X greater than those of $CD4^+$ and $CD8^+$ T cells primed with MAGE-$A6_{172-187}$, respectively. Consequently, HF-$2_{216–229}$-stimulated T cells are superior at recognizing APCs pulsed with MAGE-$A6_{172-187}$ or recombinant MAGE-A6, as well as HLA-matched MAGE-$A6^+$ melanoma cell lines(111,112).

1.10.2 APC Based Strategies

Many types of APCs have been investigated, including peripheral blood mononuclear cells, activated B cells, and, more commonly, DC. As indicated above, DC are a heterogeneous population of APCs that can efficiently take up antigens and sample their environment. They then process and present these antigens to $CD4^+$ and $CD8^+$ T cells and incorporate immune response modulating cues (including the secretion of cytokines such as interleukin 12 (IL-12) p70, which skews the immune response to a type 1 response) to modulate the type of response. A type 1 response involves IFN-γ, IL-2, and tumor necrosis factor and it promotes the activation of cytotoxic $CD8^+$ T cells. Several recent reviews summarize the history, biology, and clinical application of these cells(20,121,122).

Clinical trials of autologous DC vaccines involve individualized patient vaccination approaches and single clinical trial arms. It is difficult to compare trials and draw firm conclusions about the efficacy or different approaches(123-125). Natural $CD11c^+$ DC as well as DC generated from monocytes(126-128) and $CD34^+$ progenitor cells have been tested with various antigen formats, including complex tumor lysates that contain normal, TAA and tumor specific antigens, or synthetic MHC class I restricted peptides. Vaccines have been injected into the blood, skin (subcutaneously or intradermally), and lymph nodes. A schematic of the generation of DC vaccines is shown in Figure 3. The initial lessons learned were that DC vaccines are safe, feasible and immunogenic and can promote clinically significant tumor regression in 4.2-7.1% of patients(104,109,129-134).

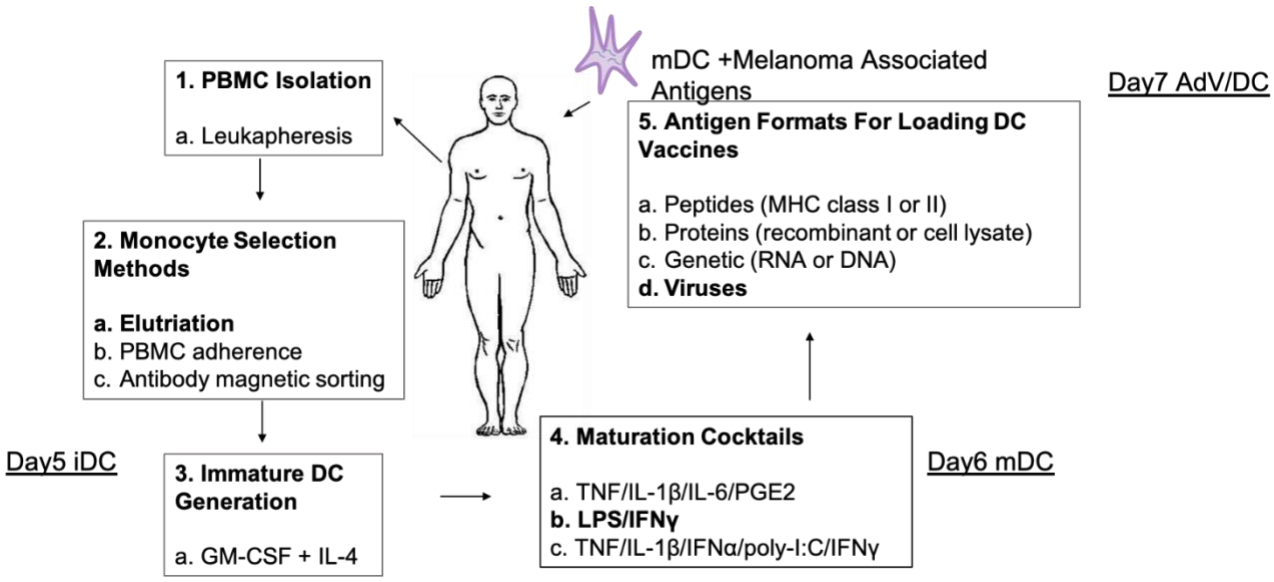

Figure 3. Monocyte-derived DC-based Immunization Protocol.
DC-based vaccines are generated by the selection of CD14+ monocytes from isolated PBMC. Monocytes are cultured with GM-CSF and IL-4, often for 5 days, to obtain immature DC. Immature DC are matured using various maturation cocktails as previously described by Kaka et al. (2009), Vujanovic et al. (2010), and Kalinski et al. (2005). After 24-48hr maturation, matured DC are delivered to patients. DC are loaded with antigens either before, during, or after maturation. The methods and reagents highlighted in bold were the methods chosen for the UPMC 09-021 trial referenced in Chapter 3.

One therapeutic cancer vaccine—Sipuleucel-T manufactured by Dendreon—was approved by the Food and Drug Administration in 2010. It consists of autologous APC loaded with the TAA prostatic acid phosphatase and GM-CSF and is approved for metastatic prostate cancer on the basis of a 4.1-month improvement in overall survival seen in data from large scale phase III clinical trials(135).

1.10.3 Tumor Based Strategies

Early cancer vaccine studies found that mice could be immunized with tumor cells that were killed and engineered to express immune stimulatory cytokines(136,137) including GM-CSF. The data supporting syngeneic, autologous, or allogeneic tumor cells transfected to express

high amounts of GM-CSF supported clinical testing, with some immune and clinical responses(77,138-141). Other strategies that use the personalized approach of harnessing autologous tumor antigens include using tumor lysates to load APCs ex vivo and fusion of tumor cells and autologous APCs. Immunity to undefined tumor lysates and foreign helper proteins has been demonstrated in some cases(142-144). Autologous tumor cells can also be used to transfect APCs (autologous or derived from allogeneic cell lines) with tumor genomic DNA(145). This allows uncharacterized mutated gene products specific to the tumor to be processed and presented for immune activation.

1.11 Determinant Spreading

Although antigen choice is critical for generating antitumor immunity, the spread of the immune response from one antigen to another antigen expressed in the same tissue ("determinant spreading"(146) or "epitope spreading") has been linked to superior clinical outcome(103,147-152) in multiple tumor types and vaccination settings. The phenomenon of *in vivo* cross presentation of tumor derived antigens released in one wave of T cell attack to promote subsequent waves of anti-tumor T cells directed against different antigens may be an important mechanism for tumor rejection(149). A vaccine that targets shared antigens may set the stage for subsequent rounds of immunity to mutated neoantigens. The most important role of vaccines containing TAAs may be to induce determinant spread to tumor specific antigens that activate higher avidity T cells, which more effectively mediate tumor rejection. The *in vivo* mechanism of cross priming may also result in autoimmunity(153), which has been found to represent a biomarker of clinical response to interferon in patients with melanoma(154).

1.12 DC Vaccine Clinical Trials for the Treatment of Melanoma

DC vaccines have been used in the clinic as a potential therapeutic modality for patients with melanoma. Researchers have tried to optimize DC priming abilities by the use of different maturation cocktails, such as LPS and IFN-γ, IFN-α and polyinosinic:polycytidylic acid (poly p:IC), and TNF-α, IL-1β, and PGE_2 combinations(155). Each of these maturation cocktails are designed to enhance DC priming abilities by increasing DC secretion of Th1-skewing chemokines, such as IL12p70 , in addition to T cell-recruiting chemokines.

Researchers have tried to optimize DC vaccines by the use of different DC subtypes. For example, one study isolated primary $CD1c^+$ blood DCs from Stage IV melanoma patients. The DCs were activated briefly (16hrs.) with tumor associated antigens. 4/14 participants showed long-term progression free survival (12-35 months) by the presence of circulating antigen-specific T cells(130). Another study pulsed matured DC with neo-antigens from stage III melanoma patients, which was then injected as a vaccine. Blood isolated from the vaccinated patients revealed presence of antigen-specific T cells in circulation(156). Recently, DC vaccines have also been used in combination with current checkpoint blockade therapy. A clinical trial using monocyte-derived DCs loaded with shared melanoma antigens in combination with ipilimumab yielded 8 complete responders and 7 partial responders, out of the 39 melanoma patients(157). The results of this trial are encouraging and suggest combination therapeutics might produce the best immunogenic response associated with clinical benefit in melanoma patients.

1.13 Adenovirus Vectors in DC-Based Vaccination

Recombinant Adenovirus Vectors (AdV) were first shown to be superior to other traditional methods of transfection of DCs, such as electroporation, in 1997(158). Since then, AdV have been proven to be a safe and an effective method of gene transfer in human DCs. Adenoviruses are non-enveloped, double-stranded DNA viruses that are between 30-43 kb in genome length(159,160). The genome transcript of adenoviruses can be separated into two categories: early onset genes (are transcribed before viral onset replication) and late genes (transcribed after viral replication). The E1A gene product is an essential protein for viral replication and is considered a transactivator for all other adenoviral genes(159). Because of this, the E1A gene locus is normally deleted and replaced by foreign DNA (including cDNA sequences encoding TAA) in recombinant adenovirus vectors used in vaccine formulations. There are approximately 50 adenovirus serotypes in humans. Adenovirus serotypes 2 and 5 are commonly used in the clinic(159).

A review of the literature has revealed that adenoviruses readily infect/transduce DC with greater than 95% efficiency(161). We and others have previously shown that adenovirus transduction of immature DC at an MOI up to 1,000 PFU:1 DC can result in a more matured phenotype (high level expression of CD83, CD86, HLA-DR, and increased secretion of IL12p70), with resultant DC shown to be more efficient at priming specific $CD8^+$ T cells(161). Moreover, we have shown that adenovirus transduction (using an MOI of 500PFU:1DC) of pre-matured DC results in higher expression of co-stimulatory molecules and antigen processing machinery, compared to adenovirus transduction before maturation(161).

The use of adenovirus-based DC vaccination has been reported to be superior to other forms of DC-vaccination, such as peptide loading. Studies have shown that AdV transduced DC

enhance tumor-antigen-specific T cell responses, compared to peptide-loaded DC(162,163). An advantage of adenovirus transduction is that the adenovirus vector does not restrict epitope recognition to specific human leukocyte antigen (HLA) epitopes. Adenovirus transduced DC can be transduced with full length tumor antigens can stimulate T cells to numerous class I- and class II-presented peptide epitopes(164-167). Peptide-loaded DC are limited to stimulating T cells with class I and/or class II-restricted epitopes. Since adenovirus transduced DC are not restricted to specific epitopes, they are able to increase the breadth of a generated anti-tumor immune response.

Clinical trials using AdV transduced DC have been shown to be clinically effective and immunogenic in advanced stage melanoma patients. Trials involving transduced DC with one tumor antigen vs multiple tumor antigens have yielded similar results(168-170). Both vaccination methods have been proven to be safe and immunogenic, with objective clinic response rates averaging ~5-10%. Additionally, these trials have indicated the development of determinant spreading, NK cell activation, and vaccine-induced increases of $CD8^+$ and $CD4^+$ T cell responses. All together, these data support the continued use of adenovirus-based DC vaccines for the treatment of advanced-stage cancers.

2.0 Statement of the Problem

2.1 Foreword

The data referenced in this chapter was adapted from a previous published research manuscript in *Journal for Immunotherapy of Cancer:* Butterfield, L.H., Vujanovic, L., Santos, P.M., **Maurer, D.M**., Gambotto, A., Lohr, J., Li., C., Waldman, J., Chandran, U., Lin, Y., Lin, H., Tawbi, H.A., Tarhini, A.A., and Kirkwood, J.M. Multiple Antigen-Engineered DC Vaccines with or without IFNα to Promote Antitumor Immunity in Melanoma. *Journal for Immunotherapy of Cancer*. February 2019.

2.2 Significance of Thesis to Human Health

DC based cancer vaccines provide three essential signals (antigen presentation, costimulation, and proinflammatory cytokine production) required to initiate Type-1 adaptive immune responses(134,171-174). Clinical studies have shown that DC-based vaccines are capable of generating tumor-specific immune responses and are safe. However, clinical response rates for DC vaccines in metastatic cancer patients remain low (i.e. 5-10%)(129), indicating that critical pathways for activating effective immunity remain unknown.

To improve clinical outcomes observed in patients, we developed a genetically-engineered DC-based vaccine using a recombinant adenovirus coordinately expressing three shared melanoma antigens: Tyrosinase, MART-1, and MAGE-A6 (TMM2) to promote an expanded anti-tumor

$CD4^+$ and $CD8^+$ T cell repertoire. Monocyte-derived DC were first matured with rhIFN-γ + lipopolysaccharide (LPS), and then transduced with recombinant adenovirus (AdVTMM2) before administration to patients (n = 35) 3x via bi-weekly intradermal injections(175). A subset of patients were randomly selected to receive IFNα-2b over the course of one month. IFNα-2b was chosen because of its ability to skew DC function to a type 1 immune response and benefit overall survival rates. The enrollment period for the trial was from September 2012 until November 2015. The study design, vector design, and diagnosis status of patients at the time of enrollment, are shown in Figure 4.

Thirty-five late staged melanoma patients were enrolled in the phase I clinical trial. Three out of the thirty-five patients were treatment naïve, while the others previously had received standard of care (IFN-α and/or IL-2) or checkpoint blockade therapies (Ipilimumab and/or Pembrolizumab)(175). As stated above, patients received the vaccine 3x over the course of one month. At that time, anyone who did show disease progression participated in a randomized IFN-α2B boost treatment for an additional month (n=23). A detailed patient demographic table & study design schema are located in Table 1.

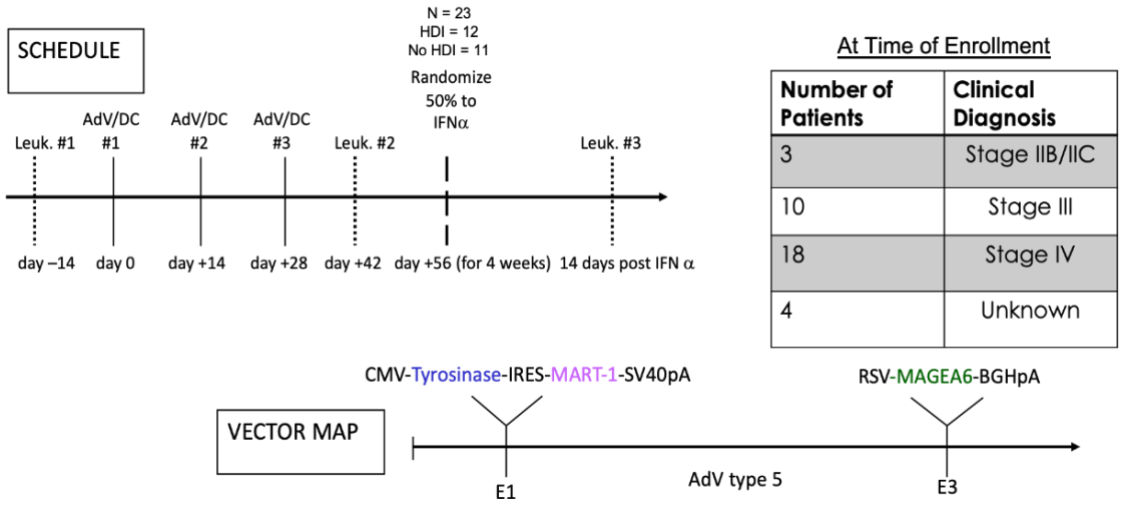

Figure 4. UPMC 09-021 AdVTMM2/DC Vaccine Study Design.
The study design of the UPMC 09-021 clinical trial is shown. As shown on the right side, late stage melanoma patients were enrolled in the trial. Patients received 3 doses of the vaccine (10^7 DC) via intradermal injections, over the course of one month. Leukaphersis was taken at baseline and post-vacanation. Patients that did not progress post-vacanation participated in a randomized IFNα-2b treatment for one month. Leukaphersis was taken post-treatment. The vector map of the AdVTMM2/DC vaccine is shown.

Table 1. **UPMC 09-021 Patient Demographics**.
Detailed patient demographics from the UPMC 09-021 phase I clinical trial.

Study Number	*Age*	*Race*	*Sex*[1]	*Stage*	*Prognosis Group*[2]	*Outcome Group*[3]	*Overall Survival*[4]	*Progression Free Survival*[4]
1	82	White	F	STAGE IIIC	PD	Bad	6.37	3.20
2	74	White	M	STAGE IIIB	PD	Bad	14.03	2.03
3	82	White	F	STAGE IV	PD	Bad	13.63	2.10
4	74	White	M	STAGE IV	PD	Bad	1.07	0.80
5	44	White	M	STAGE IV	PD	Bad	0.67	0.40
6	67	White	M	STAGE IV	SD	Good	39.80	5.53
7	42	White	M	STAGE IV	SD	Good	20.00	7.23
8	74	White	F	STAGE IV	SD	Good	13.07	8.77
9	66	White	M	STAGE IV	SD	Good	27.43	5.73
10	61	White	M	STAGE IV	PR	Good	44.33	13.47
11	56	White	M	STAGE IV	PD	Bad	14.833	1.77
12	44	White	M	STAGE IV	SD	Good	41.73	3.93
13	74	White	M	STAGE IIC	NED1	Good	42.53	18.43
14	58	White	F	UNKNOWN	PD	Bad	28.43	1.70
15	52	White	F	STAGE IV	NED2	Bad	42.70	6.97
16	75	White	F	STAGE IIB	NED2	Bad	38.60	9.30
17	64	White	M	STAGE III	PD	Bad	4.63	2.37
18	68	White	M	STAGE IV	NED2	Bad	39.90	5.07
19	64	White	M	UNKNOWN	SD	Good	3.50	3.23
20	61	White	F	UNKNOWN	NED2	Bad	20.27	19.27
21	60	White	M	STAGE IV	PR	Good	40.17	7.30
22	70	White	F	STAGE IV	PD	Bad	3.03	2.03
23	28	White	M	UNKNOWN	PD	Bad	11.20	2.13
24	42	White	F	STAGE IV	PD	Bad	3.27	2.13
25	52	White	M	STAGE IIB	PD	Bad	0.67	0.67
26	60	White	M	STAGE IIIA	NED1	Good	36.13	3.67
27	59	White	F	STAGE IIIB	NED1	Good	35.87	13.73
28	47	White	M	STAGE IV	PD	Bad	11.8	1.63
29	60	White	M	STAGE IIIA	NED1	Good	32.33	14.00
30	45	White	F	STAGE IIIB	NED1	Good	37.50	37.50
31	66	White	M	STAGE IIIC	NED1	Good	37.30	30.70
32	41	White	F	STAGE IIIB	NED2	Bad	26.57	2.53
33	46	White	F	STAGE IIIB	PD	Bad	1.67	0.90
34	88	White	M	STAGE IV	SD	Good	8.27	3.37
35	52	White	F	STAGE IV	SD	Good	24.27	13.07

[1] M: Male; F: Female
[2] 2PD: Progressive Disease, SD: Stable Disease, NED1: No Evidence of Disease at time of enrollment and remained NED for ≤ 18 months, NED2: No Evidence of Disease at time of enrollment and remained NED for ≥ 18 months, PR: Partial Responder (RECIST)
[3] Clinical Outcome groups used for experimental analysis. Patients who did not progress during the trial where considered to have a "good" outcome, while patients who progressed were considered to have a "bad" outcome
[4] Time in months

Clinical status of the patients indicated that the median overall survival was 724 days, while the median progression free survival was reported to be 336 days. 12 individuals progressed early and were not considered for the randomized IFNα-2b cytokine boost. Out of the remaining 23 patients, 8 achieved stable disease, 2 showed partial tumor regression, and 6/11 patients who had no evidence of disease at the start of the trial (had prior metastasis), remained progression free for at least 18 months. The remaining patients all showed tumor progression.

Similar to previous DC-based vaccine studies, patients had measurable $CD8^+$ and $CD4^+$ antigen-specific responses. However, expression of important DC markers (HLA-DR, CD11c, CD40, CD80, CD83, CD86 and CCR7) on vaccine DC did not correlate with immune or clinical outcomes (Figure 5A). Furthermore, Cox regression analysis revealed these markers were not prognostic factors for overall survival (OS) or progression free survival (PFS) (Table 2). Unlike some prior reports, DC production of IL12p70 (either spontaneous or after CD40L-induced activation), an essential cytokine for promotion of type 1 immunity, also failed to correlate with immune or clinical outcomes (Figure 5B). This was also the case for DC production of the immunoregulatory molecule IL-10 (Figure 5C). RNA levels of most these cell surface and secreted molecules increased with DC maturation, as expected, but RNA levels also failed to correlate with objective clinical outcomes (Figure 5D-E).

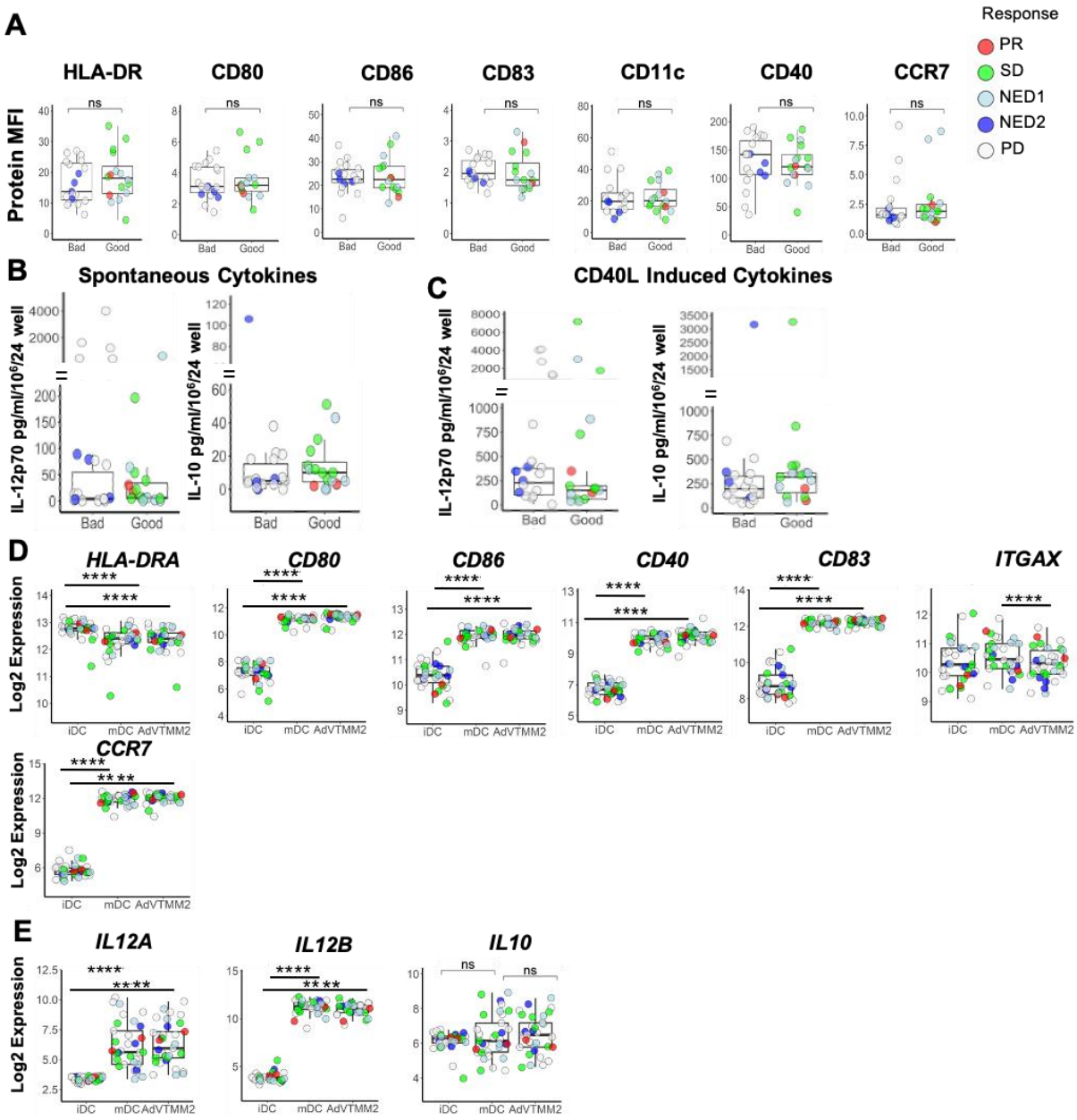

Figure 5. Consensus DC Phenotypic and Potency Biomarkers do not Correlate with Clinical Outcome.
Consensus markers associated with immunostimulatory DC were assessed by flow cytometry after patient DC adenoviral transduction (AdV/DC) (A). DC were gated based on FSC vs SSC profiles, with IgG isotype-matched antibodies used to define negative control staining patterns. Spontaneous (B) and CD40L-induced (C) IL12p70 and IL-10 secretion from DC were assessed in culture supernatants by Luminex. Patients (n=35) were segregated by clinical outcome, and data comparisons were performed using unpaired student t-tests or Wilcoxon rank sum tests (CD80, CD40, CD11c, and IL12p70/IL10 comparisons) to determine significance. ns = not significant. Microarray analysis of critical DC genes (D), spontaneous or induced IL12A, IL12B, and IL10 transcriptional levels (E) in DC subtypes from melanoma patients(n = 33). Patients are segregated based on clinical outcome, with the significance of inter-group differences for IL10 and ITAX determined using a one-way ANOVA analysis with Tukey's multiple comparison test. All other inter-group differences were assessed using the Kruskal-Wallis one-way ANOVA with Dunnett's multiple comparison test. **: p value ≤ 0.01, ****: p value≤ 0.0001, ns= not significant.

Table 2. Critical DC Markers are not Prognostic Factors for Overall Survival or Progression Free Survival in Advanced Melanoma Patients.

Univariate Cox regression analysis for associations between critical DC markers (MFI) on AdVTMM2 (n=35) assessed prior to patient administration at baseline and OS and PFS. The hazard ratio, significance values, and 95% Confidence Intervals for each of these markers are listed**.**

Endpoint	Factor	Cell Type	HR	95% CI for HR	p
OS	HLA-DR	AdV/DC	1.1	(0.73-1.7)	0.59
	CD80	AdV/DC	1.3	(0.87-1.9)	0.21
	CD86	AdV/DC	0.74	(0.43-1.3)	0.28
	CD83	AdV/DC	0.88	(0.59-1.3)	0.55
	CCR7	AdV/DC	1	(0.73-1.4)	0.9
	CD40	AdV/DC	1.2	(0.68-2)	0.57
	CD11c	AdV/DC	1	(0.95-1.06)	0.88

Endpoint	Factor	Cell Type	HR	95% CI for HR	p
PFS	HLA-DR	AdV/DC	1.1	(0.74-1.5)	0.73
	CD80	AdV/DC	1.1	(0.79-1.5)	0.61
	CD86	AdV/DC	0.82	(0.55-1.2)	0.36
	CD83	AdV/DC	1.2	(0.86-1.6)	0.32
	CCR7	AdV/DC	0.9	(0.63-1.3)	0.57
	CD40	AdV/DC	1.2	(0.73-1.8)	0.52
	CD11c	AdV/DC	1.3	(0.73-1.73)	0.59

Overall, the data suggested that the AdVTMM2 DC vaccine was immunogenic and was capable of stimulating T cell responses against melanoma. However, the clinical response rate (defined as complete or partial response) was a dismal 5.7%. This suggests melanoma patient monocyte-derived DC may be inferior at stimulating immune responses, compared to healthy donors (HD). Additionally, given clinical outcome data from these patients and our previous findings that vaccine efficacy did not correlate with administered DC expression of commonly tested costimulatory molecules (CD80, CD86) or IL-12p70 levels(175), molecules correlating with clinical outcomes need to be identified. In the current study, gene and protein expression profiling was performed to identify key biomarkers associated with *in vivo* DC immunogenicity and positive

clinical response to DC-based vaccination. By understanding the mechanisms and proteins behind DC functionality, we will be able to generate superior DC vaccines, and possible combination therapies, that will hopefully lead to a higher clinical response rates in advanced melanoma patients.

3.0 . Melanoma Patient & HD DC Increase Checkpoint Molecule Surface Protein Expression Post-Maturation, and Patient DC Have Reduced Expression of the Co-Stimulatory Molecule, ICOSL

3.1 Foreword

Portions of this chapter were adapted from the previous published research manuscript in *Cancer Immunology Research:* Maurer, D.M., Adamik, J., Santos, P.M., Shi, J., Shurin, M.R., Kirkwood, J.M., Storkus, W.J., Butterfield, L.H. Dysregulated NF-κB-dependent ICOSL Expression in Human Dendritic Cell Vaccines Impairs T Cell Responses in Melanoma Patients. *Cancer Immunology Research*, 2020.

3.2 Graphical Summary

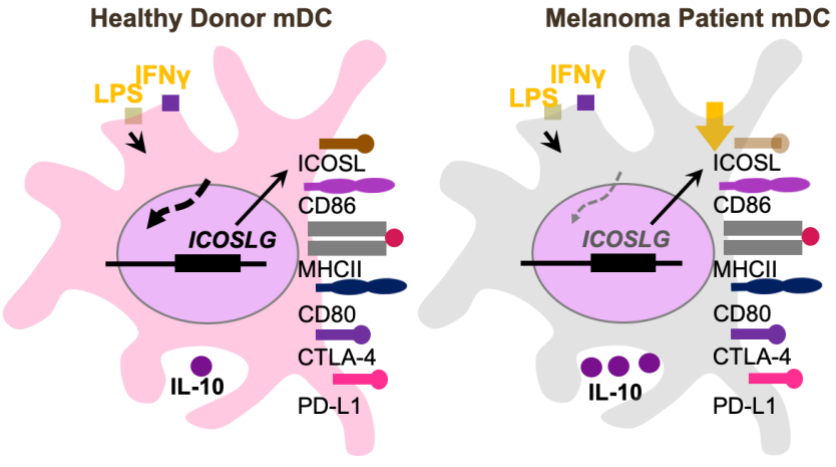

Figure 6. Graphical Summary for "Melanoma Patient & HD DC Increase Checkpoint Molecule Surface Protein Expression Post-maturation, and Have Decreased Expression of the Co-stimulatory Molecule, ICOSL, Compared to HD".

3.3 Introduction

To identify critical molecules important for promotion of anti-tumor T cell responses, 11 different costimulatory and immune checkpoint molecules that have been implicated as being important for antigen presentation and T cell activation were targeted for investigation. Cryopreserved elutriated monocytes from melanoma patients and HD were used. Clinical protocols & reagents for DC generation (day5 iDC), maturation (day6 mDC), and transduction (day7 AdVTMM2/DC) were followed to ensure *in vitro* recapitulation of the clinical trial. Cell culture supernatants were collected for each DC subtype. These supernatants would be used to test for chemokine and cytokine secretion from patient and HD cells using Luminex assays. Additionally, transcriptional profiling of patient DC was performed on day 5 iDC, day 6 mDC, and day 7 AdVTMM2/DC. Transcriptional analyses revealed significant changes in gene expression of targeted molecules due to maturation, with additional changes post-AdVTMM2 antigen engineering.

The initial protein screen observed surface protein expression of PD-1, PDL-1, PD-L2, CTLA-4, LAG-3, Galectin-9, OX40L, CD70, B7-H4, B7-H5, and ICOSL on iDC, mDC, and AdVTMM2/DC from patients and HD. Surface protein expression was examined using FACS analysis. To validate the observed mean fluorescent intensities of the targeted molecules on iDC, mDC, and AdVTMM2/DC, cryopreserved vaccine lots from two individual patients were used. Surface protein expression of eight out of the eleven molecules (PD-1, PDL-1, PD-L2, CTLA-4, LAG-3, B7-H4, B7-H5, and ICOSL) was validated using the vaccine lots; validation thresholds were set at $\leq 10\%$ change of positive frequencies.

3.4 Materials & Methods

AdVTMM2 Virus. The replication-deficient E1/E3-deleted Ad5 TMM2 virus coordinately encoding full-length cDNAs for tyrosinase, MART-1, and MAGE-A6 used in this study was manufactured as previously described(176). DCs, generation described below, were harvested 24hrs. post-maturation and transduced with the adenovirus at an MOI of 400. CellGenix GMP DC Medium, serum free (CellGenix, #20801-0500) was used for the transduction. DCs and the AdVTMM2 virus in CellGenix medium were incubated for 3hrs. at 37°C, and then washed with PBS. The vector map is shown in Figure 3.

DC Generation from Cryopreserved Monocytes. Patient and healthy donor (HD) PBMCs were isolated by leukapheresis and elutriation(175). Fractioned cells were cryopreserved using freezing cryovials, 1.8 mL internal thread (Nunc Cat. No. 368632). Freezing media contained 20% DMSO in Dulbecco's Modified Eagle Medium (Gibco/Invitrogen, Catalog #11885), complete media [20% heat-Inactivated Fetal Bovine Serum (FBS) (Gibco/Invitrogen, Catalog #16000), 1% L-glutamine (Gibco/Invitrogen, Catalog # 25030), and 1% pen/step (Gibco/Invitrogen, Catalog #15140)]. Monocyte-enriched fractions were thawed using RPMI (Gibco/Invitrogen, Catalog #11875-085) complete media [1% pen/strep, 1% L- glutamine, 10% FBS Heat-Inactivated Serum (Gibco-Invitrogen, Catalog #16000-044), and 0.5% DNase (Sigma, Catalog # DN-25)]. Cells were centrifuged at 1200 RPM (31 x g) for 10 minutes and then washed twice with PBS. Cells were counted, analyzed for viability using Trypan Blue Stain 0.4% (Gibco, Catalog #15250-061), and plated at 1 x 106/mL in CellGenix DC medium, serum free (CellGenix, Catalog #20801-0500). To culture patient DCs for checkpoint and costimulatory protein surface molecule expression, the conditions were identical to Standard Operating Procedures used in the clinical trial [Cell Genix

with GM-CSF (1000 U/mL; Genzyme and Sanofi) and IL4 (1000 U/mL; Cell Genix)](12). For all other experiments, research grade reagents were used [AIMV Media (Gibco-Invitrogen) with GM-CSF (800U/mL; Genzyme and Sanofi) and of IL4 (500 U/mL; Cell Genix)]. On day 5, immature DCs (iDCs) were matured by addition of rhIFNγ (1000 U/mL; Actimmune and R&D Systems) + LPS (250 ng/mL; Sigma-Aldrich) in CellGenix DC medium, serum free for 24hrs. (mDCs). Matured DCs were transduced with clinical-grade TMM2 adenovirus at a MOI of 400 for 3hrs. at 37°C, and then washed with PBS. Cells were rested overnight in DC media with IL4 and GM-CSF (1000 U/mL; AdVTMM2/DC).

Cell Surface FACS Analyses. DC were harvested, washed twice with PBS, prior to counting and assessment of viability by trypan blue dye exclusion. Viability was validated by the use of Zombie Aqua Viability Dye (BioLegend #423101). The viability dye was used per manufacturer's instructions. Cells were washed with FACS buffer (2% BSA, and 0.02% NaN_3 in PBS). Fc blocking was done using 5% Human Antibody Serum (Corning) for 25 min at 4°C. Antibody staining was performed for 20 min at 4°C. Cells were washed and fixed using 2% paraformaldehyde for 30 min at RT or overnight at 4°C. FACS analyses were performed using the BD LSR Fortessa II (BD Biosciences), with data analyzed using FlowJo v10 software. DC were identified as HLA-DR^+/$CD86^+$ double positive cells. Mean fluorescence intensity (MFI) or positive frequencies were determined after correcting for background staining using an isotype control. A 2% threshold was used to determine positive staining (Figure 7).

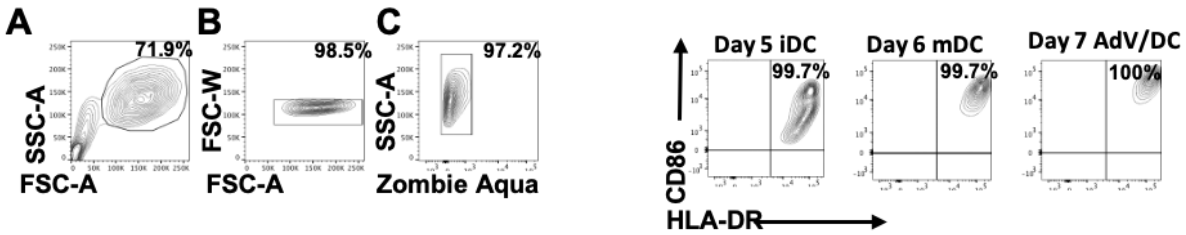

Figure 7. Gating Strategies used for DC identification.
Gating strategy used to assess checkpoint and costimulatory molecule surface expression on HD and patient DC (A). Monocytes were gated based on FSC vs SSC gating (B), followed by single-cell/viability gating (C). HLA-DR^{+}CD86^{+} double-positive DC were then analyzed for co-expression of the indicated DC markers, immune checkpoint molecules and costimulatory molecules by flow cytometry (D). Isotype controls were used to account for background staining. Molecules of interest were considered to be expressed on the surface of DC if positive staining was greater than 2%, compared to background (isotype) levels.

Antibodies. The following antibodies were used for assessment of costimulatory and checkpoint molecule expression on DC subsets: FITC Mouse Anti-Human HLA-DR (BD Biosciences Catalog#555811), PE-Cy7 Mouse Anti-Human CD86 (BD Biosciences Catalog#561128), BV 421 Mouse Anti-Human PD-L1 (BioLegend Catalog#329714), BV 711 Mouse Anti-Human PD-L2 (BD Biosciences Catalog#564258), BV711 Mouse IgG1, κ Isotype Control (Biosciences Catalog#563044), BV786 Mouse Anti-Human CTLA-4 (BD Biosciences Catalog#563931), BV786 Mouse IgG2a, κ Isotype Control (BD Biosciences Catalog#563732), ICOSL (BD Biosciences Catalog#564276), BV 421 Mouse IgG2b, κ Isotype Control Antibody (BioLegend Catalog#400342), PE Mouse Anti-human CD252 (BioLegend Catalog# 326308), PE Mouse IgG1, κ Isotype Control (BioLegend Catalog#400114), PE Mouse Anti-Human Galectin-9 (BD Biosciences Catalog #565890), PE Mouse Anti-Human CD70 (BD Biosciences Catalog#555835), PE Mouse IgG3, κ Isotype Control (BD Biosciences Catalog#556659), Human B7-H4 Alexa Fluor 647-conjugated Antibody (R&D Systems, Catalog#FAB6576R-100), Mouse IgG2B Alexa Fluor 647-conjugated Isotype Control (R&D Systems, Catalog# IC0041R), Human VISTA/B7-H5/PD-1H Alexa Fluor 750-conjugated Antibody (R&D Systems, Catalog# FAB71261S), Mouse IgG2B

Alexa Fluor 750-conjugated Isotype Control (R&D Systems, Catalog# IC0041S), Alexa Fluor® 647 Mouse anti-Human CD279 (BD Biosciences, Catalog#560838), Mouse IgG1, κ Isotype Control (BD Biosciences Catalog#557714), and Alexa Fluor® 647 Mouse Anti-Human LAG-3 (BD Biosciences, Catalog#565717).

Luminex. Human Checkpoint 14-plex (Thermo-Fisher Procarta Plex) was used for detection of checkpoint and costimulatory molecules in culture supernatants. A custom 2-Plex (Thermo-Fisher Procarta Plex) for granzyme-B and IFN-γ was used for detection of granzyme-B. Immune Monitoring 65-Plex (Thermo-Fisher Procarta Plex) was used for the detection of chemokine and cytokine secretion in DC culture supernatants. Serum was diluted 1:1 per manufacturer's instructions, analyzed in a BioRad BioPlex System 100. Experimental data was analyzed using five-parametric curve fitting and assay controls included kit standards and multiplex QC controls (R & D Systems).

Transcriptional Analysis of Costimulatory/Checkpoint Molecules. RNA from DC preparations was collected using the All Prep RNA/Protein kit (Qiagen#80404). cDNA was synthesized using the qScript cDNA Synthesis Kit (Quantabio). QPCR was performed using standard Taqman primers (listed below) and the Express qPCR supermix (Thermo Fisher #1178501K). The following primers were used: CD274 (Hs00204257_m1), CTLA-4 (Hs00175480_m1), and ICOSLG (Hs00391287_m1). HPRT1 (Hs99999909_m1) was used as a housekeeping control. All experiments were done in triplicates using the StepOne Plus Real-time PCR System (Applied Biosystems). Gene expression was calculated and normalized to the HPRT1 endogenous control using the Livak and Schmittgen method (2 -ΔCT).

DC Microarrays. Patient-derived immature, matured, and adenovirally-transduced DCs were harvested (as described above), washed with PBS, and centrifuged at 1200 RPM (30 x g). Cell pellets were collected and resuspended in RNAlater (Invitrogen; Catalog #AM7021), placed at 4°C overnight, and then moved to -80°C for storage. RNA was analyzed using HUGENE 2.0 ST gene arrays (Affymetrix) (GSE157738). Human microarray and qPCR data from patients confirmed in vitro adenovirus transduction based on increased expression of transcripts for Tyrosinase, MART-1and MAGE-A6, as well as the adenoviral hexon gene product (Figure 8A-B). A publicly-available HD DC dataset was used as for comparison (GSE111581)(177) using the same maturation protocol in preparing DC from both patients and HD. Patient and HD microarray data and differential gene expression was analyzed using R statistical packages, limma (Version 3.38.3)(178) and oligo (Version 3.9)(179). The Robust Multi-Average (RMA) method was used to normalize the data and the Benjamin-Hochberg Procedure was used to adjust for type 1 error rate. Ingenuity Pathway analysis software (QIAGEN Bioinformatics) was used for comparative analysis between patient and HD datasets. The patient and HD datasets used different gene array platforms, hence pathway analysis focused on opposing trends that might underlie differential gene profiling. Pathways and/or genes with the same directional pattern (activation or inhibition) were not prioritized for further consideration. Significant adjusted p value and log fold change thresholds were set at 0.05 and 1.2, respectively.

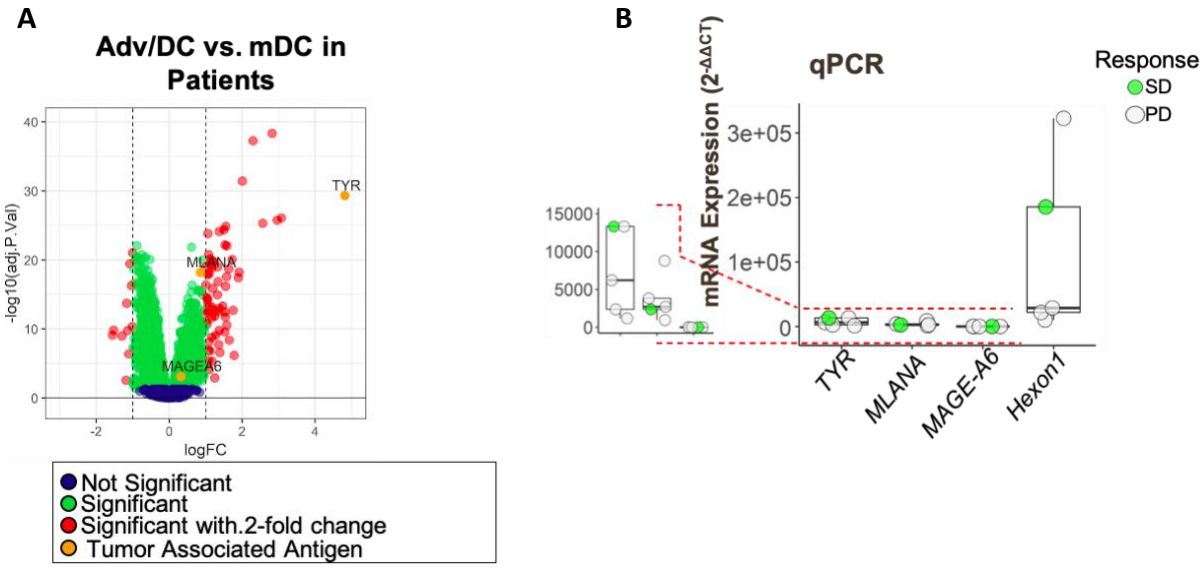

Figure 8. Confirmation of Efficient AdVTMM2 Transduction of Patient DC by Microarray and QPCR. Differential expression analysis of patient DC (pre/post AdVTMM2 infection) was performed (n=33) using microarrays focusing on vector inclusive transcripts from Tyrosinase, MART-1/MLANA, MAGE-A6 and AdV Hexon-1 (A). A volcano plot is depicted with vector-associated melanoma antigen transcripts indicated. QPCR analysis was performed in a subset of patients (n=6) to verify the microarray data (B). The Y axis is expanded on the left to show differences in encoded tumor antigen expression. Shown is a heatmap for the top 62 differentially expressed genes (FC > 2 and type 1 error rate of 0.05) in iDC, mDC and AdV/DC of melanoma patients (n=32) (A). Secreted IL-10 levels in melanoma patient mDC (n=22) compared to HD (n=4) (B).

Clinical Outcome Comparison Groups. For all analysis, clinical outcome groups were defined based on time to progression (Table 1). Patients who showed tumor regression (PR), remained stable (SD), or were considered "No Evidence of Disease" at enrollment and remained NED for at least eighteen months (NED1) were considered to have "favorable/good outcomes". Patients who had early tumor progression or were considered "No Evidence of Disease" at enrollment, but remained NED for less than eighteen months (NED2) were considered to have "bad outcomes". Eighteen months was chosen for the cutoff because it is clinically meaningful.

Statistical Analysis. Based on data distribution, t-tests or Wilcoxon rank-sum test were used for most of the analyses. The Shapiro-Wilk test was used to assess data normality. When appropriate,

one-way ANOVA or Kruskal-Wallis one-way ANOVA tests were performed. To test for multiple comparisons, a Dunnett multiple comparison or Tukey comparison test was used. Additionally, Pearson or Spearman's correlation coefficients and linear regression models were calculated to determine associations present. Kaplan-Meier (KM) curves and Cox proportional-hazards modeling were carried out using the R packages survival (version 3.1-8) and survminer (version 0.4.6). P values are represented as *$p \leq 0.05$, **$p \leq 0.01$, ***$p \leq 0.001$, **** $p \leq 0.0001$. Graphs were generated using the R package ggplot2 (Version 3.1.1) and GraphPad Prism v7.

3.5 Results

3.5.1 DC Exhibit Increased Cell Surface Expression of PD-L1, PD-L2, and CTLA-4 Post-Maturation

HD and patients expressed the co-inhibitory molecules, PD-1, LAG-3, PD-L1, PD-L2, and CTLA-4 at baseline (iDC), but then quickly lost surface expression of PD-1 and LAG-3 post-maturation (data not shown). In contrast, HD and melanoma patient DC expressed higher levels of PD-L1, PD-L2, and CTLA-4, post-maturation and after adenoviral transduction vs. baseline (Figure 9A). We observed a significant direct correlation between CTLA-4 and PD-L1 surface expression on AdVTMM2/DC from patient cells (Figure 9B). In addition to the protein surface analysis, transcriptional profiling of patient DC was performed, revealing significant changes in gene expression due to maturation, with additional changes post-AdVTMM2 antigen engineering. *CTLA4* mRNA expression in AdVTMM2/DC was inversely correlated to mRNA transcript levels

of the costimulatory molecule, *CD80*, and the Th1 polarizing cytokine subunit, *IL12p35* (Figure 9C). We also determined that *CTLA4* mRNA expression in AdVTMM2/DC was positively associated with IL10 mRNA levels (Figure 9C). Additionally, transcriptional profiling and protein analyses of patient DC revealed melanoma patients expressed high levels of immunoregulatory molecules, such as IL-10 and *IDO* (Figure 10A-B). While it is known that maturation of DC can lead to increased stimulatory capacity, these data suggest DC regulatory networks that could contribute to limitations in T cell activation.

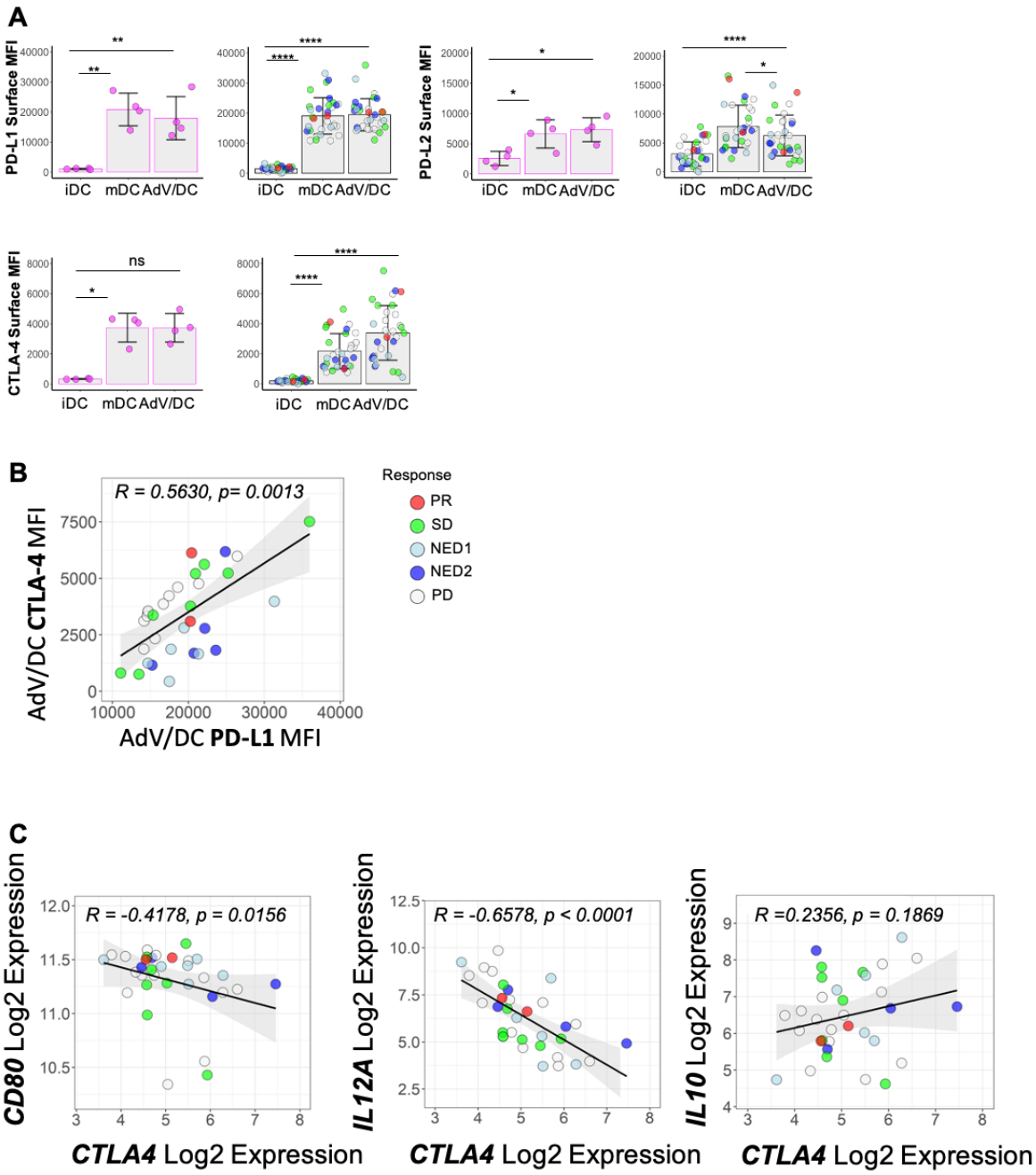

Figure 9. HD and Patient DC Express Higher Levels of Surface Expression of PD-L1, PD-L2 and CTLA-4 Post-maturation and Viral Transduction. AdVTMM2/DC Expression of Checkpoint Molecules is Directly Correlated to Cytokine and Co-Stimulatory Molecule Transcript Levels.

DC surface expression of immune checkpoint molecules PD-L1 (A, left), PD-L2 (A, right) an CTLA-4 (A, second row) on DC subtypes (Day 5 iDC, Day 6 mDC, and Day 7 AdV/DC) by flow cytometry in HD (n=4) and melanoma patients (n = 32). Patients were segregated based on clinical outcomes. Significance of inter-group differences for PD-L1 & CTLA-4 expression on patient cells and CTLA-4 expression on HD were determined using the Kruskal-Wallis one-way ANOVA with Dunnett's multiple comparison test. PD-L2 expression ion patient & HD DC and PD-L1 expression. Patient DC were determined using one-way ANOVA analysis with Tukey's multiple comparison test. *: p value ≤ 0.05, **: p value ≤ 0.01, ***: p value ≤ 0.001, ****: p value≤ 0.0001. Correlation of AdV/DC surface protein expression (flow cytometry; MFI) of PD-L1 and CTLA-4 (n=32) (B). Correlations of CTLA4 with IL12A,

CD86, and IL10 transcriptional levels in patient AdV/DC (n=33) (C). Patients are segregated based on clinical outcomes. Spearman correlations were used to assess the relationship between PDL1 and CTLA4 surface protein on AdV/DC, as well as to assess the relationship between CTLA4 and CD80. Pearson's R was used to determine the correlation between CTLA4 and IL12A and the correlation between CTLA4 and IL10.

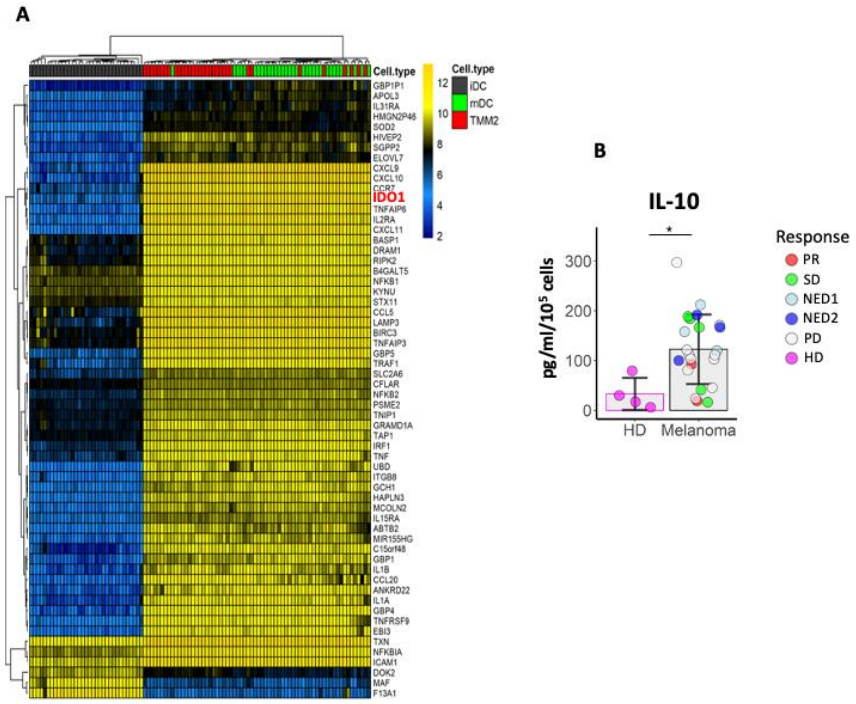

Figure 10. Melanoma Patient mDC Express the Immunosupressive Molecules, *IDO1* and IL-10.
Shown is a heatmap for the top 62 differentially expressed genes (FC > 2 and type 1 error rate of 0.05) in iDC, mDC and AdV/DC of melanoma patients (n=32) (A). Secreted IL-10 levels in melanoma patient mDC (n=22) compared to HD (n=4) (B). Patients were segregated based on clinical outcomes and unpaired student T tests were used to determine the significance of inter-group differences. *: p value ≤ 0.05.

3.5.2 ICOSL Cell Surface Expression is Reduced on Patient DC and is Negatively Associated with the Immunosuppression Molecule, IL-10

The preliminary protein screen revealed both HD and melanoma patient monocyte-derived DC rarely express the costimulatory molecules, B7-H4 and B7-H5. However, it was observed that surface expression of the costimulatory molecule, ICOSL, was reduced on both patient and HD DC upon maturation and subsequent viral transduction (Figure 11A, Figure 11). Importantly, the level of ICOSL expression on patient-derived DC was significantly lower than that of DC from HD (Figure 11A, Figure 12). Moreover, patients exhibited a more significant decrease in ICOSL cell surface expression when iDC were matured (Figure 13). No clinical correlations were observed with ICOSL surface protein expression. In addition, we observed significant negative correlations with surface ICOSL expression and IL-10 production from patient mDC and AdVTMM2/DC (Figure 11B). Unlike the maturation induced changes observed with the co-inhibitory molecules, the differences in ICOSL surface expression observed between HD and patients were patient-specific.

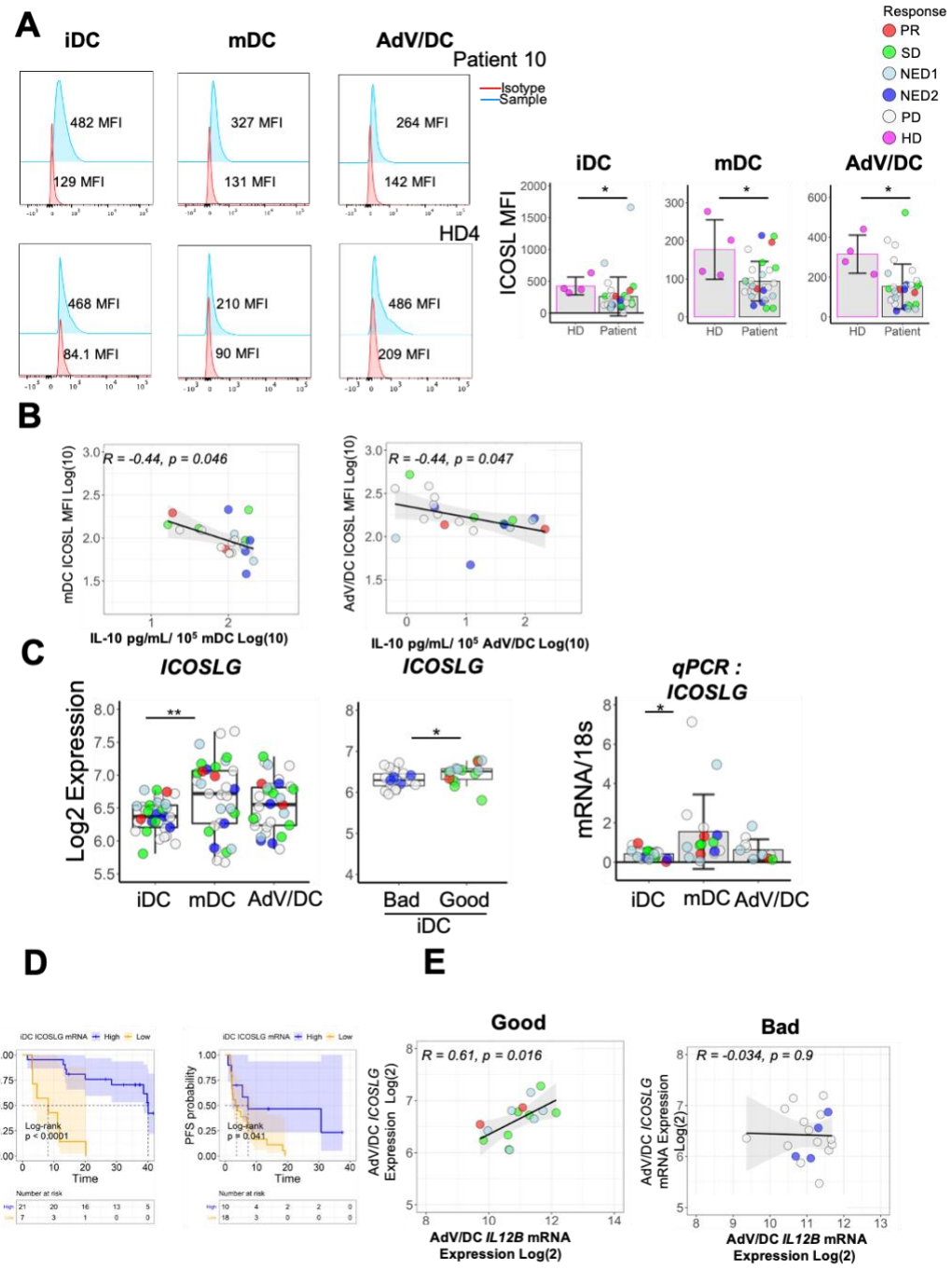

Figure 11. ICOSL Protein Expression is Reduced on Melanoma Patient DC vs HD DC and Negatively Correlates with IL-10, while ICOSLG mRNA Expression Positively Correlates with *IL12B* Expression & Patient Survival Rates.

ICOSL protein surface expression was analyzed on melanoma patient (n=30) DC subtypes and HD (n=4) by flow cytometry. Representative histograms from a patient and HD are shown for each DC subtype. Background staining was corrected with isotype (red) controls (A, left). Quantified ICOSL MFI values are shown (A, right). Patients were segregated by clinical outcomes, with intergroup significance determined using unpaired Wilcoxon rank sum test (A). mDC and AdV/DC ICOSL levels positively correlate with IL-10 levels (n=22) (B). Microarray and qPCR analysis of *ICOSLG* transcript levels in patient DC (n=33, iDC, mDC, AdV/DC) (C). Patients were segregated by clinical outcomes, with intergroup significance determined using unpaired Kruskal-Wallis one-way ANOVA (C, left and right

panels) or paired student t-test (one-tailed) (C, middle panel). Kaplan-Meier (KM) curves reveal iDC mRNA levels of *ICOSLG* are associated with OS and PFS in patients (n=33) (D). AdV/DC *ICOSLG* mRNA expression positivity correlates with *IL12B* mRNA expression in favorable clinical outcome patients (E). Correlations were calculated using Pearson's correlation coefficients and the data was log transformed to meet normality assumptions (E). *: p value ≤ 0.05, **: p value ≤ 0.01.

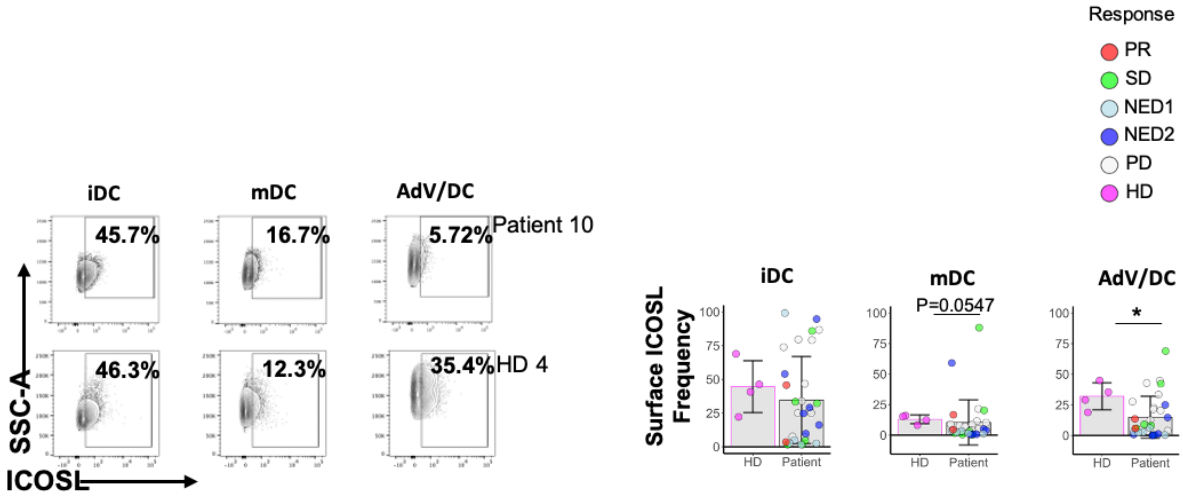

Figure 12. ICOSL Protein Expression is Reduced on Melanoma Patient DC vs HD DC.
Gating for positive frequencies of ICOSL are shown for a representative patient and HD. Quantified frequencies are also graphed for each DC subtype**.** *: p value ≤ 0.05

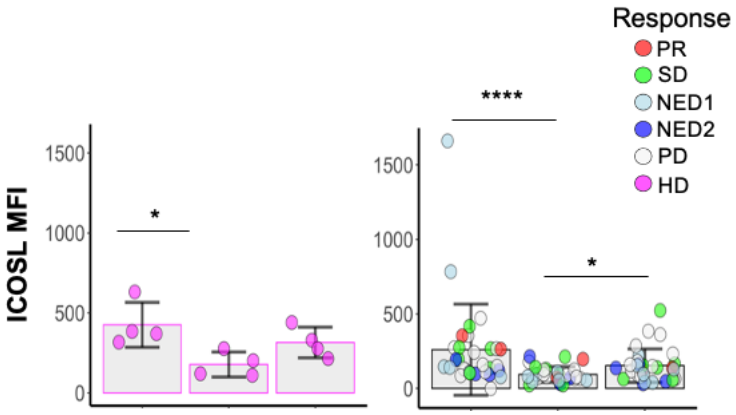

Figure 13. Patient DC Express Significantly Less Surface ICOSL Post-maturation, Compared to HD.
ICOSL protein surface expression (flow cytometry, MIF) was analyzed in HD (n=4) and melanoma patient (n=30) DC subtypes. *: p value ≤ 0.05, ****: p value≤ 0.0001.

3.5.3 ICOSLG iDC Expression Correlates with Clinical Outcome and OS in Melanoma Patients

Transcriptional profiling of patient iDC, mDC, and AdVTMM2/DC indicated that baseline expression levels of *ICOSLG* correlated with clinical outcome (Figure 11C, middle panel). Additionally, survival analysis revealed that higher *ICOSLG* expression at baseline was associated with OS and PFS in patients (Figure 11D). No direct association was observed with mDC or AdVTMM2/DC *ICOSLG* expression and survival. Interestingly, when patients were separated by clinical outcome, *IL12B* (IL12p40) expression had a significant positive association with *ICOSLG* expression (Figure 11E) in AdVTMM2/DC.

3.6 Discussion

Based on the observation that classical DC markers did not correlate with clinical responsiveness, we sought out to identify molecules and signaling pathways that impact patient T cell responses to vaccination and clinical outcomes. We initially targeted 11 co-stimulatory and co-inhibitory molecules that have either been reported or suggested to be important for antigen presentation and T cell activation. Protein expression of these checkpoint and costimulatory molecules was examined in iDC, mDC and AdVTMM2/DC. Protein surface expression of the checkpoint molecules, PD-L1, PD-L2, and CTLA-4, were significantly upregulated in DC post-maturation. PD-L1 and CTLA-4 have both been independently shown to be regulated by JAK2 and STAT1 via IFN-γ signaling(50,180), which may explain the increase in surface expression of these molecules. We have recently shown that the blockade of PD-1 during recall antigen

presentation by DC had minimal impact on induced T cell responses(181). However, *CTLA4* mRNA expression correlated negatively with *CD86, CD80* and *IL12p35* mRNA expression levels in patient DC, and was positively correlated with *IL10* mRNA. Together, these findings suggest that melanoma patient-derived DC are hypo-stimulatory and suggest areas for targeted improvement.

We identified ICOSL as being differentially expressed between patient and HD DC. Importantly, the differential surface protein expression of ICOSL observed between HD and patients was patient-specific. iDC, mDC, and AdVTMM2/DC from patients displayed lower surface expression levels of ICOSL, compared to HD. There was a gradual decline in ICOSL expression post-maturation in DC from both HD and patients, which differs from what has been previously reported for monocyte-derived DC from healthy donors(182).

Transcriptional profiling of patient DC revealed that *ICOSLG* mRNA expression overall was not significant in the differential expression analysis. However, we did observe a significant difference in *ICOSLG* mRNA expression in iDC, when patients were separated by clinical outcome. Additionally, survival analysis indicated baseline levels of *ICOSLG* mRNA expression was significantly associated with OS and PFS. These data suggest that the clinical associations observed with ICOSL, noted above, may be imprinted and due to deficiency in patient precursor cells.

4.0 ICOSL Protein Expression from Melanoma Patient DC Correlate with a Th1-skewing Phenotype, and is Associated with *In vivo* Antigen-Specific T Cell Responses and Survival Rates

4.1 Foreword

Portions of this chapter were adapted from the previous published research manuscript in Cancer Immunology Research: •Maurer, D.M., Adamik, J., Santos, P.M., Shi, J., Shurin, M.R., Kirkwood, J.M., Storkus, W.J., Butterfield, L.H. Dysregulated NF-κB-dependent ICOSL Expression in Human Dendritic Cell Vaccines Impairs T Cell Responses in Melanoma Patients. Cancer Immunology Research, 2020.

4.2 Introduction

The data in the previous chapter highlighted that melanoma patients have significantly less ICOSL protein surface expression on their DC, compared to HD counterparts. Additionally, protein surface expression of ICOSL significantly negatively correlated with IL-10 secretion levels. The transcriptional profiling of *ICOSLG* revealed an increase in mRNA expression post-maturation and viral transduction, which is the inverse of what was observed at the protein level. It was hypothesized that post-translational modifications of ICOSL protein, such as shedding, was responsible for the decrease in cell surface expression of this molecule on DC. ICOSL-specific ELISA assays were used to measure soluble ICOSL (sICOSL) in cell culture supernatants

collected from the *in vitro* recapitulation experiments discussed in Chapter 3. Importantly, *ICOSLG* mRNA expression at baseline positively correlated with survival rates and clinical outcome in patients, further supporting the possible functional importance of human DC.

Overall, these data indicate that ICOSL might be functionally important for the generation of optimal anti-tumor immune responses as a consequence of specific vaccination. It was therefore hypothesized that ICOSL protein expression from melanoma patient DC would correlate with *in vivo* antigen-specific immune responses and a Th1-skewing phenotype. To investigate this, IFN-γ ELISPOT assays and Luminex assays (measuring levels of secreted chemokines and cytokines) were used to assess specific T cell responses against Tyrosinase, MAGE-A6, and MART-1 post-vaccination.

4.3 Materials & Methods

Soluble ICOSL ELISA. Soluble ICOSL concentrations were determined using the Human B7-H2 Duo Kit ELISA (R&D #DY165-05) and the DuoSet ELISA Ancillary Reagent Kit 2 (R&D #DY008). R&D company protocols were followed. Cell culture supernatants were diluted at either a 1:5 ratio (AdV/DC supernatants) or 1:2 ratio (mDC supernatants). All standards and samples were run in triplicate. Absorbance readings were read using the Spectramax 340PC Microplate Reader (Molecular Devices). The concentrations of the standard controls were used to generate a standard curve using SoftMax Pro Software (Version 4). Sample concentrations were determined by interpolating absorbance readings of samples to the generated standard curve.

Clinical Comparison Groups. Please refer to "Materials & Methods", Chapter 3, page 38.

Statistical Analysis. Please refer to "Materials & Methods", Chapter 3, page 38.

4.4 Results

4.4.1 sICOSL Levels from Patient mDC are Associated with Survival Rates in Patients and Correlate with Th1 Polarizing Chemokines

The transcriptional analysis of patient DC mentioned above indicated baseline levels of *ICOSLG* increased post-maturation (Figure 11C, right and left panels), which was in contrast to the ICOSL surface protein expression. Therefore, post-translational processing of ICOSL in DC, such as shedding, was investigated. sICOSL levels were detected in patient and HD DC culture supernatants. Interestingly, sICOSL levels increased significantly post-maturation, compared to iDC levels, in patient cells (Figure 14A), which might explain the differences observed between mRNA expression and protein expression of ICOSL. Additionally, sICOSL levels from patient mDC correlated with clinical outcome (Figure 14A). No significant changes were observed in sICOSL levels from HD DC, post-maturation (Figure 14B). Survival analysis comparing sICOSL levels from patient mDC revealed higher production of sICOSL was associated with longer OS and PFS rates (Figure 14C). Additionally, sICOSL secretion from patient mDC significantly correlated with the Th1 polarizing and effector T cell recruiting chemokines, MIP-1α and CCL9 (Figure 14D). sICOSL was also detected 24hrs post-viral transduction in AdVTMM2/DC supernatants from both HD and patients (Figure 15). It is important to note that there was a washout

period after viral transduction, so the levels of sICOSL detected in AdVTMM2/DC should not be viewed as the “net total”. We calculated cumulative totals (mDC + AdV/DC sICOSL levels) to estimate the total of sICOSL produced from day 7 AdV/DC for each patient/HD.

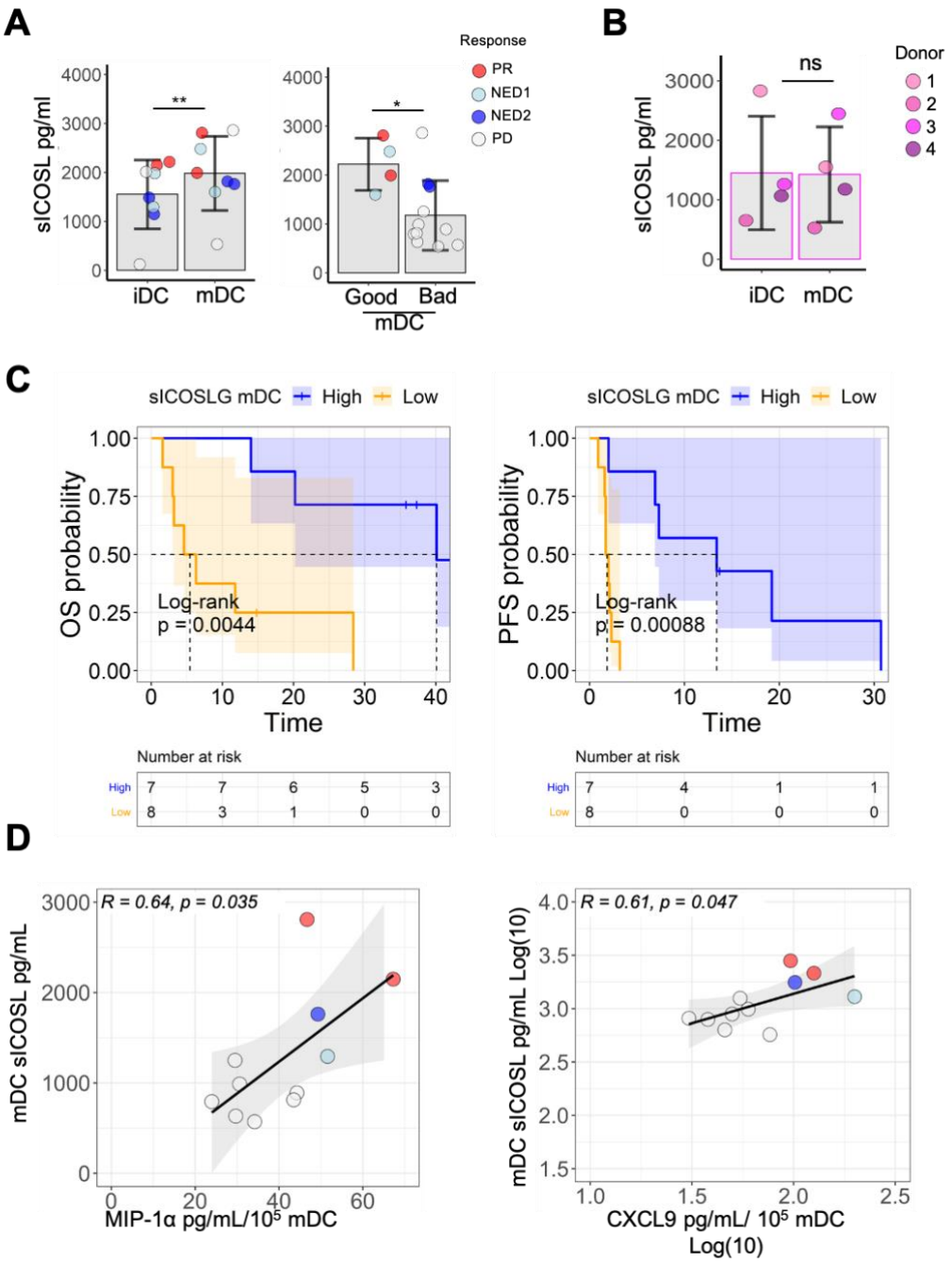

Figure 14. sICOSL Correlates with Favorable Clinical Outcomes, Th1 chemokines, and Survival Rates in Patients.

Soluble ICOSL (sICOSL) levels were determined in patient (n=16) matched pairs (n=8) (iDC and mDC, panel A (left)) and nonmatched (n=16, panel A (right)) DC culture supernatants using a specific ELISA. sICOSL of HD was determined in matched pairs (n=4, panel(B)). Patients were segregated by clinical outcomes, with intergroup significance determined using unpaired (A, left panel)) or paired (A, right panel)) Wilcoxon rank sum tests. KM curves reveal mDC sICOSL levels correlate with overall survival and PFS in patients (n=15) (C). The log-rank p value is indicated on the KM plot (C). mDC sICOSL levels positively correlate with the Th1 chemokines, MIP-1α

and CXCL9 (n=11) (D). Correlations were calculated using Pearson's correlation coefficients (D). The data was log transformed to meet normality assumptions (D, right panel). *: p value ≤ 0.05, **: p value ≤ 0.01, ns= not significant.

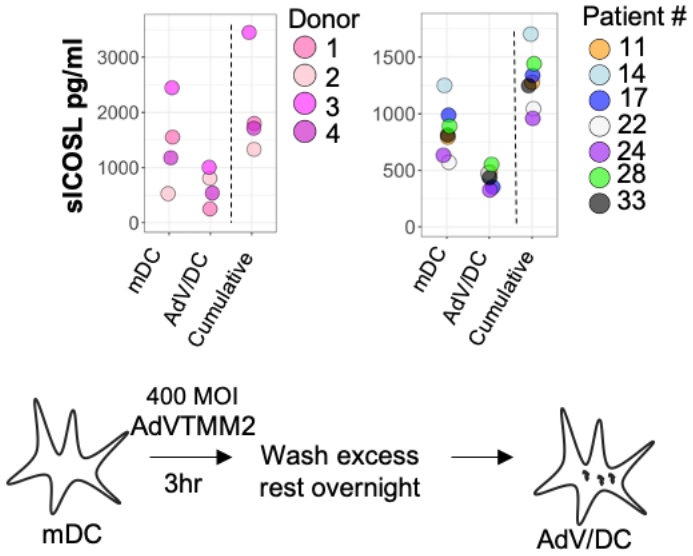

Figure 15. Patient and HD AdVTMM2/DC Secrete sICOSL.
sICOSL levels were determined in patient (n = 7) or HD (n=4) matched pairs mDC & AdV/DC culture supernatants using a specific ELISA. Due to a washout step following viral transduction, the levels of sICOSL detected in AdVTMM2/DC do not represent "net total". We calculated cumulative totals (mDC + AdV/DC sICOSL levels) to estimate the total of sICOSL produced from day 7 AdV/DC for each patient/HD

4.4.2 ICOSL Surface Protein Expression on AdVTMM2/DC is Associated with *In vivo* Antigen -Specific T Cell Responses and sICOSL Correlates with Aggregate Vaccine-induced T cell Responses

Once we observed the correlations between ICOSL expression and patient survival rates, we hypothesized that ICOSL expression was potentially important for generation of optimal immune responses. ICOSL surface protein expression on patient AdVTMM2/DC was positively associated ($p = 0.002$) with the ability of these APCs to induce specific $CD8^+$ T cell responses

against Tyrosinase *in vivo* (Figure 16A). In addition, increased levels of sICOSL positively correlated with the magnitude of aggregate vaccine-induced $CD8^+$ T cell responses (Figure 16B), suggesting the functional importance of sICOSL in anti-tumor immunity. Calculated hazard ratios determined sICOSL was a positive predictive prognostic factor for OS and PFS in these patients, while surface ICOSL on AdVTMM2/DC was a positive predictive prognostic factor only for OS (Table 3). Together, these data suggest ICOSL might be important for antigen-specific T cell responses.

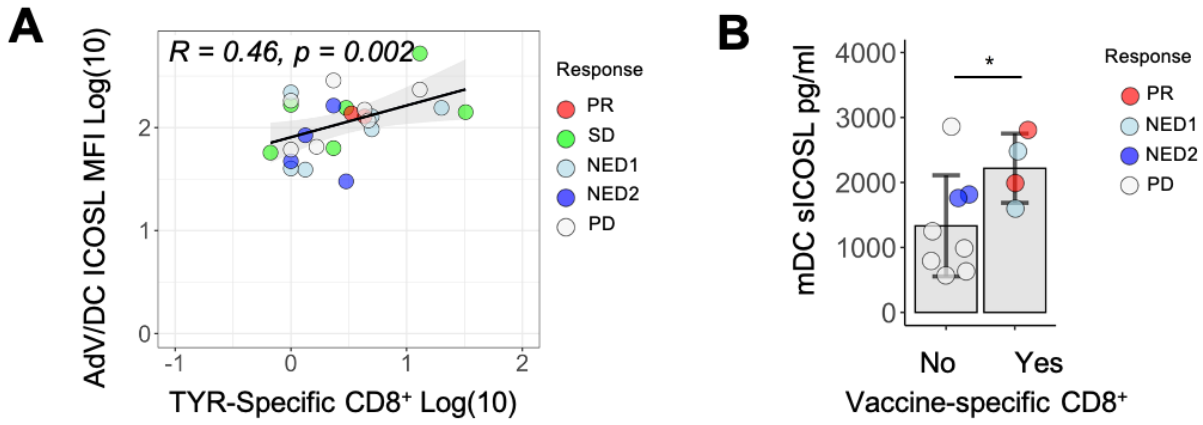

Figure 16. ICOSL Surface Protein Expression on Patient AdV/DC and sICOSL from Patient mDC are Associated with *in vivo* Antigen-specific T cell Responses.
ICOSL protein surface expression on AdV/DC correlates with *in vivo* vaccine-specific Tyrosinase $CD8^+$ responses (determined using IFN-γ ELISPOT assays) (n=25). The data was log transformed to meet normality assumptions. Pearson's R correlation was used to determine the correlation significance (A). ICOSL detected in supernatants from patient mDC correlated with bulk tumor-associated $CD8^+$ T cell responses in patients (n=12). Patients were segregated by clinical outcomes, with intergroup significance determined using paired student t-tests (B). *: p value ≤ 0.05

Table 3. sICOSL is a Prognostic Index for Extended Overall Survival and Progression Free Survival of Melanoma Patients.
Univariate Cox regression analysis for sICOSL protein levels (n=15) or surface ICOSL MFI values (n=30) from baseline mDC culture supernatants or mDC and AdV/DC cells, respectively. The hazard ratios, significance values, and 95% Confidence Intervals for OS and PFS are listed.

Endpoint	Factor	Cell Type	HR	95% CI for HR	p
OS	sICOSL	mDC	1	(0.082-0.81)	0.02
	ICOSL MFI	mDC	0.66	(0.30-1.47)	0.312
	ICOSL MFI	AdV/DC	1.72	(1.18-2.45)	0.00452
PFS	sICOSL	mDC	1	(0.22-1.01)	0.053
	ICOSL MFI	mDC	1.33	(0.68-2.60)	0.409
	ICOSL MFI	AdV/DC	1.32	(0.96-1.81)	0.088

4.5 Discussion

The increase of mRNA expression of *ICOSLG* post-maturation in patient cells suggested ICOSL might be shed from DC. ELISA assays revealed that melanoma patient and HD cells secrete ICOSL at baseline, post-maturation, and viral transduction. The levels of sICOSL remain relatively unchanged post-maturation, compared to baseline from HD. However, patient sICOSL levels increase post-maturation.

While it has been previously reported ICOSL expression on activated APCs plays a critical costimulatory role for T cell activation(182), the physiological role for soluble form of ICOSL is not well understood. In recent studies, plasma sICOSL was significantly increased in patients with acute pancreatitis and its elevated expression was associated with disease severity in patients with systemic lupus erythematous(183,184). Significant positive correlations between sICOSL levels and antigen-specific $CD8^+$ T cell responses and survival rates in melanoma patients were observed. Additionally, higher levels of sICOSL from patient mDC significantly correlated with the Th1

chemokines, MIP-1α and CCL9. Moreover, we have shown continuous production of sICOSL by HD and patient AdVTMM2/DC. In addition to the soluble data, it was observed that surface expression on AdVTMM2/DC significantly correlated with vaccine-induced Tyrosinase $CD8^+$ T cell responses. In all, these data support the importance of cell surface, as well as secreted forms of ICOSL, as biomarkers of the clinical efficacy of DC vaccination in patients with melanoma.

5.0 ICOSL Protein Expression is Critical for the Priming and Cytotoxic Capacity of Antigen-Specific T Cells

5.1 Foreword

Portions of this chapter were adapted from the previous published research manuscript in Cancer Immunology Research: •Maurer, D.M., Adamik, J., Santos, P.M., Shi, J., Shurin, M.R., Kirkwood, J.M., Storkus, W.J., Butterfield, L.H. Dysregulated NF-κB-dependent ICOSL Expression in Human Dendritic Cell Vaccines Impairs T Cell Responses in Melanoma Patients. Cancer Immunology Research, 2020.

5.2 Graphical Summary

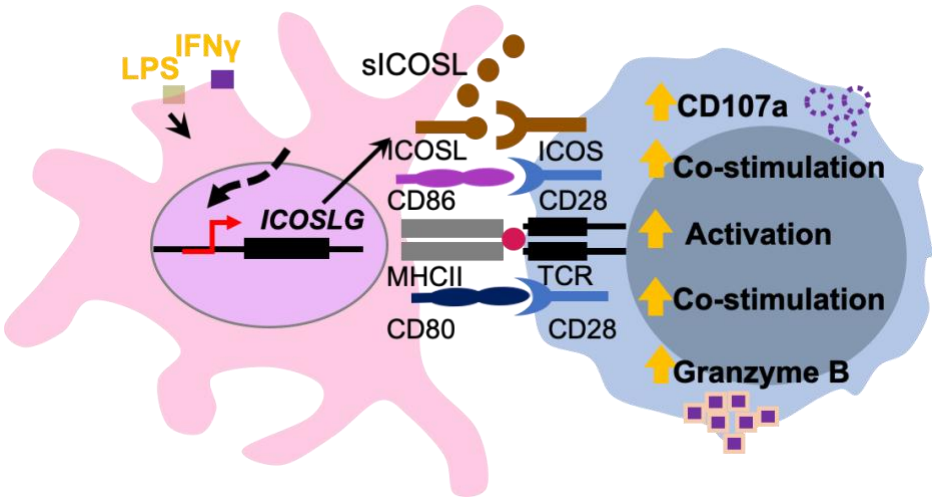

Figure 17. Graphical Summary for "ICOSL Protein Expression is Critical for the Priming and Cytotoxic Capacity of Antigen-specific T cells".

5.3 Introduction

The positive linear associations observed between ICOSL and patient $CD8^+$ antigen-specific T cell responses, as well as survival rates, implicated ICOSL as having potential functional importance in DC-mediated (cross)priming of antigen-specific T cell responses *in vivo.* Additionally, use of publicly-available datasets identified a significant positive association with *ICOSLG* expression and $CD8^+$ T cell infiltration at sites of metastasis in cutaneous melanomas, which further supports the possible importance of ICOSL in activating T cell responses (Figure 18A-B).

To determine if the level of ICOSL expression on DC was critical for the initiation of T cell activation (priming) or for recall responses (boosting) *in vitro*, a cytomegalovirus (CMV) pp65 antigen model was chosen. mDC were split into three conditions (mDC negative control, IgG control group, or α-ICOSL-treated group) and stimulated with CMV peptide before being cocultured with autologous T cells. Responder T cells were restimulated after seven days. Effector T cell cytotoxic activity was determined by T cell CD107a and granzyme B protein expression assays.

A

Primary Lesion: T cell CD8+ CIBERSORT in SKCM-Primary (n=103):

	se(coef)	HR	95%CI	p.value
CD8+ T cell	1.638	0.027	(0.001-0.664)	0.027
ICOSLG	0.234	0.932	(0.59-1.475)	0.765

Metastasis: T cell CD8+ CIBERSORT in SKCM-Metastasis (n=368):

	se(coef)	HR	95%CI	p.value
CD8+ T cell	0.727	0.102	(0.025-0.424)	0.002
ICOSLG	0.066	0.844	(0.742-0.961)	0.01

Primary Lesion + Metastasis: T cell CD8+ CIBERSORT in SKCM (n=471):

	se(coef)	HR	95%CI	p.value
CD8+ T cell	0.672	0.092	(0.025-0.343)	0
ICOSLG	0.062	0.832	(0.737-0.94)	0.003

B

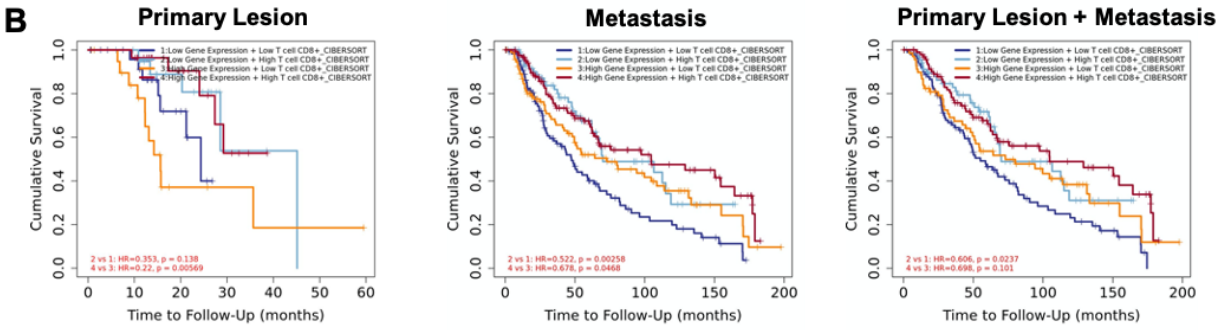

Figure 18. Datasets for cutaneous melanomas (SKCM) suggest ICOSLG expression is important for CD8+ T cell infiltrate in primary lesions and metastasis.

Cox proportional hazard model for $CD8^+$ T cell infiltration and ICOSLG expression in SKCM tumors (A). KM curves for the corresponding immune infiltrates in SKCM (both primary tumor and metastasis). The $CD8^+$ T cell infiltration and *ICOSLG* gene expression are divided into low and high levels. The hazard ratio and p value for Cox model and the log-rank p value indicated on the KM plot (B).

5.4 Materials & Methods

Detection of IgM and IgG Antibodies against CMV in HD Serum. The Bioplex 2200 System and Infectious Disease Panel (BioRad) were used to detect antibodies against CMV in HD serum collected from whole blood. Testing was performed according to the manufacturer's instructions using the BioPlex ToRC IgG and IgM kits on the BioPlex 2200 analyzer (Bio-Rad). The BioPlex used a total input volume of 5 µL serum or plasma for the analytes. Following flow cytometric analysis, the data were initially calculated in relative fluorescence intensity (RFI) and were then converted to a fluorescence ratio (FR) using the internal standard bead. The FR was compared to an assay-specific calibration curve to determine analyte concentration in antibody index units (AI). The interpretive criteria were established by the manufacturer, and results were defined as negative (≤0.8 AI), equivocal (0.9 to 1.0 AI), or positive (≥1.1 AI). The BioPlex 2200 Software Version 4.2. was used for all calculations.

ICOSL *In vitro* Function Assays. HD PBMCs were purified by Ficoll-hypaque gradient centrifugation (GE Healthcare - #17144022). $CD14^{+}$ monocytes were selected using CD14 microbeads (Miltenyi Biotec #130-050-201) and DC were generated as outlined above. Autologous $CD14^{neg}$ cells were cryopreserved in 10% (v/v) DMSO (Protide Pharmaceuticals, Inc., Catalog #PP1400) + 90% (v/v) human serum (Gemini Bio Products, Catalog #100-512) for later use. Day 5 immature DC cultures were split into 2 fractions: half of the cells were frozen for future use and the other half were matured as outlined about. Following 24h maturation, DC were pulsed with a CMV pp65 peptide pool (15 mer peptides, with 11 amino acid overlap; total 2ng per peptide added) (Miltenyi Biotec #130-093-435) for 2h at 37°C. The cells were then washed and split into three groups: negative control (mDC alone), IgG-treated control (10 µg/mL; eBioscience, Catalog

16-4714-82), or an α-ICOSL-treated group (10 μg/mL; eBioscience, Catalog #16-5889-82). DC were incubated with nothing or the respective antibodies for 3h at 37°C in AIMV media. Following incubation, DC were cocultured with autologous CD14neg (i.e. T cell-enriched) cells (at a 1:10 ratio) in AIMV media and 5% human serum for 7 days. rhIL-7 (10 ng/ml final concentration; Sigma-Aldrich) was added to the co-culture on day 1, with rhIL-15 (10 ng/mL final concentration; Sigma-Aldrich, Catalog # IL013) added on day 4. On day 7 of the coculture, activated T cells were harvested, counted, and a viability test performed using trypan blue. Cryopreserved autologous iDC were thawed, pulsed with the CMV peptides (2 ng per peptide added, please see above) and cocultured with activated autologous T cells (at a 1:10 ratio) for seven days. Responder T cells were restimulated in an identical manner, with rhIL-15 added every 2-3 days (10 ng/mL final concentration). Seven days after boosting, T cell function was assessed. T cells were harvested, counted, and each group (T cells pulsed with mDC control, IgG-treated control, or an α-ICOSL-treated DC), were split into 4 stimulation groups: No stimulation (responder T cells alone), Negative Control (Non-pulsed DC + responder T cells), Positive Control (T cells stimulated with PMA(20ng/mL; Sigma-Aldrich, Catalog #P8139) and Ionomycin (1 μg/mL; Sigma-Aldrich, Catalog #I0634)), and CMV peptide pulsed (CMV pulsed DC + responder T cells (at a 1:10 ratio)). For each condition, a CD107a antibody or an isotype control was added. Cells were stimulated for 5hrs at 37°C. CD107a expression was determined using FACS analysis. MFI was determined after subtracting isotype control values from the stained samples. A 2% threshold was used to determine positive staining, compared to isotype controls. CD107a MFI values for the negative control was subtracted from the MFI of the CMV experimental group to determine true CD107a staining. Because CD8 and CD4 molecules are downregulated on the T cell surface for several days after antigen-specific activation, $CD3^{+}CD4^{dim}$ or $CD3^{+}CD8^{dim}$ cells were gated for subsequent

assessment of CD107a expression. A Zombie Aqua Dye was used to confirm viability (Figure 19A-D). Culture supernatants were collected on day 7 (time of boost), day 9 (2 days after boosting), day 11 (4 days after boosting) and day 16 (7 days after boosting) for analysis of secreted products in ELISA or Luminex assays.

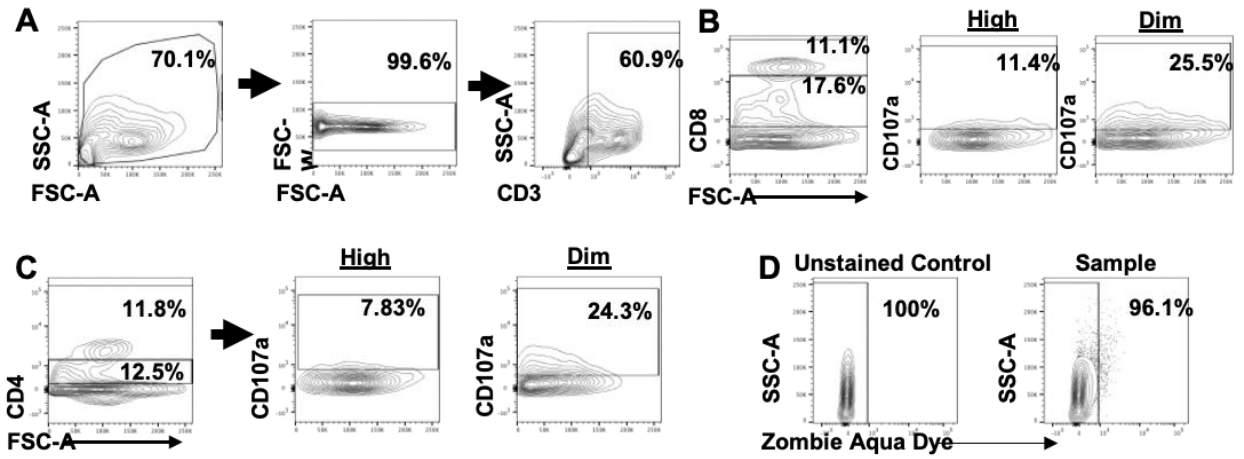

Figure 19. Gating Strategies used for *In vitro* T cell assays.
$CD8^{dim+}$ and $CD4^{dim+}$ T cells were selected to assess functional T cell interactors in flow cytometry analyses. The following gating strategy was used to analyze DC-activated T cells from in vitro co-cultures: Lymphocyte cells were selected based on an FSC vs SSC gate, with $CD3^+$ single-cells selected for consequent analysis (A). $CD8^+$ and $CD4^+$ T cells were then separated into high (resting, non-activated) and dim (recently activated) expressor populations (B-C). The CD4/CD8 dim populations were then assessed for expression of CD107a as a surrogate marker of their cytotoxic potential. DC viability was monitored by flow cytometry using zombie aqua dye (to validate data obtained by visual inspection based on trypan blue exclusion) (D).

Antibodies. The following antibodies were used for ICOSL functional assays: FITC Mouse Anti-Human CD3 (HIT3α; BD Biosciences #555339), APC-Cy7 Mouse Anti-Human CD4 (RPA-T4) (BD Biosciences #557871), PE-Cy7 Mouse Anti-Human CD8 (RPA-T8) (BD Biosciences #557746), PE Mouse Anti-Human CD107a (H4A3) (BD Biosciences #555801), PE Mouse IgG1, κ Isotype Control (MOPC-21) (BD Biosciences #559320), CD275 (B7-H2) Monoclonal Antibody (MIH12) (eBioscience #16-5889-82), and Mouse IgG1 kappa Isotype Control(eBioscience#16-4714-82).

Statistical Analysis. Please refer to the "Materials & Methods" section, Chapter 3, page 38. In addition, associations between ICOSLG expression and CD8+ T-cell infiltrates across cutaneous melanoma tumors were evaluated using publicly available software Timer 2.0. (http://timer.cistrome.org/).

Clinical Comparison Groups. Please refer to the "Materials & Methods", Chapter 3, page 38.

5.5 Results

5.5.1 DC-Expressed ICOSL is Critical for the Priming of Antigen-specific T cell Responses

HD were identified as CMV-naïve or CMV-experienced based on serum antibody (IgG, IgM) reactivity against CMV. Autologous mDC were cultured with or without a blocking ICOSL mAb and pulsed with a CMV pp65 peptide pool. $CD4^+$ and $CD8^+$ T cells primed with ICOSL-blocked DC expressed less CD107a and produced significantly less granzyme B than T cells primed using ICOSL expressing DC (Figure 20A). In marked contrast, we observed no impact for ICOSL antibody-mediated antagonism on T cell responses to CMV antigen on recall responses (Figure 20B). Since activation, measured by CD107a expression, of recall responses did not appear to be influenced by ICOSL blockade, granzyme B activity was not measured for these. This data suggests that ICOSL expression on DC plays a role in optimal (cross)priming of effector $CD8^+$ and $CD4^+$ T cells and does not appear to play a dominant role in modulating memory/recall T cell responses.

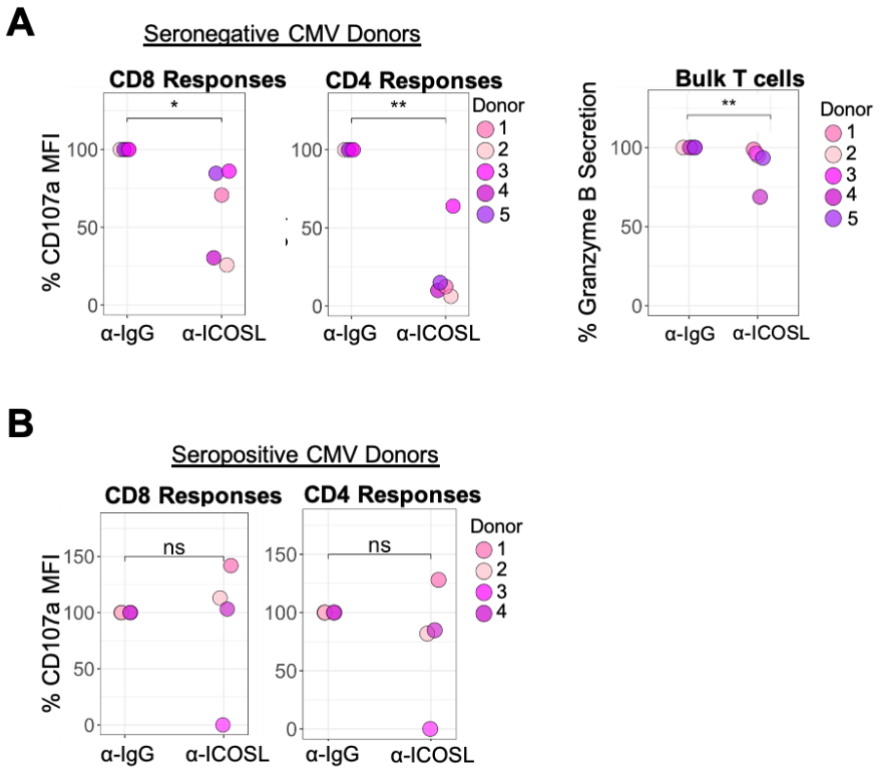

Figure 20. ICOSL on DC is Critical for Their Ability to (Cross)prime Antigen-specific T cell responses *In vitro*. CD107a MFI levels from CMV-specific T cells when primed (C) (n = 5) or boosted (D) (n = 4) with autologous mDC previously treated with blocking α-ICOSL (10 μg/mL) antibody or an IgG control. Granzyme B secretion levels from CMV-specific T cells when primed with autologous mDC previously treated with blocking α-ICOSL (10 μg/mL) antibody or an IgG control (n=5) (C). Data is displayed as normalized percentages against the IgG control and unpaired Wilcoxon rank sum test was used to determine significance (A,B). *: p value ≤ 0.05, **: p value ≤ 0.01, ns= not significant**.**

5.6 Discussion

We were technically unable to assess the importance of ICOSL in generating immune responses using patient samples, as the circulating T cells were mainly memory T cells (73.7% $CD8^+$, 91.9% $CD4^+$) or exhausted effector T cells (25.7%$CD8^+$, 6.6% $CD4^+$)(175). To properly investigate this paradigm, we employed a CMV-based *in vitro* vaccine model, assessing T cell expression of granzyme B and CD107a as effector cell cytotoxic activity. $CD8^+$ T cells from CMV seronegative donors primed with antigen-loaded DC pretreated with an anti-ICOSL blocking

antibody were significantly impaired in their ability to differentiate into effector T cells. Notably, the DC expressed high surface levels of the costimulatory molecule, CD86, stressing the important early role for DC-expressed ICOSL in initiating antigen-specific responses from antigen-naïve T cells.

In the context of melanoma, $CD4^+$ cytotoxic T cells have been isolated from patients in high frequencies and these cells can kill autologous $MHCII^{high}$ melanoma tumor cells. Additionally, murine models have indicated antigen-specific $CD4^+$ T cells can aid in the expansion of infiltrating $CD8^+$ T cells(185). Murine and human studies have both shown that anti-PD1 and anti-CTLA-4 treatment increases the cytotoxic activity of these cells, indicting an important role for $CD4^+$ T cells in anti-tumor immunity(186,187). In the CMV-based *in vitro* vaccine model, $CD4^+$ T cells primed with pretreated anti-ICOSL antigen loaded DC were functionally impaired. These data reveal that ICOSL is critical for the priming of cytotoxic antigen-specific $CD4^+$ and $CD8^+$ T cells, and both $CD4^+$ and $CD8^+$ T cells impact anti-tumor immunity in melanoma patients. This suggests that increasing expression of ICOSL on patient DC may improve antigen-specific vaccine responses in cancer patients.

6.0 Canonical NF-κB Signaling and ADAM10/17 Sheddase Activity are Critical for the Regulation of ICOSL Gene and Protein Expression in DC

6.1 Foreword

Portions of this chapter were adapted from the previous published research manuscript in Cancer Immunology Research: •Maurer, D.M., Adamik, J., Santos, P.M., Shi, J., Shurin, M.R., Kirkwood, J.M., Storkus, W.J., Butterfield, L.H. Dysregulated NF-κB-dependent ICOSL Expression in Human Dendritic Cell Vaccines Impairs T Cell Responses in Melanoma Patients. Cancer Immunology Research, 2020.

6.2 Graphical Summary

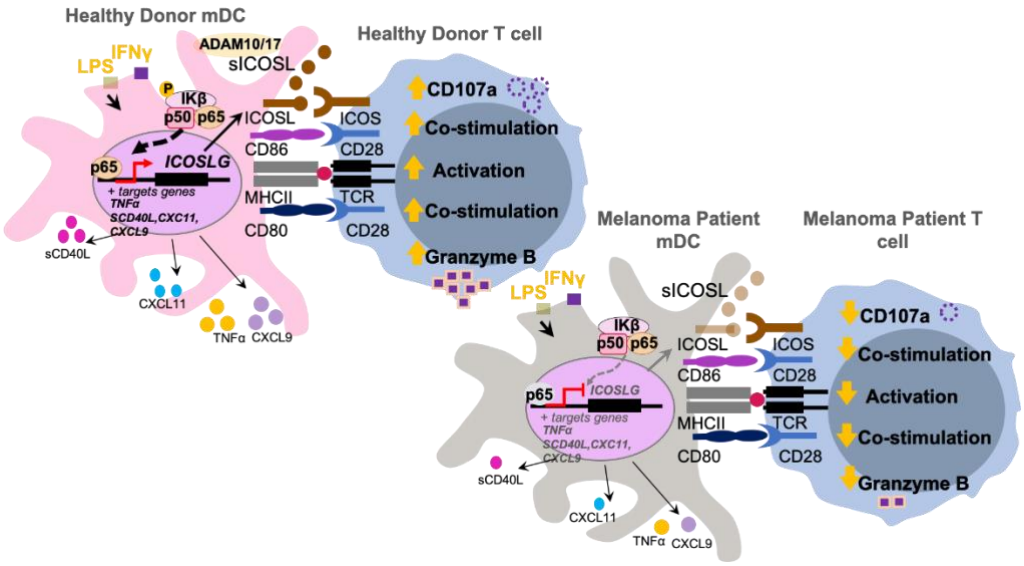

Figure 21. Graphical Summary for "Canonical NF-κB Signaling and ADAM10/17 Sheddase Activity are Critical for the Regulation of ICOSL Gene and Protein Expression in DC".

6.3 Introduction

The previous chapters have revealed that mature DC generated from melanoma patients express less cell surface ICOSL as well as sICOSL, compared to healthy donor counterparts. The work in the above chapters have highlighted that surface expression of ICOSL is critical for the priming of antigen-specific T cell responses, and that both DC surface expression and sICOSL correlate with overall survival and progression-free survival rates in patients. These data support the notion that ICOSL may represent a cogent biomarker for clinical efficiency of DC-based vaccines.

It is not yet known how ICOSL is regulated on the surface of DC. Previous literature reports suggest that *ICOSLG* expression is regulated, in part, by noncanonical NF-κB signaling in other immune cells(188). Additionally, the literature suggests that ICOSL is shed from the surface of B cells by metalloproteinases(189).

Little is understood about the regulation of ICOSL in human DC. To investigate the regulation of *ICOSLG* at the transcript levels, Ingenuity Pathway Analysis Software (IPA) was used to identify differences in activation of signaling pathways, based on gene expression, between HD and melanoma patient DC. A publicly-available HD dataset was used as a control comparator (GSE111581). It is important to note that HD and patient-derived DC were generated using analogous methodologies. Canonical NF-κB signaling was predicted to be inactivated in patient DC post-maturation. HD DC were predicted to activate canonical NF-κB signaling post maturation, consistent with numerous literature reports. Therefore, NF-κB signaling in patient cells was validated using ImageStream and its regulation of ICOSL was studied using pharmacologic inhibitors. To explore the observed difference in protein levels of ICOSL,

compared to transcript levels in patient DC, ADAM10/17 sheddase activity was investigated. Patient DC expressed both ADAM10/17 at the transcript level. The role ADAM10/17 played in ICOSL regulation was determined by the use of pharmacologic inhibitors of these metalloproteinases.

6.4 Materials & Methods

DC Microarray. Please refer to the "Materials and Methods", Chapter 3.

NF-κB Inhibition. Day 5 iDC were generated from HD and divided into the following groups: 1) iDC control (untreated), 2) stimulated with rhIFN-γ + LPS, 3) DMSO control (rhIFN-γ + LPS + DMSO) and 4) NF-κBi 15μM (rhIFN-γ + LPS + Parthenolide; Abcam #120849)). On day 5, iDC were incubated with the above reagents for 5 min at 37°C in DC media. After stimulation and/or blocking, total p65, phospho-p65, and ICOSL protein surface expression was measured by FACS analysis. A Zombie Aqua Dye was used to confirm viability.

Chromatin Immunoprecipitation (ChIP) Assay. Chromatin from mDC was analyzed using a modification of the ChIP Cell Signaling technology protocol (9005) using Micrococcal Nuclease (CST, 10011) and Magna ChIP Protein A+G Beads (16-663, Millipore). NF-κB antibody (Santa Cruz, sc-8008) was used for ChIP. Aliquots for input and non-specific IgG control samples were included with each experiment. ChIP-qPCR primers are listed below.

ICOSLG Forward – GCTTCCCAGGGCACCTAC;

ICOSLG Reverse- CTCCGGAAAGTTCGGCTCT;

ICOSLG (Exon) Forward – GAAGGAAGTCAGAGCGATGG;

ICOSLG (Exon) Reverse – GGAGCTGTTCTGTGGGATGT;

TNFα NF-κB Site Forward – TGAGCTCATGGGTTTCTCCACCAA ;

TNFα NF-κB Site Reverse – ACAACTGCCTTTATATGTCCCTGG;

TNFα (Exon) Forward – TGGGTGAAAGATGTGCGCTGATAG;

TNFα (Exon) Reverse- TTGCCACATCTCTTTCTGCATCCC

ADAM10/17 Inhibition. Day 5 iDC were generated from HD and divided into the following groups: 1) iDC baseline control, 2) mDC (rhIFN-γ + LPS 24hrs), and 3) ADAM10/17i 20μM((rhIFN-γ + LPS + Tapi-2; Tocris #6013)). On day 5, iDC were matured using rhIFN-γ + LPS alone or in the presence of Tapi-2 for 24hrs. Tapi-2 has been shown to inhibit the sheddase activity for ADAM10, ADAM17, and other metalloproteases(190,191) Cell culture supernatants were collected post-maturation for observation of sICOSL. Surface ICOSL was assessed by FACS analysis. A Zombie Aqua Dye was used to confirm viability.

Antibodies. The following antibodies were used for intracellular staining of NF-κB molecules: NF-κB p65 (D14E12) Rabbit mAb (Alexa Fluor® 647 Conjugate) (Cell Signaling #8801S), Phospho-NF-κB p65 (Ser536) Rabbit mAb (PE Conjugate) (Cell Signaling #5733S), Rabbit IgG Isotype Control (Alexa Fluor® 647 Conjugate) (Cell Signaling # 3452S), Rabbit (DA1E) mAb IgG XP® Isotype Control (PE Conjugate) (Cell Signaling #5742). The following antibodies were used for ImageStream Analysis: NF-κB p65 (D14E12) Rabbit mAb (Alexa Fluor® 647 Conjugate) (Cell Signaling #8801S), PE Mouse Anti-IκBα (Clone 25/IkBa/MAD-3) (BD Biosciences

#560818), DAPI Solution (BD Biosciences #564907). ImageStream analysis was done using the ImageStreamX Mark II (Amnis) and analyzed with IDEAS software.

Clinical Comparison Groups. Please refer to the "Materials & Methods", Chapter 3.

Statistical Analysis. Please refer to the "Materials & Methods", Chapter 3.

6.5 Results

6.5.1 NF-κB Signaling is Dysregulated in Patient DC and Targets of NF-κB signaling Correlate with Clinical Outcome

Since ICOSL expression on DC was shown to be important for optimal priming of T cells, we were interested in investigating molecular pathways responsible for the deficiency in surface expression of ICOSL on patient DC; gene expression profiles from patient iDC, mDC, and vaccines were analyzed. Differentially expressed genes in iDC and mDC from patients were then compared to HD DC.

Patient mDC exhibited profiles with dysregulation in metabolic, toll-like receptor, IL-8, and NF-κB signaling pathways (Figure 22A). Of these, the predicted dysregulation of the NF-κB pathway was of interest because the non-canonical NF-κB signaling pathway has been previously reported to regulate *ICOSLG* expression in murine B cells(188). The microarray data revealed significant increases in expression of NFKBID, an inhibitor of the NF-κB signaling pathway, in patient mDC. No changes in *NFKBID* mRNA expression was observed in HD mDC (Figure 22B).

To further investigate the NF-κB dysregulation observed in patients, inflammatory and Th1-polarizing molecules known to be regulated by NF-κB signaling were examined. Cell culture supernatants were collected after maturation of patient and HD DC. Expression of cytokines and chemokines revealed patient mDC expressed lower levels of soluble TNF-α, soluble CD40L, and CXCL9 compared to HD mDC (Figure 22C). Moreover, the level of secretion of these important molecules, as well as CXCL11 secretion levels, positively correlated with patient clinical outcomes (Figure 22C). Functional validation of dysregulation in the canonical NF-κB pathway in patient DC was confirmed using cellular imaging. HD DC showed an expected significant increase in NF-κB p65 translocation from cytoplasm into the nucleus upon *ex vivo* maturation, which was not observed for patient DC (Figure 22D-E).

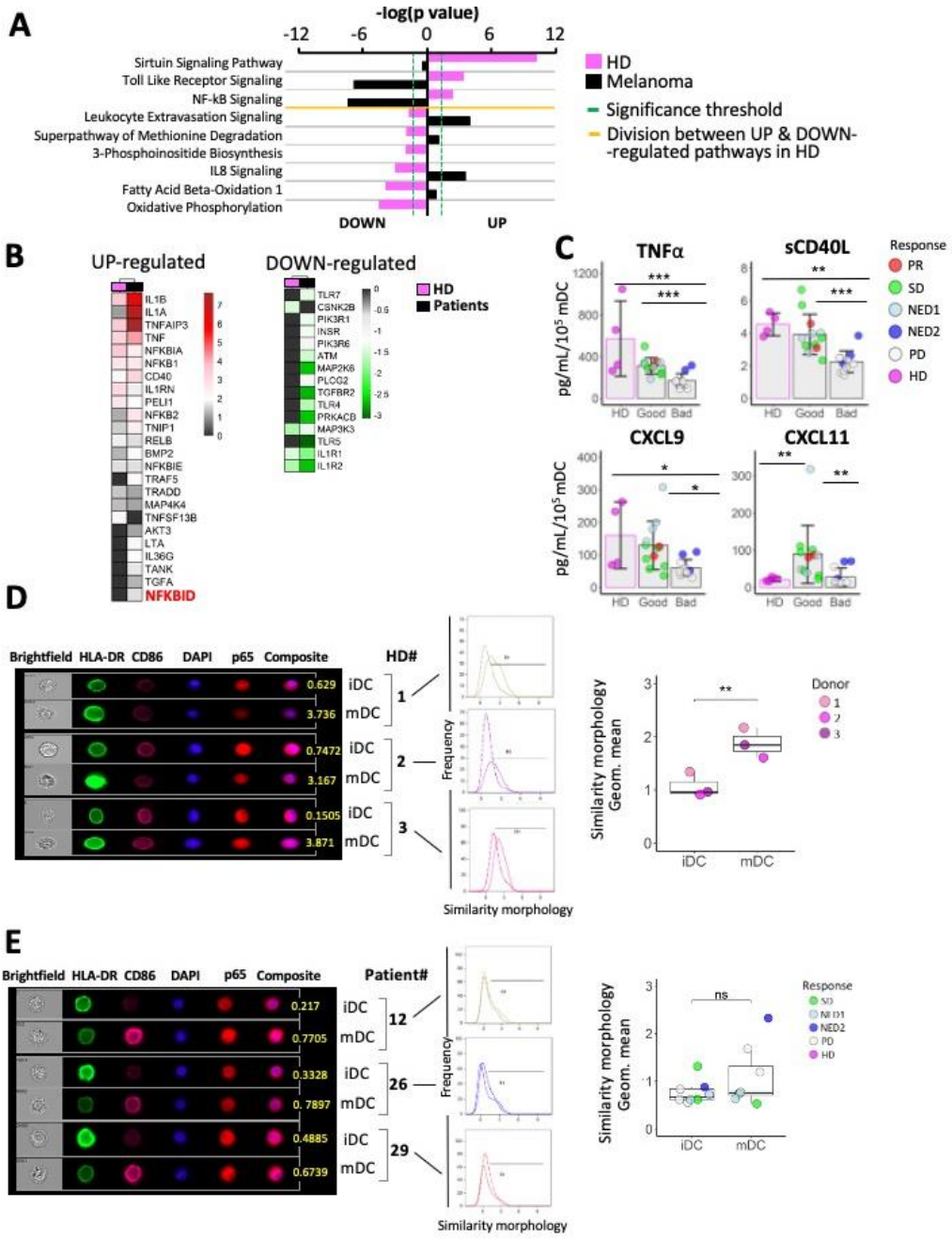

Figure 22. NF-κB Signaling is Dysregulated in Melanoma Patient mDC vs HD and Expression of NF-κB targets Correlate with Clinical Outcome.

Comparative Ingenuity Pathway Analysis of microarray data indicates that mDC from patients (n=35) exhibit differential expression of metabolic, NF-κB, and TLR signaling biomarkers when compared to mDC from HD (n=6). The -log p values were calculated for each pathway, with a -log (0.05) considered to be significant (dashed green line). Predicted calculated z scores for the indicated signaling pathways are represented as being activated (UP) or down-regulated (DOWN) (A). Depicted are heatmaps for differentially expressed NF-κB-dependent gene transcripts in patient vs. HD mDC (B). Human immune monitoring 65-Plex (Thermo-Fisher Procarta Plex) was used to analyze pro-inflammatory cytokines in cell-free supernatants harvested from HD (n=4) vs. melanoma patient (n=23) DC (C). Patients were segregated based on clinical outcomes. CXCL9 and sCD40L inter-group differences were analyzed for significance using one-way ANOVA analysis with Tukey's multiple comparison test, and TNFα and CXCL11 inter-

group differences were analyzed for significance Kruskal-Wallis one-way ANOVA with Dunnett's multiple comparison test (C). Validation of the IPA analysis using Image Stream revealed that HD DC exhibit a significantly increased degree of p65 translocation into the nucleus vs. melanoma patients DC post-maturation (D, E). Patients are segregated based on clinical outcomes, with the significance of differences between cohorts determined using matched paired student t-tests (HD panel) (D) or paired Wilcoxon rank sum test (patient data)(E) . *: p value ≤ 0.05, **: p value ≤ 0.01, ***: p value ≤ 0.001, ns= not significant.

6.5.2 NF-κB p65 is a Direct Transcriptional Regulator of *ICOSLG*

After observing operational NF-κB dysregulation in patient matured DC, we hypothesized that *ICOSLG* expression might be dependent on canonical NF-κB signaling. To investigate this, we analyzed direct binding of NF-κB p65 to the *ICOSLG* promoter region. Chromatin immunoprecipitation revealed a direct p65 binding site in the *ICOSLG* gene promoter region in HD mDC (Figure 23A & Figure 24A-B).

To further confirm the role of NF-κB on ICOSL regulation, we assessed the impact of adding the NF-κB inhibitor, Parthenolide, which directly modifies the p65 subunit by inhibiting IkB proteins(192,193), on ICOSL after stimulation with rhIFNγ + LPS (15mins). Inhibition of NF-κB activation resulted in a significant decrease in phospho-p65 levels in the Parthenolide-treated DC group (Figure 22B-C). ICOSL surface protein levels were significantly decreased in Parthenolide-treated DC compared to control DC (Figure 23B-C), supporting canonical NF-κB signaling in the regulation of ICOSL surface protein expression levels in DC.

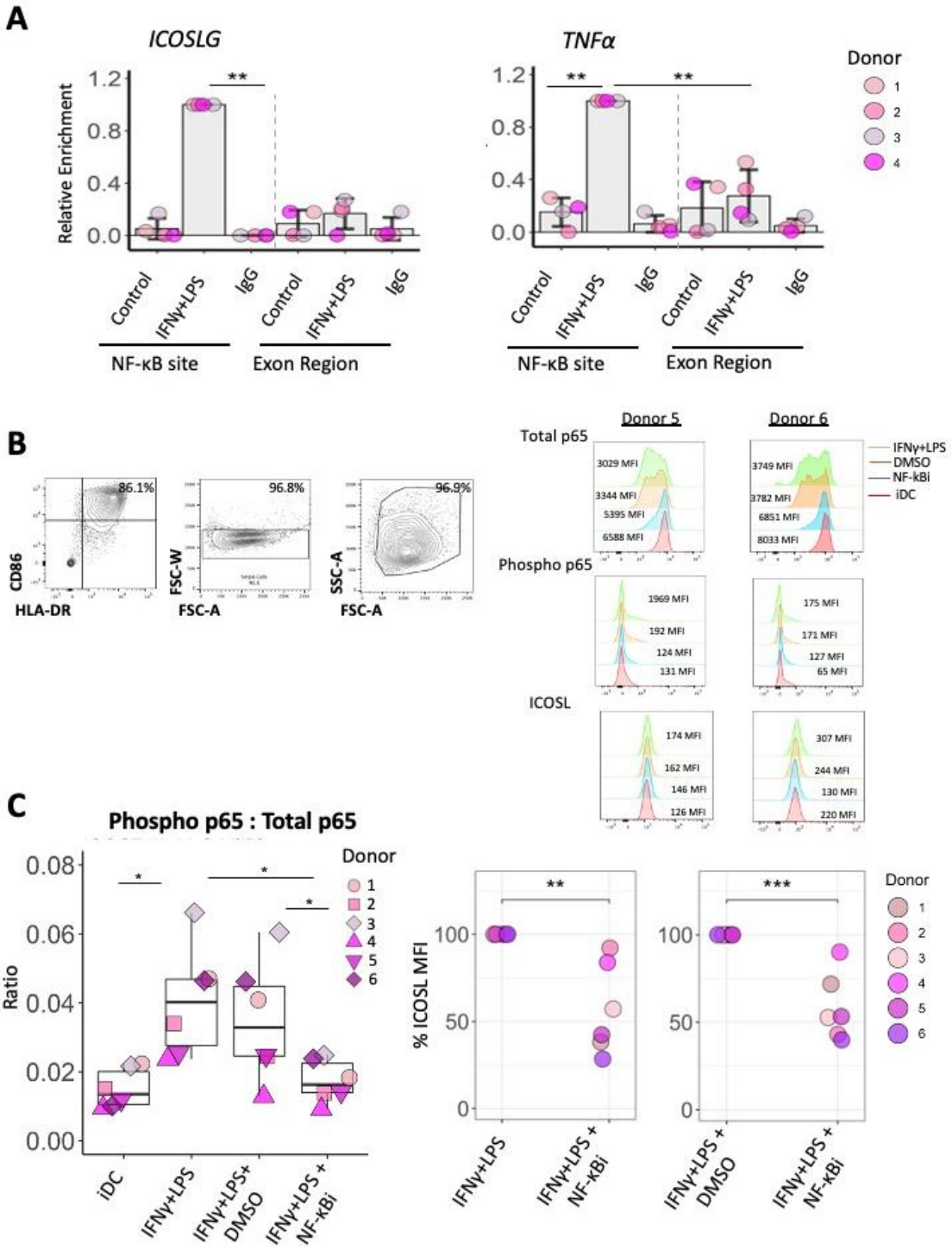

Figure 23. Canonical NF-κB Signaling Regulates ICOSL Protein Surface Expression on Human DC. Chromatin Immunoprecipitation assays performed on HD (n=4) cells revealed that NF-κB p65 binds directly to the *ICOSLG* promoter region in IFNγ + LPS treated (matured) DC by 30 min. TNFα was used as a positive control. Fold enrichment was calculated based on Ct as 2(ΔCt), where ΔCt = (CtInput – CtIP). The IgG ΔCt was subtracted from the specific antibody ΔCt to generate ΔΔCt = (ΔCtspecific Ab – ΔCtIgG) (A). ICOSL surface expression analyzed from HD DC (n=6) at baseline (day 5 iDC), stimulated with IFNγ + LPS (15 mins), IFNγ + LPS with DMSO (15 mins), or IFNγ + LPS with the NFκB inhibitor, Parthenolide (15 □M, 15 mins) (B, C). Histograms are shown from two representative

donors for total p65, phospho-p65, and ICOSL MFI values (B). Isotype antibodies were used to control for background staining. The ratio of phospho-p65 levels to total p65 levels is shown (panel C, left). ICOSL MFI values are shown for each treatment group (panel C, right). Data is displayed as normalized percentages against the positive control (IFNγ + LPS) and unpaired student t-test (two-tailed) was used to determine significance. *: p value ≤ 0.05, **: p value ≤ 0.01.

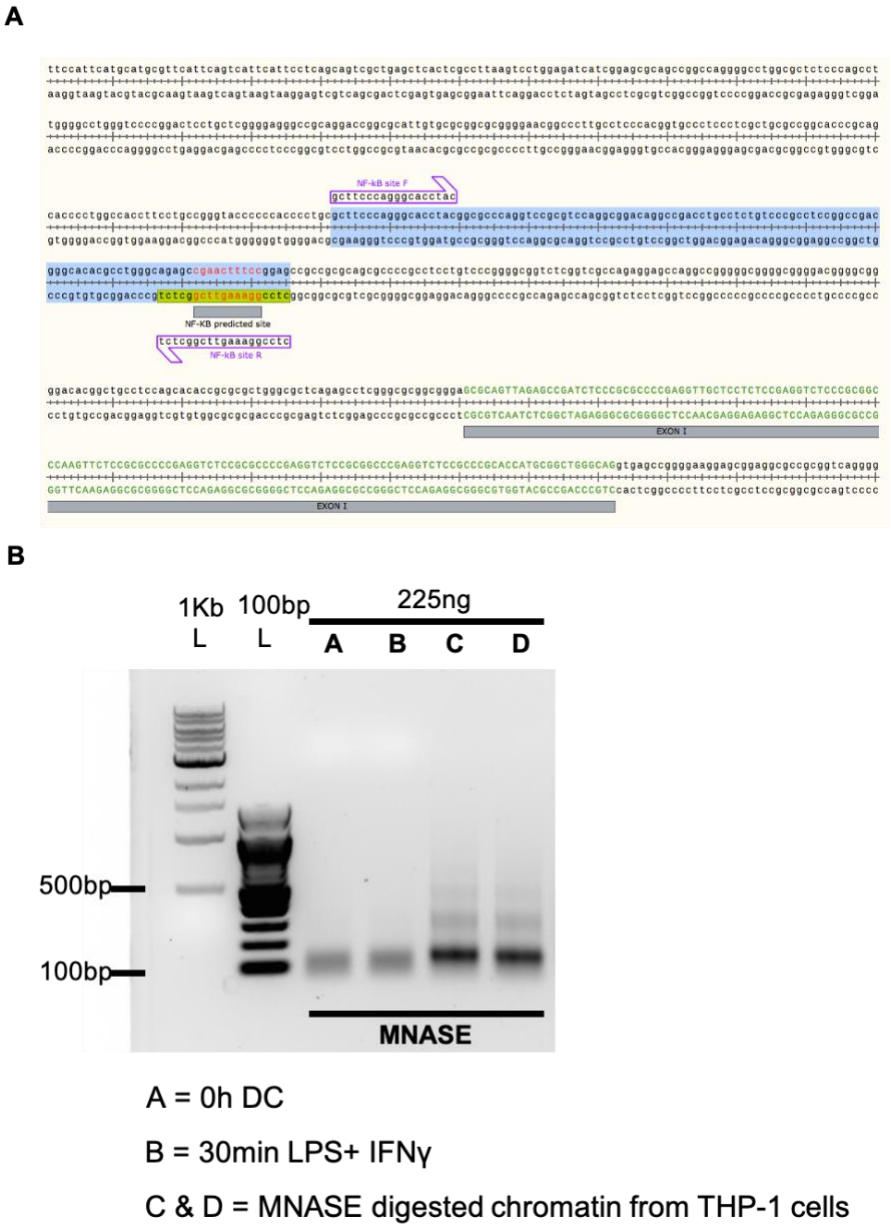

Figure 24. Primer Design and DNA Input used in Chromatin Immunoprecipitation (ChIP) Assays.
The predicted NF-κB binding site in the ICOSLG promoter is highlighted in red. Purple regions denote primer sequences used to amplify N-κB enrichment in ChIP assays. Additional primer pairs (see Methods section) targeting downstream EXON sequence was used for negative/background binding control (A). Shown is the distribution of micrococcal nuclease-digested DNA fragments from one representative donor used in the ChIP assay (B).

6.5.3 Inhibition of ADAM10/17 Sheddase Activity Stabilizes ICOSL Surface Protein Expression on Mature DC

We have shown that canonical NF-κB signaling regulates ICOSL surface protein expression. However, our data also has also suggested ICOSL is shed from the surface of DC, which correlates with clinical outcomes in patients. Our microarray data revealed that patient DC express the metalloproteases ADAM10 and ADAM17 (Figure 25A). ADAM10 is significantly reduced post-maturation, while ADAM17 expression increases (Figure 25A). To investigate the mechanisms underlying the shedding of surface ICOSL, we inhibited ADAM10/17 activity using Tapi-2, during DC maturation conditions. HD DC matured in the presence of Tapi-2 exhibited a significant increase in surface ICOSL protein expression and a decrease in sICOSL (Figure 25B-C). These data suggest that both canonical NF-κB signaling and metalloproteinase activity contribute to the steady-state regulation of cell surface levels of ICOSL in DC.

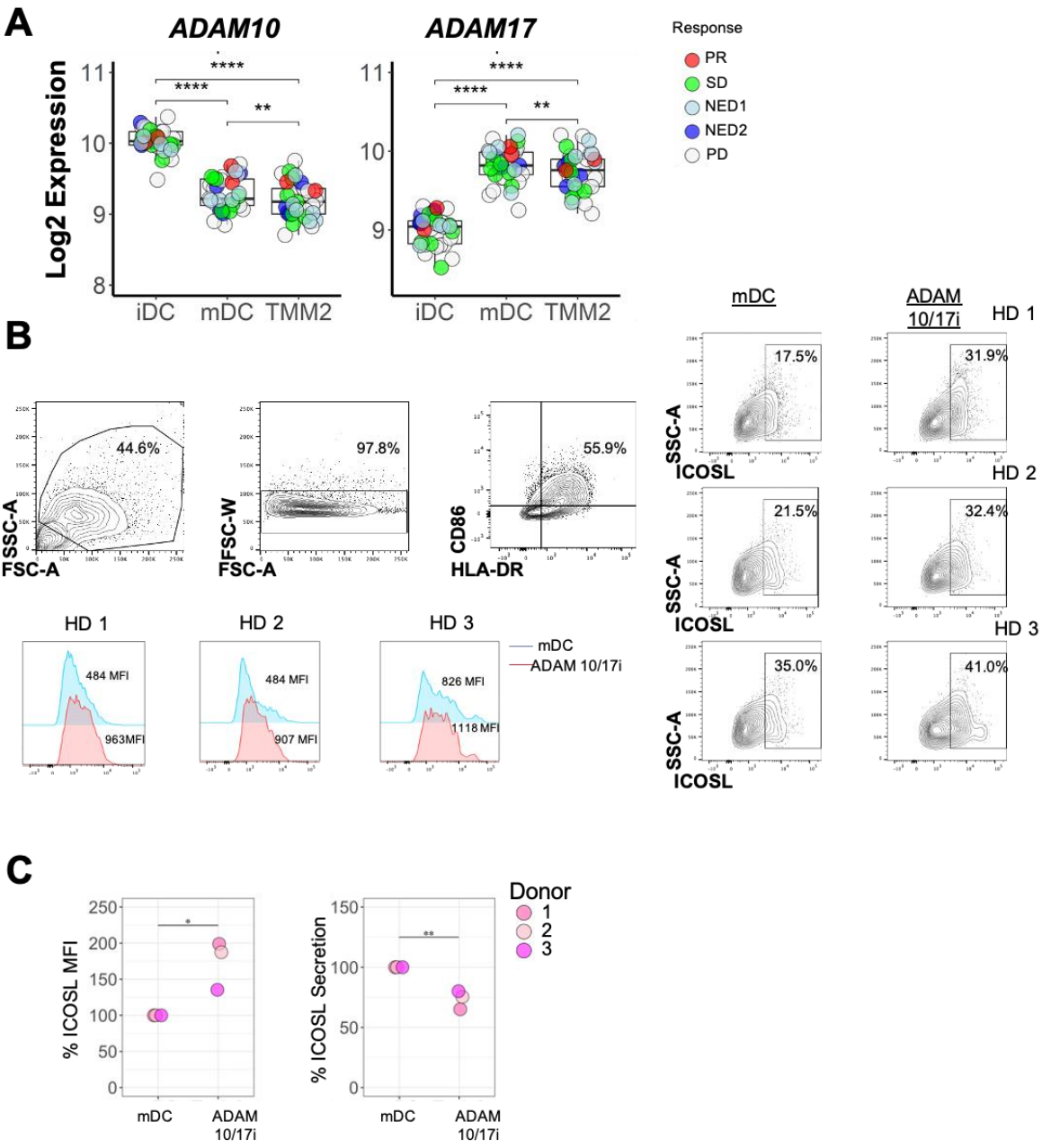

Figure 25. DC Surface Expression of ICOSL and RC-released sICOSL are Regulated in-part by the Metalloproteases, ADAM10 and ADAM17.

Log2 mRNA expression of ADAM10 and ADAM17 for iDC, mDC, and AdV/DC in melanoma patients (n=33) (A). Patients were segregated by clinical outcomes, with intergroup significance determined using one-way ANOVA. ICOSL surface expression analyzed from HD DC (n=3) at baseline (iDC), stimulated with IFNγ + LPS (24hrs), or stimulated with IFNγ + LPS with the ADAM10/17 inhibitor, Tapi-2 (20uM, 24hrs). Gating is shown from a representative HD and ICOSL frequencies and histograms are shown for mDC and Tapi-2 treated cells (B). ICOSL MFI values or sICOSL levels are shown for mDC controls and Tapi-2 treated cells (C). Data is displayed as normalized percentages against the mDC control and an unpaired student t-test (two-tailed) was used to determine significance (C). *: p value ≤ 0.05, **: p value ≤ 0.01, ***: p value ≤ 0.001.

6.6 Discussion

ICOSL has also been previously reported to be shed from B cells based on the action of the "sheddase" ADAM10. By cleaving surface ICOSL, ADAM10 modulates availability of ICOSL costimulation during humoral immune activation(189). Our microarray data revealed that patient DC express ADAM10 and significantly increase mRNA transcript levels of another metalloproteinase molecule, ADAM17, post-maturation (data not shown). Here, we have shown that inhibition of ADAM10/17 sheddase activity in HD DC increased surface expression of ICOSL and decreased sICOSL levels, revealing the importance of metalloproteinase activity in regulating ICOSL surface expression on DC. To our knowledge, the importance of ADAM10/17 sheddase activity for ICOSL regulation on human DC has yet to be reported.

Our data further revealed that ICOSL expression levels in DC are in part dictated by canonical NF-κB signaling, with p65 directly interacting with the promoter region of *ICOSLG.* To our knowledge, this regulatory pathway in DC has not been previously reported, as only the noncanonical pathway of NF-κB signaling has been suggested to regulate *ICOSLG* expression(188). We have also shown that patient mDC exhibit a decrease in canonical NF-κB signaling, as evidenced by significant reductions in nuclear translocation of p65 when compared to HD counterparts.

As predicted by dysregulation of NF-κB signaling, proinflammatory cytokine secretion was also reduced in cell culture supernatants from patient DC. CXCL9, TNFα, soluble CD40L, and CXCL11 secretion levels from mDC correlated with clinical outcome. Moreover, CXCL11 secretion from mDC seemed to be unique to melanoma patients, as CXCL11 production from HD mDC was marginal. The observed correlation with clinical efficiency indicates these molecules

may represent salient biomarkers for assessing clinical efficiency in patients. The decreased activation of the canonical NF-κB signaling pathway did not affect the maturation-induced upregulation of the costimulatory molecule CD86 on DC. This finding can be explained by CD86 regulation in human DC by RelB, which is predominately associated with the noncanonical NF-κB signaling pathway(194). In addition, complementary pathways are being activated, such as IFNγ signaling, which has also been reported to upregulate CD86 expression(195).

The comparative pathway analysis revealed that matured DC from melanoma patients have increased transcriptional expression of natural NF-κB inhibitors post-maturation. Some of these inhibitors, such as NFκBIA, are regulatory molecules that are transcriptionally activated upon NF-κB activation. Transcript levels of these molecules were increased in both patient and healthy donor cells. However, transcriptional expression of the inhibitor molecule, *NFκBID*, was only upregulated in patient DC post-maturation. This was of interest because previous studies have shown that *NFκBID* expression in DC leads to an immunoregulatory phenotype with increased secretion of IL-10(196). As stated in the above chapters, transcriptional profiling and protein analyses of patient DC have shown that melanoma patients express high levels of immunoregulatory molecules, such as IL-10 and *IDO*. Overall, these data indicate that genetic manipulation of NF-κB targets in patient DC may mitigate their immunoregulatory phenotype and lead to increased expression of costimulatory and proinflammatory molecules believed critical to the efficacy of DC-based vaccines. This dysregulation of canonical NF-κB signaling in patients may in part explain the observed reductions in ICOSL protein expressed on the surface of DC cultured from melanoma patients. Indeed, we now show that NF-κB signaling, via both the canonical and noncanonical pathways, is important for DC immunogenicity and the anti-tumor efficacy of DC-based vaccines.

7.0 Conclusion

7.1 Summary & Future Directions

DC-based vaccination for the treatment of solid cancers have been shown to be safe and immunogenic in the clinic(129). However, the overall clinical response rate remains low(129). The main objective of this thesis was to identify and analyze DC vaccine gene expression profiles that correlate with potent vaccine-antigen-specific T cell immune responses and a favorable clinical outcome. By understanding the mechanisms and proteins involved in optimal DC functionality, we will be able to generate superior DC vaccines, and possible combination therapies, that will hopefully lead to a higher clinical response in advanced melanoma patients.

In Chapters 3-6 of this thesis, we used cryopreserved HD and patient monocytes from a recent autologous adenovirus-based DC vaccine engineered with three full length common melanoma antigens. Surprisingly, conventional markers and cytokines associated with DC maturation did not correlate with clinical outcomes or immune responses. We performed gene and protein expression profiling to identify key novel biomarkers associated with *in vivo* DC immunogenicity and positive clinical response to DC-based vaccination. We report here that cell surface expression of Inducible T Cell Costimulator Ligand (ICOSL) is selectively reduced on DC from melanoma patients and partially regulated by canonical NF-κB signaling, resulting in a vaccine that is sub-optimal for T cell (cross)priming. We further show that levels of soluble ICOSL (sICOSL) positively correlates with production of Th1 immune chemokines, objective clinical response rates, and overall survival in advanced-staged melanoma patients. Additionally, we show that sICOSL is partially regulated by ADAM10/17 sheddase activity on monocyte-derived DC.

These data suggest that targeted manipulation of patient-derived DC to improve ICOSL expression may improve therapeutic T cell responses and treatment outcomes in cancer patients.

7.1.1 ICOSL mRNA Expression is Associated with Favorable Clinical Outcomes at Baseline

ICOSL expression may be imprinted (or conditioned) in DC from melanoma patients with active disease. This was suggested by the correlation between *ICOSLG* expression levels and clinical response and survival rates in baseline blood-derived iDC. No significant correlations were observed with mDC or AdVTMM2/DC. This might suggest that the patient-derived monocytes are intrinsically defective. Future studies will involve the profiling of HD and patient monocytes and investigate epigenetic changes within these cells that may underlie dysregulated ICOSL expression.

7.1.2 sICOSL and Protein Surface Expression of ICOSL on AdVTMM2/DC Correlate with Antigen-Specific Vaccine Responses and Overall Survival

We have shown here that sICOSL levels from *in vitro* cell culture supernatants correlated with overall survival rates observed and favorable clinical outcomes observed in patients. Moreover, univariate cox regression analysis for sICOSL indicated sICOSL from patient mDC is a good predictive prognostic index for PFS and OS. Prospective studies will include exploring the physiological role of sICOSL in regulating anti-tumor T cell responses.

Additionally, it was observed that surface ICOSL expression on AdVTMM2/DC had a significant positive correlation with vaccine-induced immune responses and is considered a good

predictive prognostic index associated with OS. We were unable to test the importance of ICOSL in priming immune responses using patient cells, as circulating T cells were predominantly memory T cells. Future studies will include the generation of a novel adenovirus vector, encoding the 3 melanoma-associated antigens plus ICOSL (full length or the ectodomain to equate to sICOSL) for the engineering of vaccine DC, and testing of such vaccines for their ability to generate specific immune responses from autologous patient-derived naïve T cells. If these studies cannot be carried out using human samples, it might be of interest to explore the efficiency of such genetic vaccine approaches in mouse models.

7.1.3 Canonical NF-κB Signaling Regulates ICOSLG Expression in DC

The data presented in this thesis revealed that dysregulated NF-κB signaling observed in melanoma patients resulted in reduced protein expression of ICOSL. However, a target resulting in the dysregulation of NF-κB signaling has yet to be identified. Preliminary transcriptional data has suggested that the NLR Family Pyrin Domain Containing 2 gene (*NLRP2)* expression has a significant, negative correlation with clinical outcome (Figure 26). The literature suggests that the protein encoded by *NLRP2* is an inhibitor of canonical NF-κB signaling. We have hypothesized that the dysregulation of NF-κB signaling might be the result of increased *NLRP2* expression observed in patient DCs. This hypothesis is summarized in the graphic below (Figure 27). Future studies will involve lentiviral-mediated knockdown of *NLRP2* in HD and patient DC to explore the broader effects of *NLRP2*-deficiency in DC.

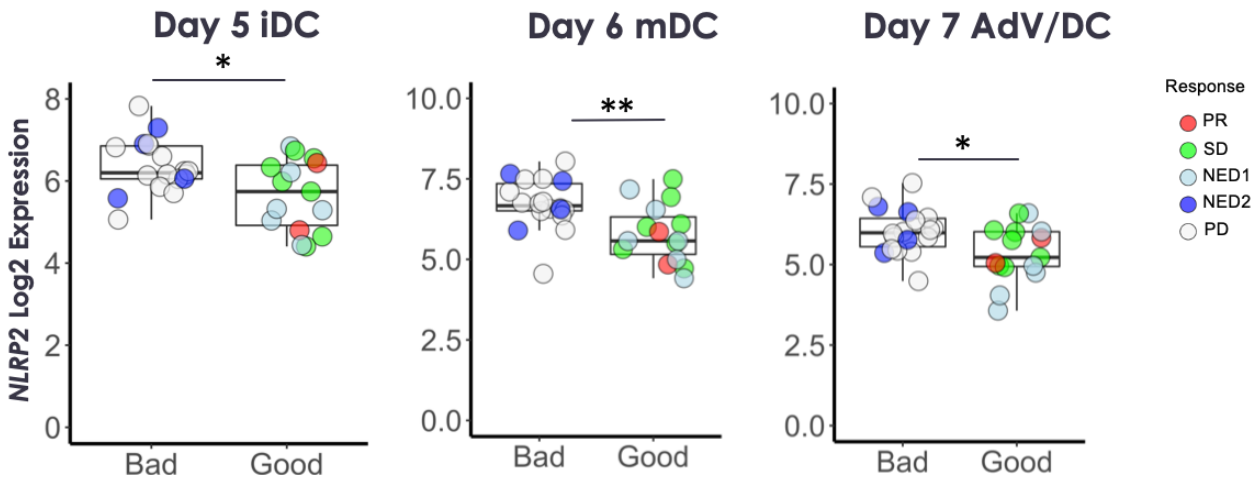

Figure 26. NLRP2 mRNA Expression in Patient DC Correlate with Clinical Outcomes.
NLRP2 mRNA expression for patient iDC, mDC, and AdVTMM2/DC. Patients were segregated based on clinical outcomes. Differences between cohorts were determined using unpaired student t-tests. *: p value ≤ 0.05, **: p value ≤ 0.01.

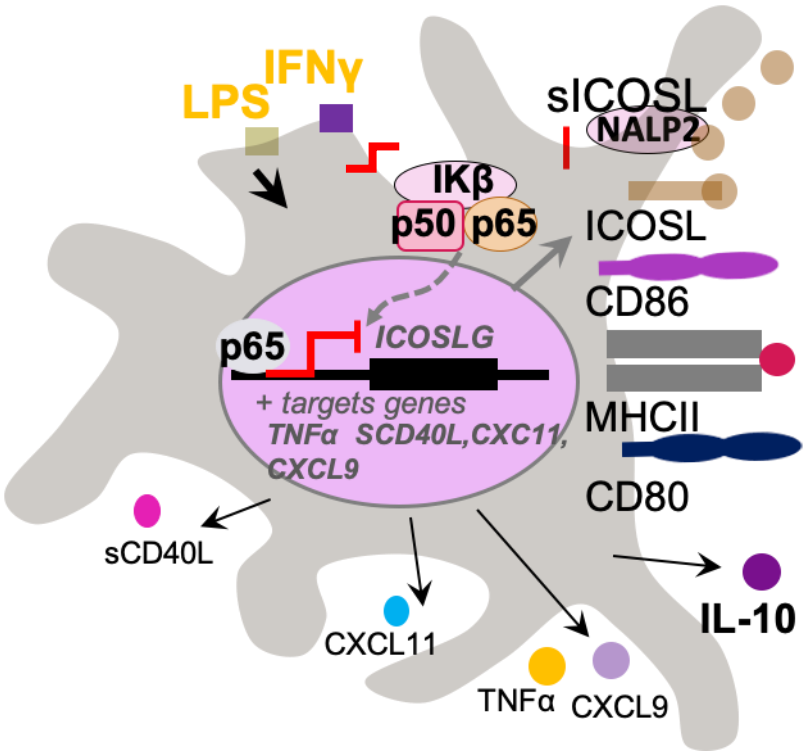

Figure 27. Hypothesized NALP2 Regulation of ICOSL Through NF-κB Signaling.

7.1.4 ADAM10/17 Sheddase Activity Regulates Surface Protein Expression of ICOSL on HD DC

We have reported here that ADAM10/17 sheddase activity partially regulates ICOSL surface expression on DC, which to our knowledge has yet to be reported. The pharmacologic inhibitors used in these experiments were not specific, and have been reported to target several metalloproteinases, including ADAM10/17. Because patient DC transcriptionally express both ADAM10 and ADAM17, it will be of significant interest in future experiments to determine which metalloproteinase is the dominant sheddase in the regulation of ICOSL expression on DC. Prospective studies will include the selective knockdown of ADAM10/17 in order to determine which sheddase is more critical in the regulation of ICOSL on DC.

7.1.5 Summary

In summary, this study is the first to reveal that canonical NF-κB signaling and ADAM10/17 sheddase activity are critical for the regulation of ICOSL gene and protein expression in DC. Our data suggest that the dysregulation in NF-κB signaling and the expression of ADAM10/17 may explain the decrease in ICOSL protein surface expression observed in patient DC. We have identified ICOSL as a potential potency biomarker for the *in vivo* immunogenicity of DC-based vaccines in melanoma patients. Reduced expression of ICOSL on monocyte-derived DC limits their ability to prime anti-tumor immune responses *in vitro* and *in vivo*. We also show that baseline mRNA expression levels of *ICOSLG* in patient DC correlate with favorable clinical outcomes and are associated with overall patient survival, suggesting the clinical associations observed with ICOSL may be imprinted in dysregulated patient DC precursor cells. Future studies will involve the profiling of HD and patient

monocytes and investigate epigenetic changes within these cells that may underlie dysregulated ICOSL expression. It will also be important to determine the impact of enforced DC expression of ICOSL on vaccine-induced, antigen-specific T cell responses in patients. Conditioning of increased and stabilized ICOSL expression on patient DC may yield a vaccine capable of more effectively driving the development of clinically-effective anti-tumor immunity in support of superior clinical outcomes.

Appendix A: Metabolic Profiling of Melanoma Patient DC

Appendix A.1 : Foreword

The data shown in Appendix A will contribute to future publications. The work shown here is in collaboration with Dr. Juraj Adamik

Appendix A.2 : Introduction

The pathway analysis discussed in the main text was used to identify signaling pathway activation differences between HD and melanoma patient DC. The significant differences in pathway activation between HD and patient DC suggests possible targets for future DC vaccine studies. Figure 21A displays the significant pathway activation differences between HD and patient DC. Of those pathways, several metabolic pathways were of significant interest.

The literature has suggested that oxidative phosphorylation and fatty acid β-oxidation are critical for the activation of human monocyte-derived DC(197), but little is understood about the role these metabolic pathways play in DC differentiation. The IPA analysis mentioned in the above chapters highlighted that genes in the oxidative phosphorylation and fatty acid β-oxidation signaling pathways are significantly reduced in HD DC upon maturation (Figure 21A). However, these pathways did not appear to be significant in patient mDC . There was little to no change in the expression of genes involved in oxidative phosphorylation or fatty acid β-oxidation. To investigate the potential significance of this pathway on DC differentiation, the microarray data

was first validated using QPCR. Additionally, to investigate the functional importance of oxidative phosphorylation and fatty acid β-oxidation on DC function, seahorse analysis was done on immature and matured DC from HD and patient samples. The preliminary data presented in this chapter indicates that metabolic manipulation might be used to enhance the efficiency and overall clinical response rates of DC-based vaccines.

Appendix A.3 : Materials & Methods

DC Generation. Please refer to the information listed in the "Materials & Methods", Chapter 3.

DC Microarrays. Please refer to the information listed in the "Materials & Methods", Chapter 3.

Transcriptional Analysis of Metabolic Genes. RNA from DC preparations was collected using the All Prep RNA/Protein kit (Qiagen#80404). cDNA was synthesized using the qScript cDNA Synthesis Kit (Quantabio). QPCR was performed using standard Taqman primers (listed below) and the Express qPCR supermix (Thermo Fisher #1178501K). The following primers were used: NDUFS3 (Hs01549083_m1), NDUFA10 (Hs01071117_m1), HADHA (Hs00426191_m1), ECHS1 (Hs00187943_m1), and IVD (Hs01064832_m1). HPRT1 (Hs99999909_m1) was used as a housekeeping control.

Seahorse Analysis. Immature and matured DC from patients and HD were collected. Cells were plated at 100,000 cells/well on Seahorse culture plates in assay media consisting of minimal, unbuffered DMEM supplemented with 1% BSA and 25 mmol/L glucose, 1 mmol/L pyruvate, and

2 mmol/L glutamine and analyzed using a Seahorse XFe96 (Agilent). Basal oxygen consumption and extracellular acidification rates were taken for the first 30 minutes. Then, cells were stimulated with oligomycin (2 μmol/L), FCCP (0.5 μmol/L), and rotenone/antimycin A (0.5 μmol/L) to obtain maximal respiratory and control values. For Fatty Acid β-Oxidation measurements, cells were either treated with a BSA control or 1 mM palmitate-BSA, conjugated to 0.17 mM BSA in 150 mM NaCl, pH 7.2. All experimental conditions were performed in triplicates per the manufacturer's instructions.

Appendix A.4 : Preliminary Results

Appendix A.4.1 Melanoma Patient DC Express Higher Levels of Metabolic Gene Transcripts, Compared to DC from HD

The *in silico* pathway analysis suggested that the activation of oxidative phosphorylation and fatty acid β-oxidation was relatively unchanged post-maturation in patient DC. Yet, the pathway analysis using HD samples suggested oxidative phosphorylation and fatty acid β-oxidation are significantly reduced in activation post-maturation with IFN-γ + LPS. To validate this, genes that displayed reduced expression post-maturation from HD cells, but not patients, were selected. The target genes selected for analysis were *NDUFS3*, *NDUFA10*, *HADHA*, *ECHS1*, and *IVD*.

QPCR analysis revealed that melanoma patient DC express higher transcript expression of *NDUFS3, NDUFA10, HADHA*, *ECHS1*, and *IVD* in both immature and mature DC subtypes,

compared to HD (Figure 28 & Figure 29). HD iDC and mDC showed relatively little to no mRNA expression of the above genes. When separated by clinical outcome, the degree of change in expression of *NDUFA10*, *HADHA*, *ECHS1*, and *IVD* was larger in patients who clinically progressed versus those who did not (Figure 30). Additionally, patients who displayed tumor progression had an increase in mRNA expression of *NDUFA10*, *HADHA*, *ECHS1*, and *IVD* post-maturation. mRNA expression of NDUFS3 increased across all patient DC post-maturation, regardless of their clinical status.

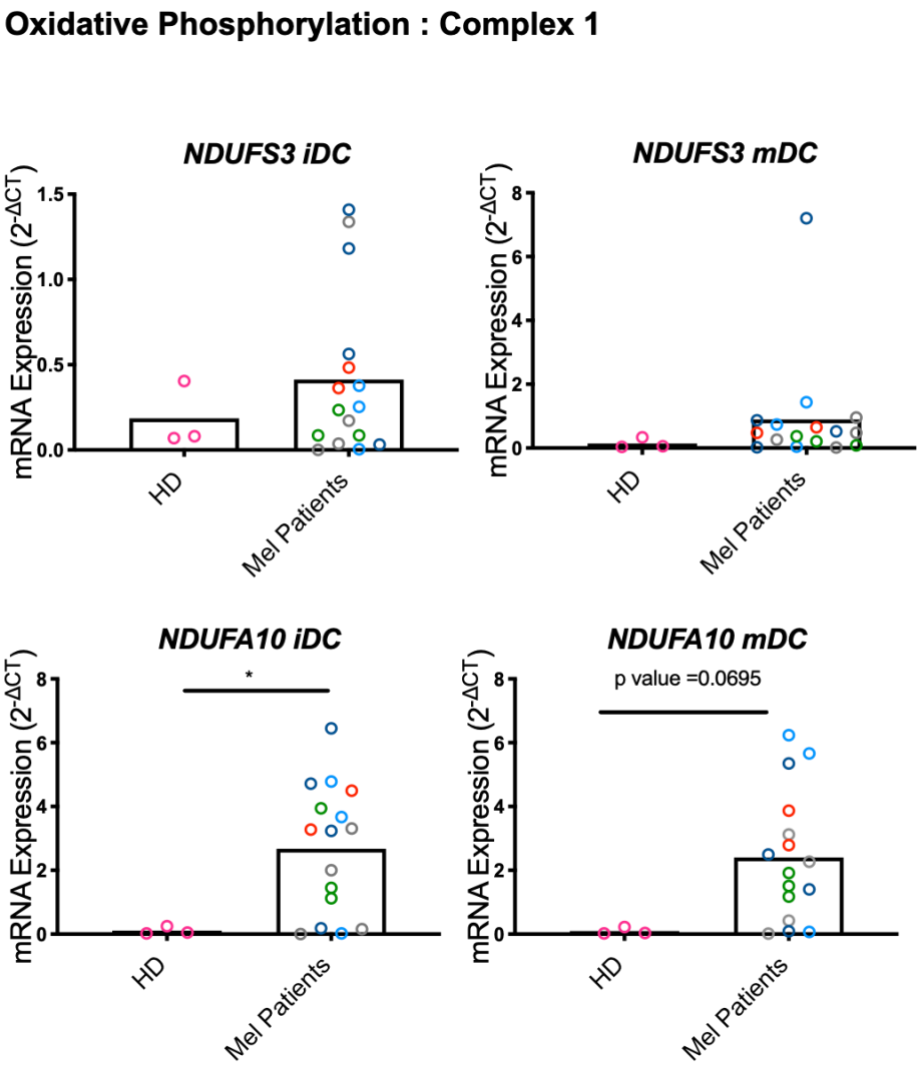

Figure 28. Melanoma Patient DC Express Higher mRNA Transcrpit levels of Complex 1 Genes, Compared to HD DC.
QPCR analysis of genes in Complex 1 of the Oxidative Phosphorylation pathway. Unpaired student t-test (two-tailed) was used to determine significance. *: p value ≤ 0.05.

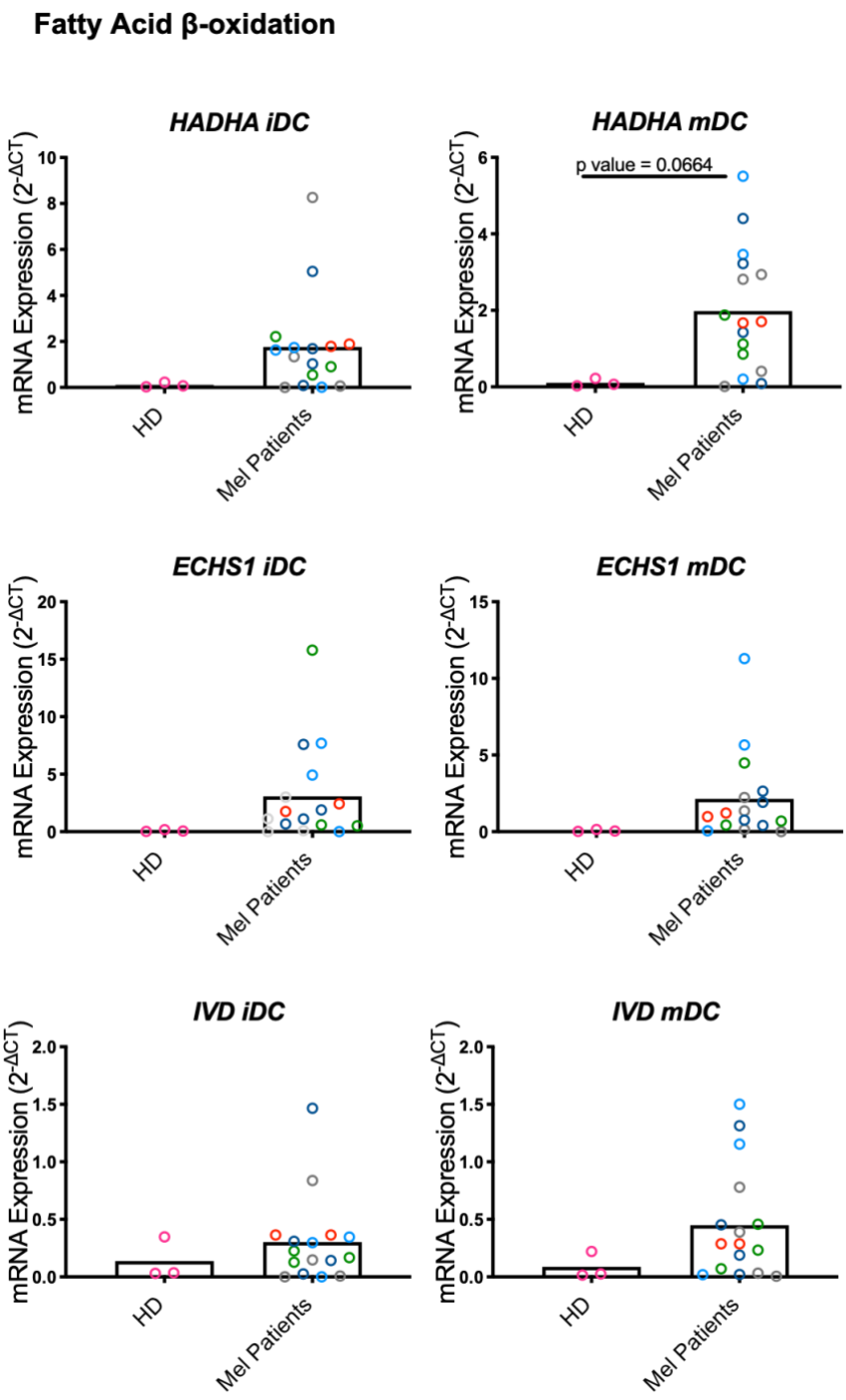

Figure 29. Melanoma Patient DC Express Higher Transcript Levels of Genes in the Fatty Acid β-oxidation Pathway, Compared to HD DC.
QPCR analysis of genes in the Fatty acid β-oxidation pathway. Unpaired student t-test (two-tailed) was used to determine significance.

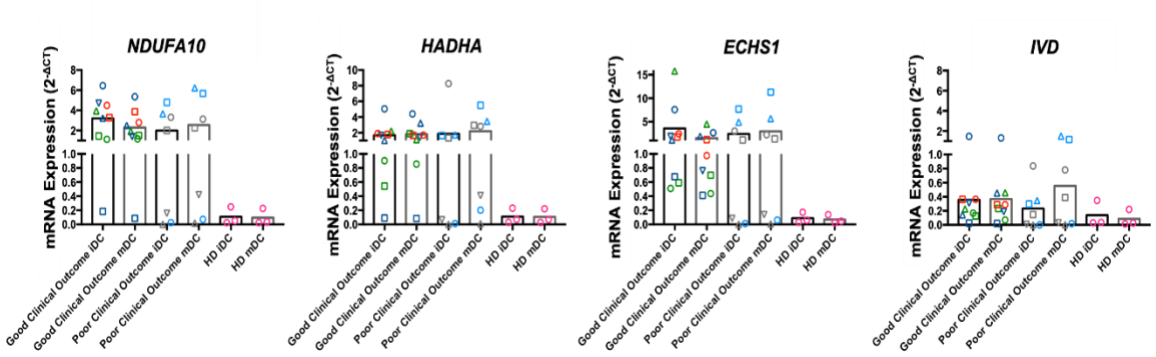

Figure 30. *NDUFA10, HADHA,ECSH1,* and *IVD* mRNA Expression Decreases Post-maturation in Favorable Clinical Outcome Patients & HD DC.
QPCR analysis of metabolic genes. Patients are segreagted by clinical outcome and seperated by DC subtype. One-way ANOVA was used to determine significance.

Appendix A.4.2 Activation of Oxidative Phosphorylation and Fatty Acid β-Oxidation are Associated with Disease Progression and Suboptimal Immune Responses in Melanoma Patients

The gene expression analysis indicated that oxidative phosphorylation and fatty acid β-oxidation may be functionally important in DC. To investigate this, Metabolic flux analysis was performed using the Seahorse XF. It was observed that change in OCR levels post maturation was largely reduced after an injection with oligomycin in patients who did not display tumor progression, compared to OCR levels in DC from patients who displayed tumor progression. Additionally, basal OCR levels were higher in patients who progressed (Figure 31A).

Fatty acid β-oxidation levels were measured by OCR rates in response to palmitate injections. It was observed that OCR levels increased post-maturation in patients who displayed disease progression. Additionally, when patients were segregated by immune response, OCR levels were higher in mDC from patients who did not generate vaccine induced immune responses

(Figure 31B). These data suggest that fatty acid β-oxidation activation in mDC is associated with disease progression and the generation of suboptimal immune responses.

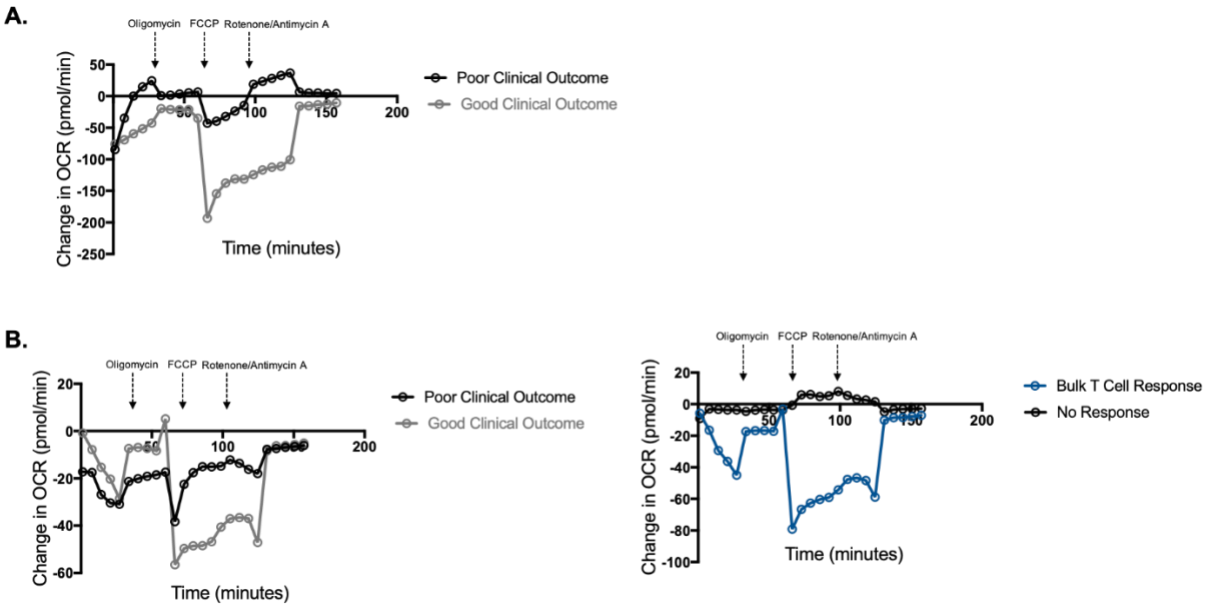

Figure 31. Oxidative Phosphorylation and Fatty Acid β-Oxidation Activation Levels in Patient mDC are Associated with Disease Progression and Subpar Immune Responses.
Seahorse analysis of patient DC. OCR levels are represented as "change in OCR" (mDC – iDC). This was done in order to normalize the data. Graphs shown display "change in OCR" levels with (B) or without (A) the addition of palmitate to the cells.

Appendix A.5 Discussion

The preliminary data on metabolic profiling discussed in this chapter suggests that oxidative phosphorylation and fatty acid β-oxidation signaling pathways are dysregulated in melanoma patient DC. It has been previously reported in mouse studies that DC reduce activation of oxidative phosphorylation and fatty-acid β-oxidation post-maturation(197). The reduction in oxidative phosphorylation and fatty-acid β-oxidation is thought to be associated with metabolic fitness and immunogenicity. The pathway analysis performed on the HD DC dataset confirmed the previous reports of murine studies. Post-maturation with IFN-γ + LPS, HD DC decrease

expression of metabolic genes in oxidative phosphorylation and fatty-acid β-oxidation signaling pathways. However, patient DC do not express reduction in mRNA expression of these genes. Importantly, functional assays revealed that both of these metabolic signaling pathways are associated with clinical outcomes and the generation of immune responses. All together, these data suggest that melanoma patient DC undergo metabolic reprogramming post-maturation *in vitro*. By targeting these pathways, patient DC can be engineered to become metabolically fit and be used to enhance the clinical responses rates of DC-based cancer vaccines. Prospective studies will explore how these metabolic pathways influence the "fitness" of human DC and we will investigate how the activation of fatty-acid β-oxidation and oxidative phosphorylation signaling pathways influence the generation of regulatory immune cells.

The literature has suggested that classical NF- κB activation has a direct relationship with oxidative phosphorylation and glycolysis in sarcoma cell line models(198). This is of significant interest, given our data revealing NF-κB dysregulation in melanoma patient DC. Future experiments could involve the investigation the relationship between NF-κB dysregulation and the metabolic gene transcripts listed above. Additionally, activation of classical NF-κB signaling could revert the metabolic phenotype observed in patient mDC, making them more metabolically fit, which will hopefully increase objective clinical responses to DC-based vaccination.

Appendix A.6 Conclusions & Future Directions

In this appendix section, preliminary data on metabolic dysregulation in melanoma patient DC was reported. We identified that the metabolic signaling pathways, oxidative phosphorylation and fatty acid β-oxidation, were predicted to be significantly reduced post-maturation in HD DC.

However, these metabolic pathways were not significant in the patient cells. Preliminary functional assays, using the Seahorse XF, revealed that higher OCR levels (with and without the addition of palmitate) post-maturation were associated with disease progression and negatively correlated with immune response.

These preliminary data suggest that metabolic dysregulation might be associated subpar DC function. Prospective studies will continue to investigate these metabolic pathways and will investigate metabolic dysfunction on the generation of tolerogenic DCs. First, we will investigate the presence of tolerogenic DC surface and soluble markers. It is hypothesized that patient DC will have a more "tolerogenic phenotype", compared to HD DC. T cell response assays will also be helpful in the determination of whether patient DC are in fact, tolerogenic. Prospective studies will also include culturing HD DC in tolerogenic conditioning media to try and reprogram metabolic pathways in HD to mimic what is observed in patient DC.

Appendix B : DC Vaccination Plus Dasatinib for the Treatment of Advanced-Stage Melanoma

Appendix B.1 : Foreword

The data shown in Appendix B will contribute to future publications. The work shown here is part of a broad analysis on UPMC 12-048 clinical trial. This work was performed in collaboration with Dr. Walter J. Storkus, University of Pittsburgh, and Dr. Timothy Looney, Thermo Scientific.

Appendix B.2 : Introduction

The use of tyrosinase kinase inhibitors (TKI) in combination with immunotherapy has been indicated to help improve the immune dysregulation observed in late-staged melanoma patients(199). Recently, we have developed an autologous type 1-polarized DC vaccine loaded with six separate tumor blood vessels associated antigens (TBVAs; NCT01876212). The use of TBVAs in DC vaccines allow for selectively targeting of tumor-associated blood vessels, which led to vascular normalization and T cell-mediated control of tumor growth in mouse melanoma models. This vaccine, in combination with the TKI, Dasatinib, was used in a single-center, randomized phase II clinical trial. Sixteen HLA-A2+ patients with advanced-stage melanoma (metastatic, stage IV or unresectable, Stage IIIB/IIIC) were enrolled on trial. Patients were randomized into two treatment groups) 1) Treatment A: received 2 intradermal injections (10e7

DC) of the autologous DC vaccine on day 1 and day 15 of cycle 1 and then immediately begin Dasatinib treatment in cycle 2 (70mg, 2x a day). 2) Treatment B: Received both the autologous DC vaccine and Dasatinib during cycle 1. Both cohorts then received both DC-based vaccines + Dasatinib in subsequent treatment cycles. The design of the clinical trial is shown below (Figure 32).

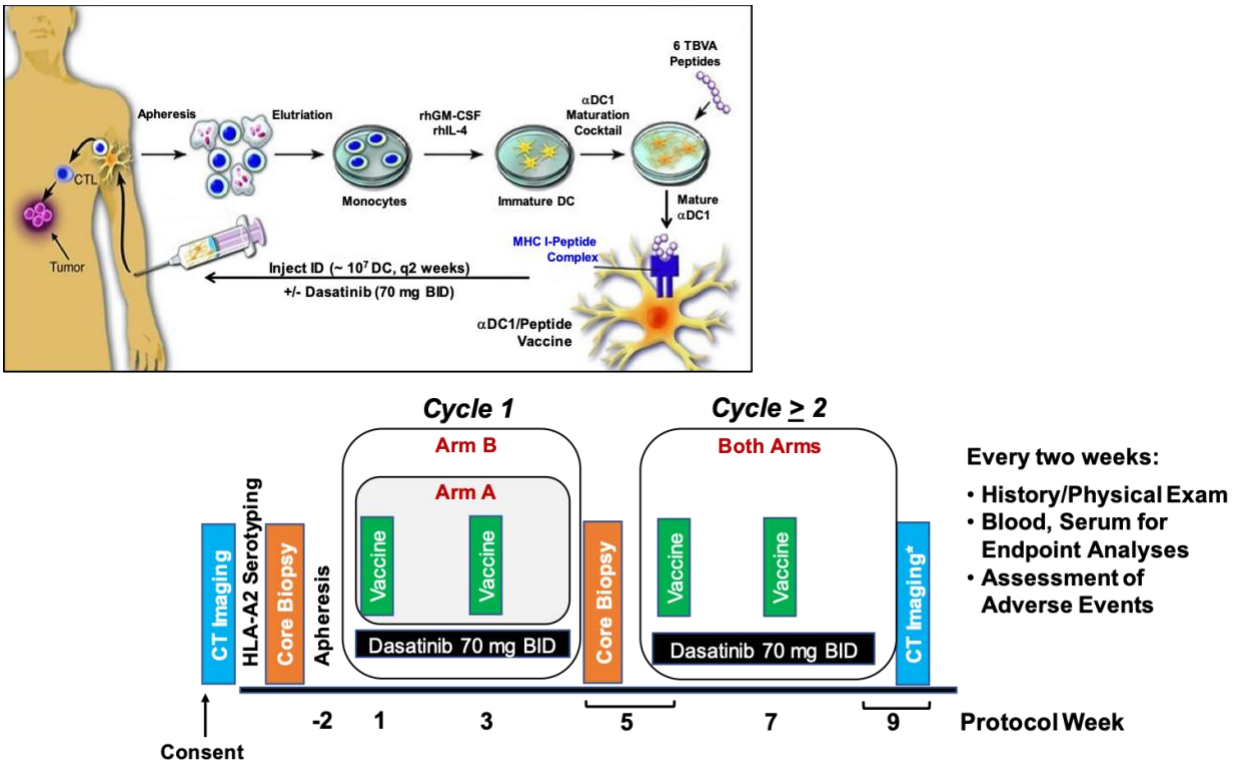

Figure 32. UPMC 12-048 Study Design.

Defined by RECSIT 1.1, clinical data on 13 evaluable patients revealed that 4 patients displayed tumor regression (PR), 6 patients showed tumor progression (PD), and 3 individuals remained stable (SD) on-treatment. Interestingly, all 4 partial responders were randomized to treatment B on the trial, indicating that timing of Dasatinib treatment might be important for clinical responsiveness.

Appendix B discusses a broad analysis of the clinical trial to identify gene expression profiles that might correlate with overall survival and clinical response rates in melanoma patients. Additionally, in collaboration with Thermo Scientific, TCR convergence frequencies were investigated in the periphery and within tumor samples at baseline and post-treatment. The preliminary data discussed here helps target future areas of investigation to increase optimal immune response rates using combination therapies.

Appendix B.3 : Materials & Methods

DC Microarrays. RNA from patient-derived cryopreserved matured αDC1cells were isolated and analyzed using Clariom S Gene Chip (Affymetrix). Patient microarray data was normalized using Robust Multi-Average (RMA) normalization. The R package, oligo (Version 3.9)(179), was used. After attempting normalization, the data followed a non-normally distributed pattern so, Wilcoxon tests were used for differential gene expression analysis.

TCR Sequencing. TCR sequencing was done in collaboration with Thermo Scientific and used the Oncomine TCR Beta-LR Assay (Thermo Fisher Scientific Cat. No. A35386), and protocol as described in the Oncomine TCR Beta Assay User Guide MAN0017438 Revision A.0.

Next-generation Sequencing on Tumor Biopsies. Next-generation sequencing was done in collaboration with Thermo Scientific and used the Oncomine Immune Response Research Assay(200).

Statistical Analysis. Based on data distribution, Wilcoxon rank-sum test were used for most of the analyses. Spearman's correlation coefficients were calculated to determine associations present. Kaplan-Meier (KM) curves were carried out using the R packages survival (version 3.1-8) and survminer (version 0.4.6). P values are represented as *$p \leq 0.05$, **$p \leq 0.01$, ***$p \leq 0.001$, **** $p \leq 0.0001$. Graphs were generated using the R package ggplot2 (Version 3.1.1) and GraphPad Prism v7.

Appendix B.4 : Results

Appendix B.4.1 TCR Convergence Frequencies in Circulating T cells are Associated with Immune response and Favorable Clinical Outcomes at Baseline

Generation of immune responses should result in the expansion of antigen-specific T cells. TCR convergence is defined as the culminative frequency of T cell clones that have identical variable region sequences in their TCRs(201). We sequenced circulating T cells from advanced melanoma patients pre and post-treatment to investigate the breadth and diversity of TCR clones.

It was hypothesized that TCR Convergence frequencies would correlate with overall immune response and clinical outcomes. When separated by clinical outcome and immune response, it was observed that TCR convergence frequencies in circulating T cells were increased in patients with favorable clinical outcomes at baseline (Figure 33, left panel). Additionally, patients who generated vaccine-induced immune response also had higher TCR convergence

frequencies in circulating T cells at baseline (Figure 33, right panel). No significant difference was observed pre- vs post-treatment in the periphery or from tumor samples.

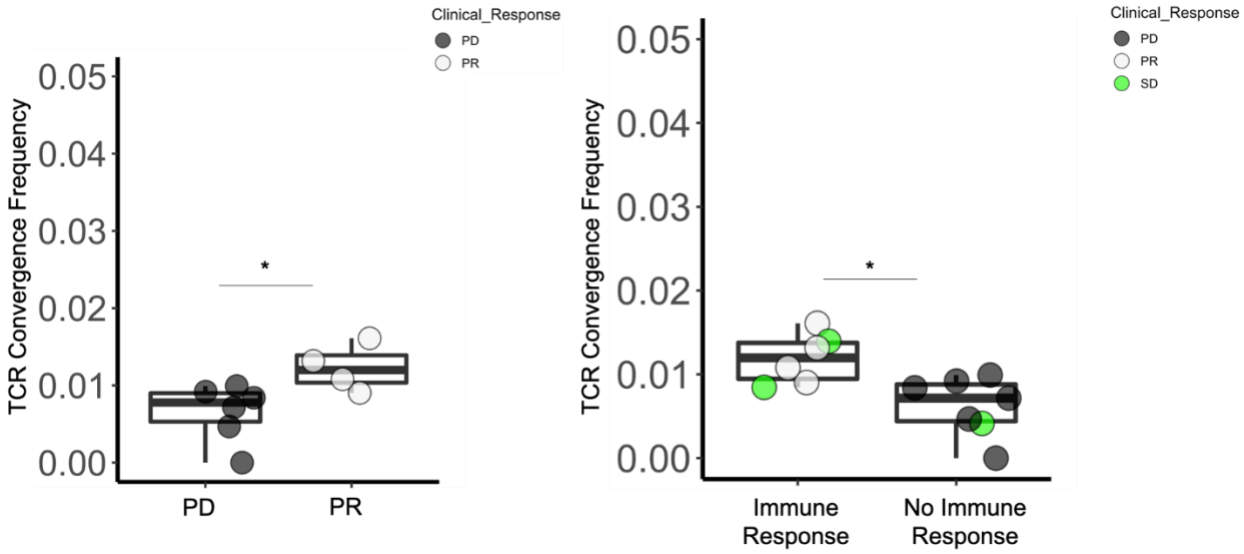

Figure 33. TCR Convergence Frequencies in Circulating T cells are Associated with Clinical Outcome and Immune Responses.
TCR sequencing of patient PBMC at baseline. Patients are segregated by clinical outcome and vaccine-induced immune responses. Wilcoxon rank-sum tests were used to determine significance**.** *$p \leq 0.05$

Appendix B.4.2 Microarray Analysis Reveals Gene Signatures that Correlate with Favorable Clinical Outcomes and Immune Responses in Matured DC from Patients

Genomic analysis revealed that there were 640 shared differently expressed genes (DEG) between patients who progressed early and did not generate a vaccine-induced immune response. Out of the 640 DEGs, many genes involved in immunosuppression were upregulated. These genes included *TLR7*, *TGFβ1*, *PTGES2*, *CLEC4A*, *SIRT1*, and *SATB1* (Figure 34A). In addition, *ITGB3BP*, a co-repressor NF-κB signaling(202), expression was upregulated in patients with poor clinical outcome and those who did not generate vaccine-induced immune responses. Importantly, the mRNA expression of *TLR7* and *SIRT1* had significant strong negative correlations with overall survival rates (Figure 34B).

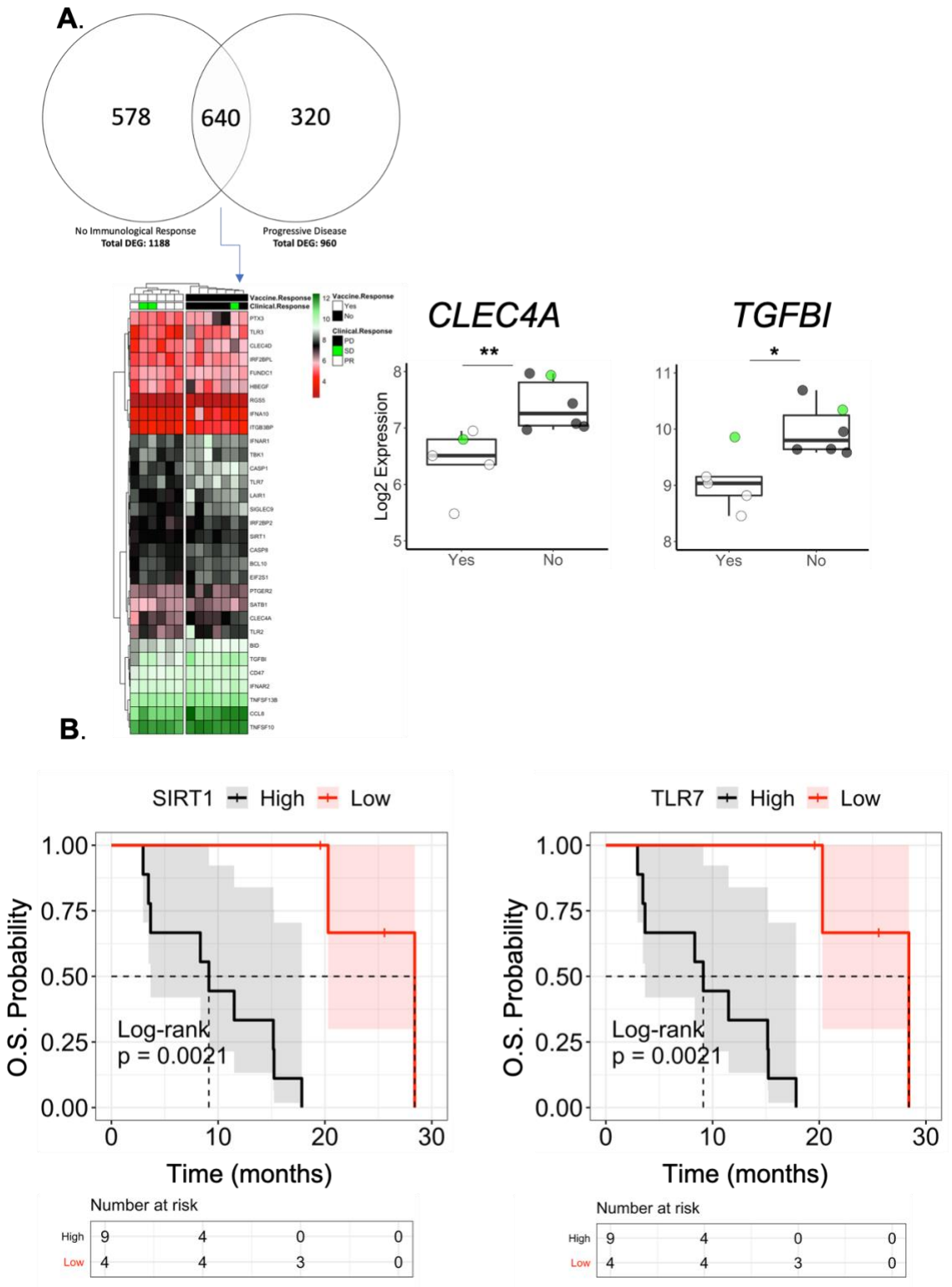

Figure 34. Immunosuppressive and Regulatory Molecule mRNA Expressions are Associated with Poor Prognosis in Patient Matured DC.

Venn Diagram of DEG from patients with a poor clinical outcome and patients who did not generate a vaccine-induced immune response (A). Heatmap hierarchical clustering of the overlapping genes between "Poor Clinical Outcome"

and “No Immune Response” (A). mRNA expression of *CLEC4A* and *TGFB1* are shown as examples (A). Patients are segergated by immune response. Wilcoxon rank-sum tests were used to determine significance. KM curves of overall survival rates. Patients are segregated based on high and low mRNA expression of *SIRT1* (B, left panel) and *TLR7* (B, right panel). *$p \leq 0.05$, **$p \leq 0.01$

It was determined that 1217 DEG overlapped between patients with favorable clinical outcomes (i.e. PR) and immunological response. Many of these genes were associated with immunogenicity of DC, antigen presentation, and costimulation. Specifically, *BTNL8*, *LAMP3*, *RELB*, *NOTCH3*, and *CXCL14* were all upregulated in these patients (Figure 35A). Moreover, *BTNL8* and *RELB* mRNA expression had significant positive correlations with overall survival rates (Figure 35B).

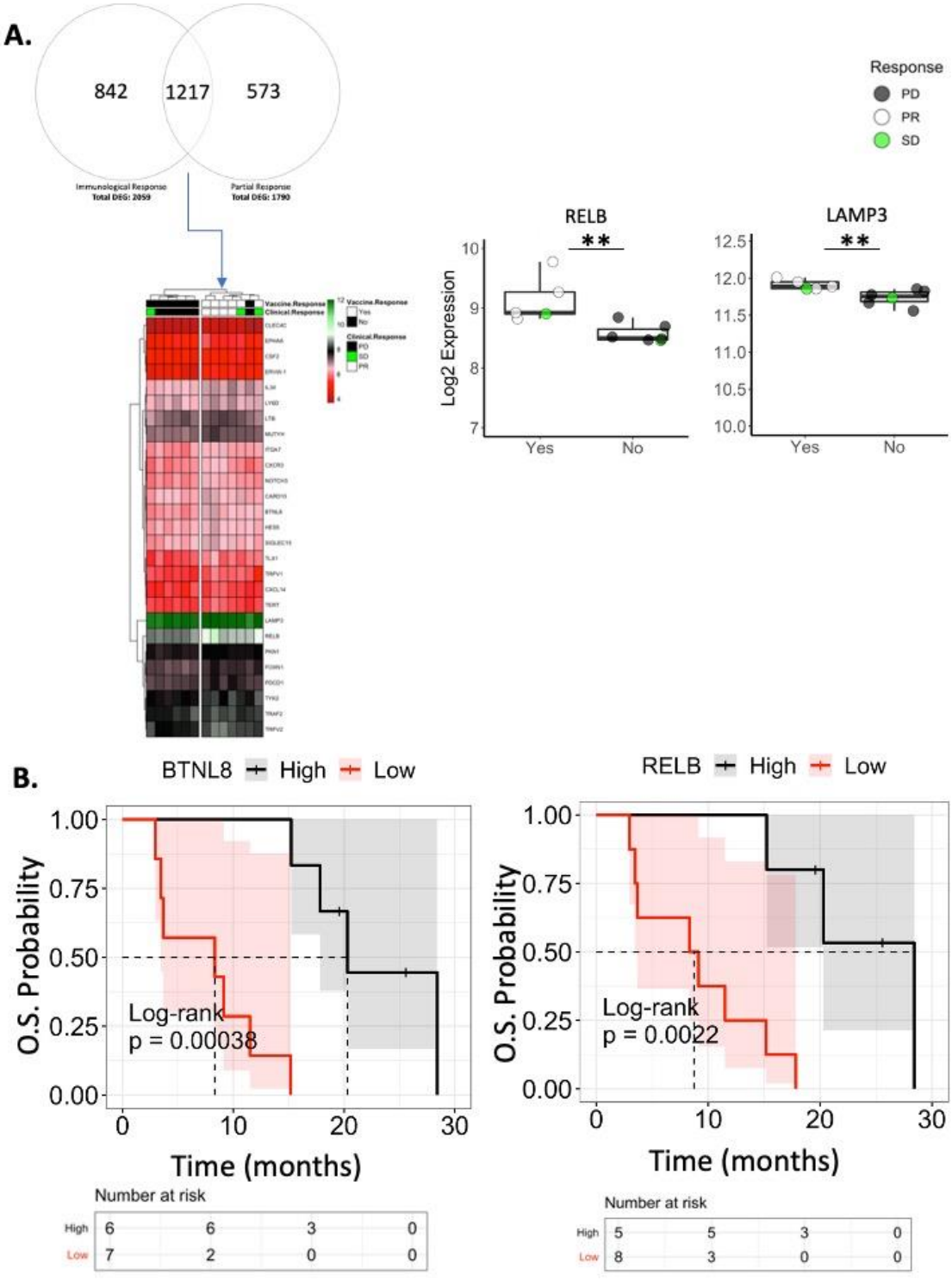

Figure 35. mRNA Expression Levels of Genes Important for Antigen Presentation, DC Function, and Co-stimulation are Associated with Favorable Clinical Outcomes, Immune Responses, and Survival Rates in Patients.

Venn Diagram of DEG from patients with a good clinical outcome and patients who did generate a vaccine-induced immune response (A). Heatmap hierarchical clustering of the overlapping genes between "Good Clinical Outcome" and "Immune Response" (A). mRNA expression of *RELB* and *LAMP3* are shown as examples (A). Patients are

segergated by immune response. Wilcoxon rank-sum tests were used to determine significance. KM curves of overall survival rates. Patients are segregated based on high and low mRNA expression of *BTNL8* (B, left panel) and *RELB* (B, right panel). **$p \leq 0.01$

Appendix B.4.3 Next-generation Sequencing on Bulk Tumors Identify Genes that Correlate with Clinical Outcomes in Patients

Next-generation sequencing was performed on bulk tumor samples pre- and post-treatment to identify gene signatures that correlate with favorable clinical outcomes. At baseline, patients who progressed early had relatively lower mRNA expression of *NCR3, NCR1, CD226, CD86, and CCL3* (Figure 36A). Additionally, post-treatment, these patients had increased mRNA expression of the immunosuppressive genes, *HIF1α, TOP2A, and ISG15* (Figure 36B). *ISG15* high mRNA expression had a significant negative correlation with overall survival (Figure 36C).

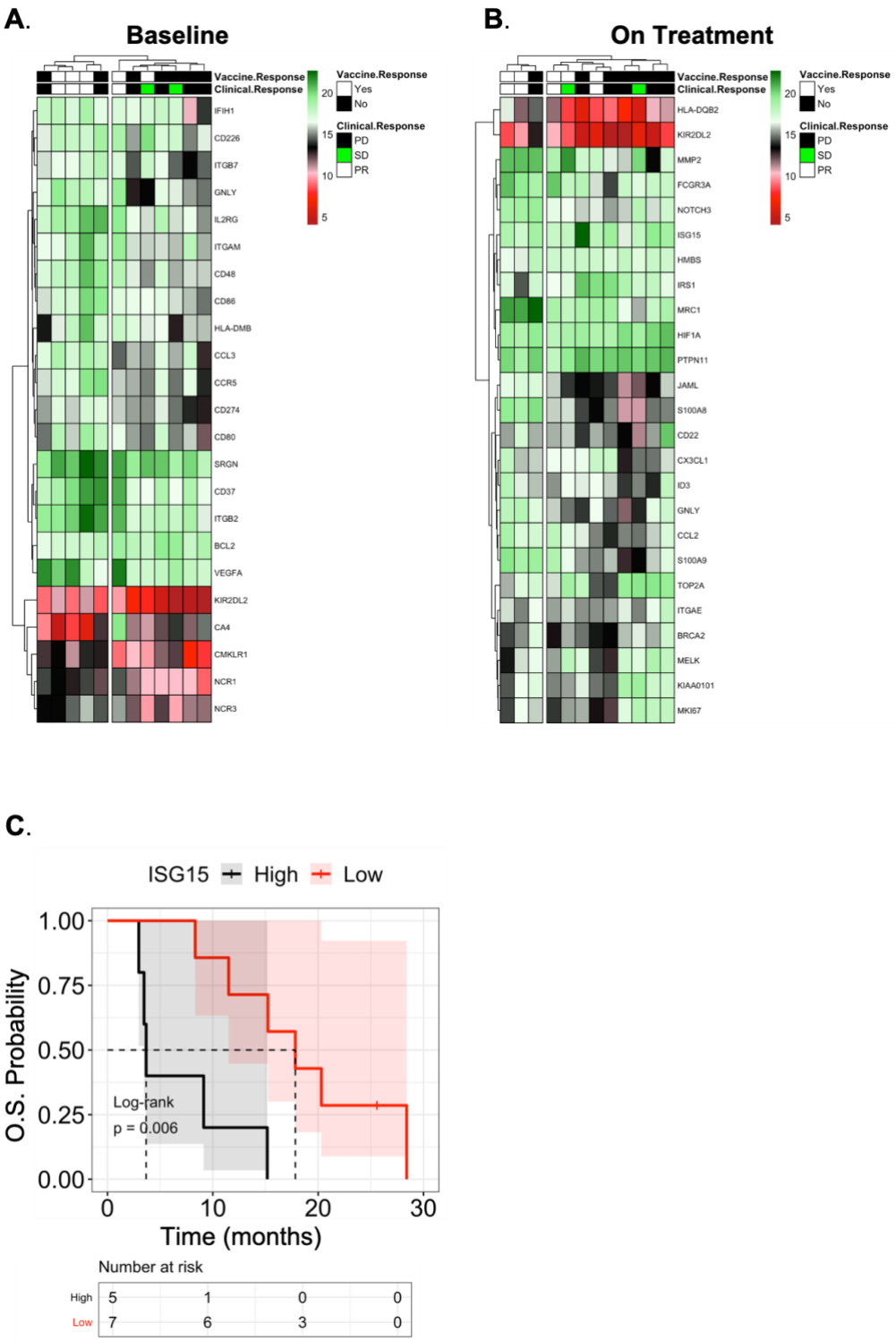

Figure 36. Patients who Progress Early Show Low mRNA Expression Levels of Genes Associated with T cell Infiltration and NK Cell Activation at Baseline, and Express hHgh mRNA expression levels of Immuosupressive molecules Post-treatnent.

Heatmap hierarchical clustering of genes from tumor samples at baseline (A) and during treatment (B). Samples are segregated based on vaccine response and clinical outcome status. KM curve of overall survival rates in

patients. Patients are segregated based on high and low mRNA expression of *ISG15* in tumor samples biopsied while on treatment.

Appendix B.5 : Discussion

The broad analysis presented here was performed to better characterize melanoma patients who respond to combination therapies with DC vaccines. The genetic analysis was used to identify targets for future investigation that might increase the responsive rates to immunotherapy. While the data presented is interesting and warrants future investigation, it is important to recognize the limitation of this clinical trial (i.e. 13 patients analyzed and not all tumor biopsies had matched pair) and to not overinterpret the data.

It was shown here that circulating T cells from patients with favorable clinical outcomes have higher TCR Convergence frequencies at baseline, compared to those who displayed tumor progression. Thee data support previous literature that TCR convergence could potentially predict response to immunotherapy(201). Additionally, next-generation sequencing of bulk tumor cells revealed patients with poor prognosis had relatively low expression of genes that have been reported to be important for co-stimulation(203), T cell infiltration(204), and receptors for natural killer cell activation(205) at baseline. Importantly, post-treatment, these patients had an upregulation of genes associated with immunosuppression and poor prognosis(206-209), compared to bulk tumors from patients with favorable outcomes.

The microarray analysis on the matured DC used in the clinical trial revealed key gene signatures that relate to DC function and immunogenicity. Patients with a poor prognosis and who did not generate a vaccine-induced immune response had an increase in expression of genes that have been reported to be associated with recruitment of MDSCs(210), immunosuppression(211-

213), the expansion of regulatory cells(214), and NF-κB signaling dysregulation(202). Patients with favorable outcomes and who generated immune responses displayed an increase in gene expression of genes critical for antigen presentation(215), co-stimulation(216), DC function(217,218), and inflammation(219). Altogether, the microarray analysis on patient mDC provided targets for future studies and identified important genes that might be part of regulatory pathways affecting DC function. By targeting these pathways in future studies, we will be able to optimize combination therapies and hopefully increase the overall clinical responsive rates to DC-based vaccine immunotherapies.

Appendix B.6 : Conclusions & Future Directions

Appendix B of this thesis examined a broad analysis of another recent autologous DC vaccine clinical trial, in combination with the TKI, Dasatinib, for the treatment of advanced melanoma. A broad genomic analysis was performed on patient DC and bulk tumor cells (pre- and post-treatment) to identify potential targets that could enhance the efficiency of clinical response rates of DC vaccines. TCR sequencing revealed TCR convergence correlated with immune response and clinical outcomes at baseline, which supports other findings in the literature. The transcriptional profiling of these cells revealed that patients who progressed early had an upregulation of immunosuppressive genes (*HIF1α*, *TOP2A*, and *ISG15*) in the tumor post-treatment. Additionally, at baseline, bulk tumor expression from patients who progressed early had a decrease in genes important for T cell infiltration, migration (*CCL3*), costimulation (*CD226*), and NK cell activation (*NCR3* and *NCR1*).

Microarray analysis on patient DC revealed that patients with favorable clinical outcomes had increases in genes important for DC function (*NOTCH3* and *RELB*), co-stimulation (*BTNL8*), and antigen presentation (LAMP3), while patients who progressed, had increased gene expression levels of regulatory markers (*CLEC4A*), recruitment of MDSCs (*TLR7*), and immunosuppressive molecules (*TGFB1* and *PTGES2*). Altogether, the data presented in Appendix B identifies potential targets for future functional assays that could facilitate higher response rates using DC vaccines.

Importantly, the transcriptional profiling of melanoma patient DC in both the UPMC 09-021 and the UPMC 12-048 clinical trials have suggested dysregulation in classical NF-κB signaling. This is important because it suggests that optimal NF- κB signaling in patient DC might influence the generated immune responses. Additionally, transcriptional profiling of the patient DC from trials has indicated NF-κB signaling correlates with favorable clinical outcomes and the presence of immune responses. This could suggest that key molecules in the NF-κB signaling pathways might be potential biomarkers for overall vaccine efficiency, which might lead to greater success with combination therapies for the treatment of advanced melanoma.

Bibliography

1. Cancer Facts & Figures 2020. Atlanta: American Cancer Society 2020.

2. Hanahan D, Weinberg RA. The hallmarks of cancer. Cell **2000**;100(1):57-70 doi 10.1016/s0092-8674(00)81683-9.

3. Burnet FM. The concept of immunological surveillance. Prog Exp Tumor Res **1970**;13:1-27 doi 10.1159/000386035.

4. Starzl TE, Penn I, Putnam CW, Groth CG, Halgrimson CG. Iatrogenic alterations of immunologic surveillance in man and their influence on malignancy. Transplant Rev **1971**;7:112-45 doi 10.1111/j.1600-065x.1971.tb00465.x.

5. Rosenberg SA, Rapp HJ. Intralesional immunotherapy of melanoma with BCG. Med Clin North Am **1976**;60(3):419-30 doi 10.1016/s0025-7125(16)31889-2.

6. Dvorak HF. Tumors: wounds that do not heal. Similarities between tumor stroma generation and wound healing. N Engl J Med **1986**;315(26):1650-9 doi 10.1056/nejm198612253152606.

7. Kim R, Emi M, Tanabe K. Cancer immunoediting from immune surveillance to immune escape. Immunology **2007**;121(1):1-14 doi 10.1111/j.1365-2567.2007.02587.x.

8. Teng MW, Swann JB, Koebel CM, Schreiber RD, Smyth MJ. Immune-mediated dormancy: an equilibrium with cancer. J Leukoc Biol **2008**;84(4):988-93 doi 10.1189/jlb.1107774.

9. Barrett WL, First MR, Aron BS, Penn I. Clinical course of malignancies in renal transplant recipients. Cancer **1993**;72(7):2186-9 doi 10.1002/1097-0142(19931001)72:7<2186::aid-cncr2820720720>3.0.co;2-2.

10. Vajdic CM, van Leeuwen MT. Cancer incidence and risk factors after solid organ transplantation. Int J Cancer **2009**;125(8):1747-54 doi 10.1002/ijc.24439.

11. Pages F, Galon J, Dieu-Nosjean MC, Tartour E, Sautes-Fridman C, Fridman WH. Immune infiltration in human tumors: a prognostic factor that should not be ignored. Oncogene **2010**;29(8):1093-102 doi 10.1038/onc.2009.416.

12. Nelson BH. The impact of T-cell immunity on ovarian cancer outcomes. Immunol Rev **2008**;222:101-16 doi 10.1111/j.1600-065X.2008.00614.x.

13. Clemente CG, Mihm MC, Jr., Bufalino R, Zurrida S, Collini P, Cascinelli N. Prognostic value of tumor infiltrating lymphocytes in the vertical growth phase of primary cutaneous melanoma. Cancer **1996**;77(7):1303-10 doi 10.1002/(SICI)1097-0142(19960401)77:7<1303::AID-CNCR12>3.0.CO;2-5.

14. Lee N, Zakka LR, Mihm MC, Jr., Schatton T. Tumour-infiltrating lymphocytes in melanoma prognosis and cancer immunotherapy. Pathology **2016**;48(2):177-87 doi 10.1016/j.pathol.2015.12.006.

15. Hanahan D, Weinberg RA. Hallmarks of cancer: the next generation. Cell **2011**;144(5):646-74 doi 10.1016/j.cell.2011.02.013.

16. Dunn GP, Bruce AT, Ikeda H, Old LJ, Schreiber RD. Cancer immunoediting: from immunosurveillance to tumor escape. Nat Immunol **2002**;3(11):991-8 doi 10.1038/ni1102-991.

17. Dunn GP, Old LJ, Schreiber RD. The three Es of cancer immunoediting. Annu Rev Immunol **2004**;22:329-60 doi 10.1146/annurev.immunol.22.012703.104803.

18. Kapsenberg ML. Dendritic-cell control of pathogen-driven T-cell polarization. Nat Rev Immunol **2003**;3(12):984-93 doi 10.1038/nri1246.

19. Steinman RM. The dendritic cell system and its role in immunogenicity. Annu Rev Immunol **1991**;9:271-96 doi 10.1146/annurev.iy.09.040191.001415.

20. Palucka K, Banchereau J. Cancer immunotherapy via dendritic cells. Nat Rev Cancer **2012**;12(4):265-77 doi 10.1038/nrc3258.

21. Boudreau JE, Bonehill A, Thielemans K, Wan Y. Engineering dendritic cells to enhance cancer immunotherapy. Mol Ther **2011**;19(5):841-53 doi 10.1038/mt.2011.57.

22. Bao K, Reinhardt RL. The differential expression of IL-4 and IL-13 and its impact on type-2 immunity. Cytokine **2015**;75(1):25-37 doi 10.1016/j.cyto.2015.05.008.

23. Na H, Cho M, Chung Y. Regulation of Th2 Cell Immunity by Dendritic Cells. Immune Netw **2016**;16(1):1-12 doi 10.4110/in.2016.16.1.1.

24. Speir JA, Stevens J, Joly E, Butcher GW, Wilson IA. Two different, highly exposed, bulged structures for an unusually long peptide bound to rat MHC class I RT1-Aa. Immunity **2001**;14(1):81-92 doi 10.1016/s1074-7613(01)00091-7.

25. Schumacher TN, De Bruijn ML, Vernie LN, Kast WM, Melief CJ, Neefjes JJ, *et al.* Peptide selection by MHC class I molecules. Nature **1991**;350(6320):703-6 doi 10.1038/350703a0.

26. Guo HC, Jardetzky TS, Garrett TP, Lane WS, Strominger JL, Wiley DC. Different length peptides bind to HLA-Aw68 similarly at their ends but bulge out in the middle. Nature **1992**;360(6402):364-6 doi 10.1038/360364a0.

27. Rammensee HG, Friede T, Stevanoviic S. MHC ligands and peptide motifs: first listing. Immunogenetics **1995**;41(4):178-228 doi 10.1007/BF00172063.

28. Raghavan M, Del Cid N, Rizvi SM, Peters LR. MHC class I assembly: out and about. Trends Immunol **2008**;29(9):436-43 doi 10.1016/j.it.2008.06.004.

29. ten Broeke T, Wubbolts R, Stoorvogel W. MHC class II antigen presentation by dendritic cells regulated through endosomal sorting. Cold Spring Harb Perspect Biol **2013**;5(12):a016873 doi 10.1101/cshperspect.a016873.

30. Fehres CM, Unger WW, Garcia-Vallejo JJ, van Kooyk Y. Understanding the biology of antigen cross-presentation for the design of vaccines against cancer. Front Immunol **2014**;5:149 doi 10.3389/fimmu.2014.00149.

31. Embgenbroich M, Burgdorf S. Current Concepts of Antigen Cross-Presentation. Front Immunol **2018**;9:1643 doi 10.3389/fimmu.2018.01643.

32. Collin M, Bigley V. Human dendritic cell subsets: an update. Immunology **2018**;154(1):3-20 doi 10.1111/imm.12888.

33. Collin M, McGovern N, Haniffa M. Human dendritic cell subsets. Immunology **2013**;140(1):22-30 doi 10.1111/imm.12117.

34. Roberts EW, Broz ML, Binnewies M, Headley MB, Nelson AE, Wolf DM, *et al.* Critical Role for CD103(+)/CD141(+) Dendritic Cells Bearing CCR7 for Tumor Antigen Trafficking and Priming of T Cell Immunity in Melanoma. Cancer Cell **2016**;30(2):324-36 doi 10.1016/j.ccell.2016.06.003.

35. Boltjes A, van Wijk F. Human dendritic cell functional specialization in steady-state and inflammation. Front Immunol **2014**;5:131 doi 10.3389/fimmu.2014.00131.

36. Mempel TR, Henrickson SE, Von Andrian UH. T-cell priming by dendritic cells in lymph nodes occurs in three distinct phases. Nature **2004**;427(6970):154-9 doi 10.1038/nature02238.

37. Ceeraz S, Nowak EC, Burns CM, Noelle RJ. Immune checkpoint receptors in regulating immune reactivity in rheumatic disease. Arthritis Res Ther **2014**;16(5):469 doi 10.1186/s13075-014-0469-1.

38. Magee CN, Boenisch O, Najafian N. The role of costimulatory molecules in directing the functional differentiation of alloreactive T helper cells. Am J Transplant **2012**;12(10):2588-600 doi 10.1111/j.1600-6143.2012.04180.x.

39. Chikuma S. Basics of PD-1 in self-tolerance, infection, and cancer immunity. Int J Clin Oncol **2016**;21(3):448-55 doi 10.1007/s10147-016-0958-0.

40. Perkins D, Wang Z, Donovan C, He H, Mark D, Guan G, *et al.* Regulation of CTLA-4 expression during T cell activation. J Immunol **1996**;156(11):4154-9.

41. Peggs KS, Quezada SA, Allison JP. Cancer immunotherapy: co-stimulatory agonists and co-inhibitory antagonists. Clin Exp Immunol **2009**;157(1):9-19 doi 10.1111/j.1365-2249.2009.03912.x.

42. Chemnitz JM, Parry RV, Nichols KE, June CH, Riley JL. SHP-1 and SHP-2 associate with immunoreceptor tyrosine-based switch motif of programmed death 1 upon primary human T cell stimulation, but only receptor ligation prevents T cell activation. J Immunol **2004**;173(2):945-54 doi 10.4049/jimmunol.173.2.945.

43. Neel BG, Gu H, Pao L. The 'Shp'ing news: SH2 domain-containing tyrosine phosphatases in cell signaling. Trends Biochem Sci **2003**;28(6):284-93 doi 10.1016/S0968-0004(03)00091-4.

44. Krummel MF, Allison JP. CD28 and CTLA-4 have opposing effects on the response of T cells to stimulation. J Exp Med **1995**;182(2):459-65 doi 10.1084/jem.182.2.459.

45. Walunas TL, Bakker CY, Bluestone JA. CTLA-4 ligation blocks CD28-dependent T cell activation. J Exp Med **1996**;183(6):2541-50 doi 10.1084/jem.183.6.2541.

46. Walunas TL, Lenschow DJ, Bakker CY, Linsley PS, Freeman GJ, Green JM, *et al.* CTLA-4 can function as a negative regulator of T cell activation. Immunity **1994**;1(5):405-13 doi 10.1016/1074-7613(94)90071-x.

47. Pen JJ, Keersmaecker BD, Heirman C, Corthals J, Liechtenstein T, Escors D, *et al.* Interference with PD-L1/PD-1 co-stimulation during antigen presentation enhances the multifunctionality of antigen-specific T cells. Gene Ther **2014**;21(3):262-71 doi 10.1038/gt.2013.80.

48. Dempsey LA. PD-1 targets CD28. Nat Immunol **2017**;18(5):487 doi 10.1038/ni.3739.

49. Gowrishankar K, Gunatilake D, Gallagher SJ, Tiffen J, Rizos H, Hersey P. Inducible but not constitutive expression of PD-L1 in human melanoma cells is dependent on activation of NF-kappaB. PLoS One **2015**;10(4):e0123410 doi 10.1371/journal.pone.0123410.

50. Garcia-Diaz A, Shin DS, Moreno BH, Saco J, Escuin-Ordinas H, Rodriguez GA, *et al.* Interferon Receptor Signaling Pathways Regulating PD-L1 and PD-L2 Expression. Cell Rep **2017**;19(6):1189-201 doi 10.1016/j.celrep.2017.04.031.

51. Valk E, Rudd CE, Schneider H. CTLA-4 trafficking and surface expression. Trends Immunol **2008**;29(6):272-9 doi 10.1016/j.it.2008.02.011.

52. Schneider H, Rudd CE. Diverse mechanisms regulate the surface expression of immunotherapeutic target ctla-4. Front Immunol **2014**;5:619 doi 10.3389/fimmu.2014.00619.

53. Wang XB, Fan ZZ, Anton D, Vollenhoven AV, Ni ZH, Chen XF, *et al.* CTLA4 is expressed on mature dendritic cells derived from human monocytes and influences their maturation and antigen presentation. BMC Immunol **2011**;12:21 doi 10.1186/1471-2172-12-21.

54. Wang B, Jiang H, Zhou T, Ma N, Liu W, Wang Y, *et al.* Expression of ICOSL is associated with decreased survival in invasive breast cancer. PeerJ **2019**;7:e6903 doi 10.7717/peerj.6903.

55. Faget J, Sisirak V, Blay JY, Caux C, Bendriss-Vermare N, Menetrier-Caux C. ICOS is associated with poor prognosis in breast cancer as it promotes the amplification of immunosuppressive CD4(+) T cells by plasmacytoid dendritic cells. Oncoimmunology **2013**;2(3):e23185 doi 10.4161/onci.23185.

56. Zhang Y, Luo Y, Qin SL, Mu YF, Qi Y, Yu MH, *et al.* The clinical impact of ICOS signal in colorectal cancer patients. Oncoimmunology **2016**;5(5):e1141857 doi 10.1080/2162402X.2016.1141857.

57. Carthon BC, Wolchok JD, Yuan J, Kamat A, Ng Tang DS, Sun J, *et al.* Preoperative CTLA-4 blockade: tolerability and immune monitoring in the setting of a presurgical clinical trial. Clin Cancer Res **2010**;16(10):2861-71 doi 10.1158/1078-0432.CCR-10-0569.

58. Fan X, Quezada SA, Sepulveda MA, Sharma P, Allison JP. Engagement of the ICOS pathway markedly enhances efficacy of CTLA-4 blockade in cancer immunotherapy. J Exp Med **2014**;211(4):715-25 doi 10.1084/jem.20130590.

59. Tran Janco JM, Lamichhane P, Karyampudi L, Knutson KL. Tumor-infiltrating dendritic cells in cancer pathogenesis. J Immunol **2015**;194(7):2985-91 doi 10.4049/jimmunol.1403134.

60. Dong Y, Sun Q, Zhang X. PD-1 and its ligands are important immune checkpoints in cancer. Oncotarget **2017**;8(2):2171-86 doi 10.18632/oncotarget.13895.

61. Michielsen AJ, O'Sullivan JN, Ryan EJ. Tumor conditioned media from colorectal cancer patients inhibits dendritic cell maturation. Oncoimmunology **2012**;1(5):751-3 doi 10.4161/onci.19570.

62. Enk AH, Jonuleit H, Saloga J, Knop J. Dendritic cells as mediators of tumor-induced tolerance in metastatic melanoma. Int J Cancer **1997**;73(3):309-16.

63. Nicholas C, Lesinski GB. Immunomodulatory cytokines as therapeutic agents for melanoma. Immunotherapy **2011**;3(5):673-90 doi 10.2217/imt.11.45.

64. Bottomley A, Coens C, Suciu S, Santinami M, Kruit W, Testori A, *et al.* Adjuvant therapy with pegylated interferon alfa-2b versus observation in resected stage III melanoma: a phase III randomized controlled trial of health-related quality of life and symptoms by the European Organisation for Research and Treatment of Cancer Melanoma Group. J Clin Oncol **2009**;27(18):2916-23 doi 10.1200/JCO.2008.20.2069.

65. McDermott DF, Regan MM, Clark JI, Flaherty LE, Weiss GR, Logan TF, *et al.* Randomized phase III trial of high-dose interleukin-2 versus subcutaneous interleukin-2 and interferon in patients with metastatic renal cell carcinoma. J Clin Oncol **2005**;23(1):133-41 doi 10.1200/JCO.2005.03.206.

66. Lissoni P, Bordin V, Vaghi M, Fumagalli L, Bordoni A, Mengo S, *et al.* Ten-year survival results in metastatic renal cell cancer patients treated with monoimmunotherapy with subcutaneous low-dose interleukin-2. Anticancer Res **2002**;22(2B):1061-4.

67. Conry RM, Westbrook B, McKee S, Norwood TG. Talimogene laherparepvec: First in class oncolytic virotherapy. Hum Vaccin Immunother **2018**;14(4):839-46 doi 10.1080/21645515.2017.1412896.

68. Welsh SJ, Corrie PG. Management of BRAF and MEK inhibitor toxicities in patients with metastatic melanoma. Ther Adv Med Oncol **2015**;7(2):122-36 doi 10.1177/1758834014566428.

69. Buchbinder EI, Hodi FS. Melanoma in 2015: Immune-checkpoint blockade - durable cancer control. Nat Rev Clin Oncol **2016**;13(2):77-8 doi 10.1038/nrclinonc.2015.237.

70. Wolchok JD, Chiarion-Sileni V, Gonzalez R, Rutkowski P, Grob JJ, Cowey CL, *et al.* Overall Survival with Combined Nivolumab and Ipilimumab in Advanced Melanoma. N Engl J Med **2017**;377(14):1345-56 doi 10.1056/NEJMoa1709684.

71. Nordlund JJ, Kirkwood JM, Forget BM, Milton G, Albert DM, Lerner AB. Vitiligo in patients with metastatic melanoma: a good prognostic sign. J Am Acad Dermatol **1983**;9(5):689-96 doi 10.1016/s0190-9622(83)70182-9.

72. Coley WB. The treatment of malignant tumors by repeated inoculations of erysipelas. With a report of ten original cases. 1893. Clin Orthop Relat Res **1991**(262):3-11.

73. Homes EC, Morton DL, Eilber FR, Golub SE, Sulit HL. Immunotherapy in malignant melanomaa. Natl Cancer Inst Monogr **1976**;44:85-6.

74. Laucius JF, Bodurtha AJ, Mastrangelo JM, Bellet RE. A Phase II study of autologous irradiated tumor cells plus BCG in patients with metastatic malignant melanoma. Cancer **1977**;40(5):2091-3 doi 10.1002/1097-0142(197711)40:5<2091::aid-cncr2820400517>3.0.co;2-h.

75. Wallack MK, Bash J, Bartolucci A. Improvement in disease-free survival of melanoma patients in conjunction with serologic response in a phase Ia/Ib Southeastern Cancer Study Group trial of vaccinia melanoma oncolysate. Am Surg **1989**;55(4):243-7.

76. Lipton A, Harvey HA, Lawrence B, Gottlieb R, Kukrika M, Dixon R, *et al.* Corynebacterium parvum versus BCG adjuvant immunotherapy in human malignant melanoma. Cancer **1983**;51(1):57-60 doi 10.1002/1097-0142(19830101)51:1<57::aid-cncr2820510114>3.0.co;2-v.

77. Soiffer R, Lynch T, Mihm M, Jung K, Rhuda C, Schmollinger JC, *et al.* Vaccination with irradiated autologous melanoma cells engineered to secrete human granulocyte-macrophage colony-stimulating factor generates potent antitumor immunity in patients with metastatic melanoma. Proc Natl Acad Sci U S A **1998**;95(22):13141-6 doi 10.1073/pnas.95.22.13141.

78. Livingston PO, Adluri S, Helling F, Yao TJ, Kensil CR, Newman MJ, *et al.* Phase 1 trial of immunological adjuvant QS-21 with a GM2 ganglioside-keyhole limpet haemocyanin conjugate vaccine in patients with malignant melanoma. Vaccine **1994**;12(14):1275-80 doi 10.1016/s0264-410x(94)80052-2.

79. Chang AE, Sondak VK, Bishop DK, Nickoloff BJ, Mulligan RC, Mule JJ. Adoptive immunotherapy of cancer with activated lymph node cells primed in vivo with autologous tumor cells transduced with the GM-CSF gene. Hum Gene Ther **1996**;7(6):773-92 doi 10.1089/hum.1996.7.6-773.

80. Stingl G, Brocker EB, Mertelsmann R, Wolff K, Schreiber S, Kampgen E, *et al.* Phase I study to the immunotherapy of metastatic malignant melanoma by a cancer vaccine consisting of autologous cancer cells transfected with the human IL-2 gene. Hum Gene Ther **1996**;7(4):551-63 doi 10.1089/hum.1996.7.4-551.

81. Kawakami Y, Eliyahu S, Delgado CH, Robbins PF, Sakaguchi K, Appella E, *et al.* Identification of a human melanoma antigen recognized by tumor-infiltrating lymphocytes associated with in vivo tumor rejection. Proc Natl Acad Sci U S A **1994**;91(14):6458-62 doi 10.1073/pnas.91.14.6458.

82. Traversari C, van der Bruggen P, Luescher IF, Lurquin C, Chomez P, Van Pel A, *et al.* A nonapeptide encoded by human gene MAGE-1 is recognized on HLA-A1 by cytolytic T lymphocytes directed against tumor antigen MZ2-E. J Exp Med **1992**;176(5):1453-7 doi 10.1084/jem.176.5.1453.

83. Van den Eynde B, Hainaut P, Herin M, Knuth A, Lemoine C, Weynants P, *et al.* Presence on a human melanoma of multiple antigens recognized by autologous CTL. Int J Cancer **1989**;44(4):634-40 doi 10.1002/ijc.2910440413.

84. Kawakami Y, Eliyahu S, Delgado CH, Robbins PF, Rivoltini L, Topalian SL, *et al.* Cloning of the gene coding for a shared human melanoma antigen recognized by autologous T cells infiltrating into tumor. Proc Natl Acad Sci U S A **1994**;91(9):3515-9 doi 10.1073/pnas.91.9.3515.

85. Coulie PG, Brichard V, Van Pel A, Wolfel T, Schneider J, Traversari C, *et al.* A new gene coding for a differentiation antigen recognized by autologous cytolytic T lymphocytes on HLA-A2 melanomas. J Exp Med **1994**;180(1):35-42 doi 10.1084/jem.180.1.35.

86. Bakker AB, Marland G, de Boer AJ, Huijbens RJ, Danen EH, Adema GJ, *et al.* Generation of antimelanoma cytotoxic T lymphocytes from healthy donors after presentation of melanoma-associated antigen-derived epitopes by dendritic cells in vitro. Cancer Res **1995**;55(22):5330-4.

87. Topalian SL, Rivoltini L, Mancini M, Markus NR, Robbins PF, Kawakami Y, *et al.* Human CD4+ T cells specifically recognize a shared melanoma-associated antigen encoded by the tyrosinase gene. Proc Natl Acad Sci U S A **1994**;91(20):9461-5 doi 10.1073/pnas.91.20.9461.

88. Finn OJ, Jerome KR, Henderson RA, Pecher G, Domenech N, Magarian-Blander J, *et al.* MUC-1 epithelial tumor mucin-based immunity and cancer vaccines. Immunol Rev **1995**;145:61-89 doi 10.1111/j.1600-065x.1995.tb00077.x.

89. Boon T, Cerottini JC, Van den Eynde B, van der Bruggen P, Van Pel A. Tumor antigens recognized by T lymphocytes. Annu Rev Immunol **1994**;12:337-65 doi 10.1146/annurev.iy.12.040194.002005.

90. Vonderheide RH, Nathanson KL. Immunotherapy at large: the road to personalized cancer vaccines. Nat Med **2013**;19(9):1098-100 doi 10.1038/nm.3317.

91. Finn OJ. The dawn of vaccines for cancer prevention. Nat Rev Immunol **2018**;18(3):183-94 doi 10.1038/nri.2017.140.

92. Kreiter S, Vormehr M, van de Roemer N, Diken M, Lower M, Diekmann J, *et al.* Mutant MHC class II epitopes drive therapeutic immune responses to cancer. Nature **2015**;520(7549):692-6 doi 10.1038/nature14426.

93. Naing A, Hu-Lieskovan S, Govindan R, Margolin KA, Moles MA, Gaynor R. An open-label, phase Ib study of NEO-PV-01 + adjuvant with nivolumab in patients with melanoma, non-small cell lung carcinoma, or transitional cell carcinoma of the bladder. Journal of Clinical Oncology
2017;35(15) doi 10.1200/JCO.2017.35.15_suppl.TPS3116.

94. Begley S. Personalized Cancer Vaccines Vanquish Melanoma in Small Study. Scientific American 2017.

95. Sahin U, Derhovanessian E, Miller M, Kloke BP, Simon P, Lower M, *et al.* Personalized RNA mutanome vaccines mobilize poly-specific therapeutic immunity against cancer. Nature **2017**;547(7662):222-6 doi 10.1038/nature23003.

96. Komita H, Zhao X, Taylor JL, Sparvero LJ, Amoscato AA, Alber S, *et al.* CD8+ T-cell responses against hemoglobin-beta prevent solid tumor growth. Cancer Res **2008**;68(19):8076-84 doi 10.1158/0008-5472.CAN-08-0387.

97. Disis ML, Gralow JR, Bernhard H, Hand SL, Rubin WD, Cheever MA. Peptide-based, but not whole protein, vaccines elicit immunity to HER-2/neu, oncogenic self-protein. J Immunol **1996**;156(9):3151-8.

98. Zhao X, Bose A, Komita H, Taylor JL, Chi N, Lowe DB, *et al.* Vaccines targeting tumor blood vessel antigens promote CD8(+) T cell-dependent tumor eradication or dormancy in HLA-A2 transgenic mice. J Immunol **2012**;188(4):1782-8 doi 10.4049/jimmunol.1101644.

99. Pollack IF, Jakacki RI, Butterfield LH, Hamilton RL, Panigrahy A, Potter DM, *et al.* Antigen-specific immune responses and clinical outcome after vaccination with glioma-associated antigen peptides and polyinosinic-polycytidylic acid stabilized by lysine and

carboxymethylcellulose in children with newly diagnosed malignant brainstem and nonbrainstem gliomas. J Clin Oncol **2014**;32(19):2050-8 doi 10.1200/JCO.2013.54.0526.

100. Kirkwood JM, Lee S, Moschos SJ, Albertini MR, Michalak JC, Sander C, *et al.* Immunogenicity and antitumor effects of vaccination with peptide vaccine+/-granulocyte-monocyte colony-stimulating factor and/or IFN-alpha2b in advanced metastatic melanoma: Eastern Cooperative Oncology Group Phase II Trial E1696. Clin Cancer Res **2009**;15(4):1443-51 doi 10.1158/1078-0432.CCR-08-1231.

101. Okada H, Butterfield LH, Hamilton RL, Hoji A, Sakaki M, Ahn BJ, *et al.* Induction of robust type-I CD8+ T-cell responses in WHO grade 2 low-grade glioma patients receiving peptide-based vaccines in combination with poly-ICLC. Clin Cancer Res **2015**;21(2):286-94 doi 10.1158/1078-0432.CCR-14-1790.

102. Slingluff CL, Jr., Lee S, Zhao F, Chianese-Bullock KA, Olson WC, Butterfield LH, *et al.* A randomized phase II trial of multiepitope vaccination with melanoma peptides for cytotoxic T cells and helper T cells for patients with metastatic melanoma (E1602). Clin Cancer Res **2013**;19(15):4228-38 doi 10.1158/1078-0432.CCR-13-0002.

103. Butterfield LH, Ribas A, Dissette VB, Amarnani SN, Vu HT, Oseguera D, *et al.* Determinant spreading associated with clinical response in dendritic cell-based immunotherapy for malignant melanoma. Clin Cancer Res **2003**;9(3):998-1008.

104. Banchereau J, Palucka AK, Dhodapkar M, Burkeholder S, Taquet N, Rolland A, *et al.* Immune and clinical responses in patients with metastatic melanoma to CD34(+) progenitor-derived dendritic cell vaccine. Cancer Res **2001**;61(17):6451-8.

105. Okada H, Kalinski P, Ueda R, Hoji A, Kohanbash G, Donegan TE, *et al.* Induction of CD8+ T-cell responses against novel glioma-associated antigen peptides and clinical activity by vaccinations with {alpha}-type 1 polarized dendritic cells and polyinosinic-polycytidylic acid stabilized by lysine and carboxymethylcellulose in patients with recurrent malignant glioma. J Clin Oncol **2011**;29(3):330-6 doi 10.1200/JCO.2010.30.7744.

106. Aranda F, Vacchelli E, Eggermont A, Galon J, Sautes-Fridman C, Tartour E, *et al.* Trial Watch: Peptide vaccines in cancer therapy. Oncoimmunology **2013**;2(12):e26621 doi 10.4161/onci.26621.

107. Pratama A, Srivastava M, Williams NJ, Papa I, Lee SK, Dinh XT, *et al.* MicroRNA-146a regulates ICOS-ICOSL signalling to limit accumulation of T follicular helper cells and germinal centres. Nat Commun **2015**;6:6436 doi 10.1038/ncomms7436.

108. Welters MJ, Kenter GG, de Vos van Steenwijk PJ, Lowik MJ, Berends-van der Meer DM, Essahsah F, *et al.* Success or failure of vaccination for HPV16-positive vulvar lesions

correlates with kinetics and phenotype of induced T-cell responses. Proc Natl Acad Sci U S A **2010**;107(26):11895-9 doi 10.1073/pnas.1006500107.

109. Kenter GG, Welters MJ, Valentijn AR, Lowik MJ, Berends-van der Meer DM, Vloon AP, *et al.* Vaccination against HPV-16 oncoproteins for vulvar intraepithelial neoplasia. N Engl J Med **2009**;361(19):1838-47 doi 10.1056/NEJMoa0810097.

110. Rosalia RA, Quakkelaar ED, Redeker A, Khan S, Camps M, Drijfhout JW, *et al.* Dendritic cells process synthetic long peptides better than whole protein, improving antigen presentation and T-cell activation. Eur J Immunol **2013**;43(10):2554-65 doi 10.1002/eji.201343324.

111. Vujanovic L, Butterfield LH. Melanoma cancer vaccines and anti-tumor T cell responses. J Cell Biochem **2007**;102(2):301-10 doi 10.1002/jcb.21473.

112. Vujanovic L, Shi J, Kirkwood JM, Storkus WJ, Butterfield LH. Molecular mimicry of MAGE-A6 and Mycoplasma penetrans HF-2 epitopes in the induction of antitumor CD8(+) T-cell responses. Oncoimmunology **2014**;3(8):e954501 doi 10.4161/21624011.2014.954501.

113. Walter S, Weinschenk T, Stenzl A, Zdrojowy R, Pluzanska A, Szczylik C, *et al.* Multipeptide immune response to cancer vaccine IMA901 after single-dose cyclophosphamide associates with longer patient survival. Nat Med **2012**;18(8):1254-61 doi 10.1038/nm.2883.

114. Slingluff CL, Jr., Petroni GR, Chianese-Bullock KA, Smolkin ME, Ross MI, Haas NB, *et al.* Randomized multicenter trial of the effects of melanoma-associated helper peptides and cyclophosphamide on the immunogenicity of a multipeptide melanoma vaccine. J Clin Oncol **2011**;29(21):2924-32 doi 10.1200/JCO.2010.33.8053.

115. Butterfield LH, Palucka AK, Britten CM, Dhodapkar MV, Hakansson L, Janetzki S, *et al.* Recommendations from the iSBTc-SITC/FDA/NCI Workshop on Immunotherapy Biomarkers. Clin Cancer Res **2011**;17(10):3064-76 doi 10.1158/1078-0432.CCR-10-2234.

116. Slingluff CL, Jr., Petroni GR, Olson W, Czarkowski A, Grosh WW, Smolkin M, *et al.* Helper T-cell responses and clinical activity of a melanoma vaccine with multiple peptides from MAGE and melanocytic differentiation antigens. J Clin Oncol **2008**;26(30):4973-80 doi 10.1200/JCO.2008.17.3161.

117. Hu Y, Kim H, Blackwell CM, Slingluff CL, Jr. Long-term outcomes of helper peptide vaccination for metastatic melanoma. Ann Surg **2015**;262(3):456-64; discussion 62-4 doi 10.1097/SLA.0000000000001419.

118. Zirlik KM, Zahrieh D, Neuberg D, Gribben JG. Cytotoxic T cells generated against heteroclitic peptides kill primary tumor cells independent of the binding affinity of the native tumor antigen peptide. Blood **2006**;108(12):3865-70 doi 10.1182/blood-2006-04-014415.

119. Rivoltini L, Squarcina P, Loftus DJ, Castelli C, Tarsini P, Mazzocchi A, *et al.* A superagonist variant of peptide MART1/Melan A27-35 elicits anti-melanoma CD8+ T cells with enhanced functional characteristics: implication for more effective immunotherapy. Cancer Res **1999**;59(2):301-6.

120. Capasso C, Magarkar A, Cervera-Carrascon V, Fusciello M, Feola S, Muller M, *et al.* A novel in silico framework to improve MHC-I epitopes and break the tolerance to melanoma. Oncoimmunology **2017**;6(9):e1319028 doi 10.1080/2162402X.2017.1319028.

121. Palucka K, Ueno H, Fay J, Banchereau J. Dendritic cells and immunity against cancer. J Intern Med **2011**;269(1):64-73 doi 10.1111/j.1365-2796.2010.02317.x.

122. Palucka K, Banchereau J. Dendritic-cell-based therapeutic cancer vaccines. Immunity **2013**;39(1):38-48 doi 10.1016/j.immuni.2013.07.004.

123. Butterfield LH. Cancer vaccines. BMJ **2015**;350:h988 doi 10.1136/bmj.h988.

124. Butterfield LH. Dendritic Cell Vaccines: release assays and potency assays. Telegraft **2015**;22(2):1-3.

125. Butterfield LH. Dendritic cells in cancer immunotherapy clinical trials: are we making progress? Front Immunol **2013**;4:454 doi 10.3389/fimmu.2013.00454.

126. Kalinski P, Millard RB, Geskin L, Giermasz A, Nakamura Y, Storkus WJ, *et al.* Polarized DC1-Based Therapeutic Cancer Vaccines. Journal of Immunotherapy **2005**;28(6):656 doi 10.1097/01.cji.0000191090.97275.78.

127. Kaka AS, Foster AE, Weiss HL, Rooney CM, Leen AM. Using dendritic cell maturation and IL-12 producing capacity as markers of function: a cautionary tale. J Immunother **2008**;31(4):359-69 doi 10.1097/CJI.0b013e318165f5d2.

128. Vujanovic L, Szymkowski DE, Alber S, Watkins SC, Vujanovic NL, Butterfield LH. Virally infected and matured human dendritic cells activate natural killer cells via cooperative activity of plasma membrane-bound TNF and IL-15. Blood **2010**;116(4):575-83 doi 10.1182/blood-2009-08-240325.

129. Rosenberg SA, Yang JC, Restifo NP. Cancer immunotherapy: moving beyond current vaccines. Nat Med **2004**;10(9):909-15 doi 10.1038/nm1100.

130. Schreibelt G, Bol KF, Westdorp H, Wimmers F, Aarntzen EH, Duiveman-de Boer T, *et al.* Effective Clinical Responses in Metastatic Melanoma Patients after Vaccination with Primary Myeloid Dendritic Cells. Clin Cancer Res **2016**;22(9):2155-66 doi 10.1158/1078-0432.CCR-15-2205.

131. Schwartzentruber DJ, Lawson DH, Richards JM, Conry RM, Miller DM, Treisman J, *et al.* gp100 peptide vaccine and interleukin-2 in patients with advanced melanoma. N Engl J Med **2011**;364(22):2119-27 doi 10.1056/NEJMoa1012863.

132. Klebanoff CA, Acquavella N, Yu Z, Restifo NP. Therapeutic cancer vaccines: are we there yet? Immunol Rev **2011**;239(1):27-44 doi 10.1111/j.1600-065X.2010.00979.x.

133. Gross S, Erdmann M, Haendle I, Voland S, Berger T, Schultz E, *et al.* Twelve-year survival and immune correlates in dendritic cell-vaccinated melanoma patients. JCI Insight **2017**;2(8) doi 10.1172/jci.insight.91438.

134. Nestle FO, Alijagic S, Gilliet M, Sun Y, Grabbe S, Dummer R, *et al.* Vaccination of melanoma patients with peptide- or tumor lysate-pulsed dendritic cells. Nat Med **1998**;4(3):328-32 doi 10.1038/nm0398-328.

135. Kantoff PW, Higano CS, Shore ND, Berger ER, Small EJ, Penson DF, *et al.* Sipuleucel-T immunotherapy for castration-resistant prostate cancer. N Engl J Med **2010**;363(5):411-22 doi 10.1056/NEJMoa1001294.

136. McBride WH, Thacker JD, Comora S, Economou JS, Kelley D, Hogge D, *et al.* Genetic modification of a murine fibrosarcoma to produce interleukin 7 stimulates host cell infiltration and tumor immunity. Cancer Res **1992**;52(14):3931-7.

137. Dranoff G, Jaffee E, Lazenby A, Golumbek P, Levitsky H, Brose K, *et al.* Vaccination with irradiated tumor cells engineered to secrete murine granulocyte-macrophage colony-stimulating factor stimulates potent, specific, and long-lasting anti-tumor immunity. Proc Natl Acad Sci U S A **1993**;90(8):3539-43 doi 10.1073/pnas.90.8.3539.

138. Nemunaitis J, Sterman D, Jablons D, Smith JW, 2nd, Fox B, Maples P, *et al.* Granulocyte-macrophage colony-stimulating factor gene-modified autologous tumor vaccines in non-small-cell lung cancer. Journal of the National Cancer Institute **2004**;96(4):326-31 doi 10.1093/jnci/djh028.

139. Luiten RM, Kueter EW, Mooi W, Gallee MP, Rankin EM, Gerritsen WR, *et al.* Immunogenicity, including vitiligo, and feasibility of vaccination with autologous GM-CSF-transduced tumor cells in metastatic melanoma patients. J Clin Oncol **2005**;23(35):8978-91 doi 10.1200/JCO.2005.01.6816.

140. Tani K, Azuma M, Nakazaki Y, Oyaizu N, Hase H, Ohata J, *et al.* Phase I study of autologous tumor vaccines transduced with the GM-CSF gene in four patients with stage IV renal cell cancer in Japan: clinical and immunological findings. Mol Ther **2004**;10(4):799-816 doi 10.1016/j.ymthe.2004.07.001.

141. Geskin LJ, Damiano JJ, Patrone CC, Butterfield LH, Kirkwood JM, Falo LD. Three antigen-loading methods in dendritic cell vaccines for metastatic melanoma. Melanoma Res **2018**;28(3):211-21 doi 10.1097/CMR.0000000000000441.

142. Chakraborty NG, Sporn JR, Tortora AF, Kurtzman SH, Yamase H, Ergin MT, *et al.* Immunization with a tumor-cell-lysate-loaded autologous-antigen-presenting-cell-based vaccine in melanoma. Cancer Immunol Immunother **1998**;47(1):58-64 doi 10.1007/s002620050504.

143. Barth RJ, Jr., Fisher DA, Wallace PK, Channon JY, Noelle RJ, Gui J, *et al.* A randomized trial of ex vivo CD40L activation of a dendritic cell vaccine in colorectal cancer patients: tumor-specific immune responses are associated with improved survival. Clin Cancer Res **2010**;16(22):5548-56 doi 10.1158/1078-0432.CCR-10-2138.

144. Geiger J, Hutchinson R, Hohenkirk L, McKenna E, Chang A, Mule J. Treatment of solid tumours in children with tumour-lysate-pulsed dendritic cells. Lancet **2000**;356(9236):1163-5 doi 10.1016/S0140-6736(00)02762-8.

145. Kim TS, Chopra A, IS OS, Cohen EP. Enhanced immunity to breast cancer in mice immunized with fibroblasts transfected with a complementary DNA expression library from breast cancer cells: Enrichment of the vaccine for immunotherapeutic cells. J Immunother **2006**;29(3):261-73 doi 10.1097/01.cji.0000197097.46100.bb.

146. Lehmann PV, Forsthuber T, Miller A, Sercarz EE. Spreading of T-cell autoimmunity to cryptic determinants of an autoantigen. Nature **1992**;358(6382):155-7 doi 10.1038/358155a0.

147. Ribas A, Timmerman JM, Butterfield LH, Economou JS. Determinant spreading and tumor responses after peptide-based cancer immunotherapy. Trends Immunol **2003**;24(2):58-61 doi 10.1016/s1471-4906(02)00029-7.

148. Disis ML, Gooley TA, Rinn K, Davis D, Piepkorn M, Cheever MA, *et al.* Generation of T-cell immunity to the HER-2/neu protein after active immunization with HER-2/neu peptide-based vaccines. J Clin Oncol **2002**;20(11):2624-32 doi 10.1200/JCO.2002.06.171.

149. Disis ML. Immunologic biomarkers as correlates of clinical response to cancer immunotherapy. Cancer Immunol Immunother **2011**;60(3):433-42 doi 10.1007/s00262-010-0960-8.

150. Hu Y, Petroni GR, Olson WC, Czarkowski A, Smolkin ME, Grosh WW, *et al.* Immunologic hierarchy, class II MHC promiscuity, and epitope spreading of a melanoma helper peptide vaccine. Cancer Immunol Immunother **2014**;63(8):779-86 doi 10.1007/s00262-014-1551-x.

151. Ribas A, Glaspy JA, Lee Y, Dissette VB, Seja E, Vu HT, *et al.* Role of dendritic cell phenotype, determinant spreading, and negative costimulatory blockade in dendritic cell-based melanoma immunotherapy. J Immunother **2004**;27(5):354-67 doi 10.1097/00002371-200409000-00004.

152. Wierecky J, Muller MR, Wirths S, Halder-Oehler E, Dorfel D, Schmidt SM, *et al.* Immunologic and clinical responses after vaccinations with peptide-pulsed dendritic cells in metastatic renal cancer patients. Cancer Res **2006**;66(11):5910-8 doi 10.1158/0008-5472.CAN-05-3905.

153. Krauze MT, Tarhini A, Gogas H, Kirkwood JM. Prognostic significance of autoimmunity during treatment of melanoma with interferon. Seminars in immunopathology **2011**;33(4):385-91 doi 10.1007/s00281-011-0247-y.

154. Gogas H, Ioannovich J, Dafni U, Stavropoulou-Giokas C, Frangia K, Tsoutsos D, *et al.* Prognostic significance of autoimmunity during treatment of melanoma with interferon. N Engl J Med **2006**;354(7):709-18 doi 10.1056/NEJMoa053007.

155. Castiello L, Sabatino M, Jin P, Clayberger C, Marincola FM, Krensky AM, *et al.* Monocyte-derived DC maturation strategies and related pathways: a transcriptional view. Cancer Immunol Immunother **2011**;60(4):457-66 doi 10.1007/s00262-010-0954-6.

156. Carreno BM, Magrini V, Becker-Hapak M, Kaabinejadian S, Hundal J, Petti AA, *et al.* Cancer immunotherapy. A dendritic cell vaccine increases the breadth and diversity of melanoma neoantigen-specific T cells. Science **2015**;348(6236):803-8 doi 10.1126/science.aaa3828.

157. De Keersmaecker B, Claerhout S, Carrasco J, Bar I, Corthals J, Wilgenhof S, *et al.* TriMix and tumor antigen mRNA electroporated dendritic cell vaccination plus ipilimumab: link between T-cell activation and clinical responses in advanced melanoma. J Immunother Cancer **2020**;8(1) doi 10.1136/jitc-2019-000329.

158. Arthur JF, Butterfield LH, Roth MD, Bui LA, Kiertscher SM, Lau R, *et al.* A comparison of gene transfer methods in human dendritic cells. Cancer Gene Ther **1997**;4(1):17-25.

159. Wold WS, Toth K. Adenovirus vectors for gene therapy, vaccination and cancer gene therapy. Curr Gene Ther **2013**;13(6):421-33.

160. Humphreys IR, Sebastian S. Novel viral vectors in infectious diseases. Immunology **2017** doi 10.1111/imm.12829.

161. Vujanovic L, Whiteside TL, Potter DM, Chu J, Ferrone S, Butterfield LH. Regulation of antigen presentation machinery in human dendritic cells by recombinant adenovirus. Cancer Immunol Immunother **2009**;58(1):121-33 doi 10.1007/s00262-008-0533-2.

162. Steitz J, Tormo D, Schweichel D, Tuting T. Comparison of recombinant adenovirus and synthetic peptide for DC-based melanoma vaccination. Cancer Gene Ther **2006**;13(3):318-25 doi 10.1038/sj.cgt.7700894.

163. Schumacher L, Ribas A, Dissette VB, McBride WH, Mukherji B, Economou JS, *et al.* Human dendritic cell maturation by adenovirus transduction enhances tumor antigen-specific T-cell responses. J Immunother **2004**;27(3):191-200 doi 10.1097/00002371-200405000-00003.

164. Lapointe R, Royal RE, Reeves ME, Altomare I, Robbins PF, Hwu P. Retrovirally transduced human dendritic cells can generate T cells recognizing multiple MHC class I and class II epitopes from the melanoma antigen glycoprotein 100. J Immunol **2001**;167(8):4758-64 doi 10.4049/jimmunol.167.8.4758.

165. Butterfield LH, Jilani SM, Chakraborty NG, Bui LA, Ribas A, Dissette VB, *et al.* Generation of melanoma-specific cytotoxic T lymphocytes by dendritic cells transduced with a MART-1 adenovirus. J Immunol **1998**;161(10):5607-13.

166. Butterfield LH, Meng WS, Koh A, Vollmer CM, Ribas A, Dissette VB, *et al.* T cell responses to HLA-A*0201-restricted peptides derived from human alpha fetoprotein. J Immunol **2001**;166(8):5300-8 doi 10.4049/jimmunol.166.8.5300.

167. Pérez-Díez A, Butterfield LH, Li L, Chakraborty NG, Economou JS, Mukherji B. Generation of CD8⁺ and CD4⁺ T-Cell Response to Dendritic Cells Genetically Engineered to Express the MART-1/Melan-A Gene. Cancer Research **1998**;58(23):5305-9.

168. Tsao H, Millman P, Linette GP, Hodi FS, Sober AJ, Goldberg MA, *et al.* Hypopigmentation associated with an adenovirus-mediated gp100/MART-1-transduced dendritic cell vaccine for metastatic melanoma. Arch Dermatol **2002**;138(6):799-802 doi 10.1001/archderm.138.6.799.

169. Butterfield LH, Comin-Anduix B, Vujanovic L, Lee Y, Dissette VB, Yang JQ, *et al.* Adenovirus MART-1-engineered autologous dendritic cell vaccine for metastatic melanoma. J Immunother **2008**;31(3):294-309 doi 10.1097/CJI.0b013e31816a8910.

170. Naveh HP, Vujanovic L, Butterfield LH. Cellular immunity induced by a recombinant adenovirus- human dendritic cell vaccine for melanoma. J Immunother Cancer **2013**;1(1):19 doi 10.1186/2051-1426-1-19.

171. Santos PM, Butterfield LH. Dendritic Cell-Based Cancer Vaccines. J Immunol **2018**;200(2):443-9 doi 10.4049/jimmunol.1701024.

172. Curtsinger JM, Schmidt CS, Mondino A, Lins DC, Kedl RM, Jenkins MK, *et al.* Inflammatory cytokines provide a third signal for activation of naive CD4+ and CD8+ T cells. J Immunol **1999**;162(6):3256-62.

173. Lafferty KJ, Warren HS, Woolnough JA. A mediator acting as a costimulator for the development of cytotoxic responses in vitro. Adv Exp Med Biol **1979**;114:497-501 doi 10.1007/978-1-4615-9101-6_82.

174. Zinkernagel RM, Doherty PC. Restriction of in vitro T cell-mediated cytotoxicity in lymphocytic choriomeningitis within a syngeneic or semiallogeneic system. Nature **1974**;248(5450):701-2 doi 10.1038/248701a0.

175. Butterfield LH, Vujanovic L, Santos PM, Maurer DM, Gambotto A, Lohr J, *et al.* Multiple antigen-engineered DC vaccines with or without IFNalpha to promote antitumor immunity in melanoma. J Immunother Cancer **2019**;7(1):113 doi 10.1186/s40425-019-0552-x.

176. Blalock LT, Landsberg J, Messmer M, Shi J, Pardee AD, Haskell R, *et al.* Human dendritic cells adenovirally-engineered to express three defined tumor antigens promote broad adaptive and innate immunity. Oncoimmunology **2012**;1(3):287-357 doi 10.4161/onci.18628.

177. Jin P, Han TH, Ren J, Saunders S, Wang E, Marincola FM, *et al.* Molecular signatures of maturing dendritic cells: implications for testing the quality of dendritic cell therapies. J Transl Med **2010**;8:4 doi 10.1186/1479-5876-8-4.

178. Ritchie ME, Phipson B, Wu D, Hu Y, Law CW, Shi W, *et al.* limma powers differential expression analyses for RNA-sequencing and microarray studies. Nucleic Acids Res **2015**;43(7):e47 doi 10.1093/nar/gkv007.

179. Carvalho BS, Irizarry RA. A framework for oligonucleotide microarray preprocessing. Bioinformatics **2010**;26(19):2363-7 doi 10.1093/bioinformatics/btq431.

180. Mo X, Zhang H, Preston S, Martin K, Zhou B, Vadalia N, *et al.* Interferon-gamma Signaling in Melanocytes and Melanoma Cells Regulates Expression of CTLA-4. Cancer Res **2018**;78(2):436-50 doi 10.1158/0008-5472.CAN-17-1615.

181. Santos PM, Adamik J, Howes TR, Du S, Vujanovic L, Warren S, *et al.* Impact of checkpoint blockade on cancer vaccine-activated CD8+ T cell responses. J Exp Med **2020**;217(7) doi 10.1084/jem.20191369.

182. Aicher A, Hayden-Ledbetter M, Brady WA, Pezzutto A, Richter G, Magaletti D, *et al.* Characterization of human inducible costimulator ligand expression and function. J Immunol **2000**;164(9):4689-96 doi 10.4049/jimmunol.164.9.4689.

183. Her M, Kim D, Oh M, Jeong H, Choi I. Increased expression of soluble inducible costimulator ligand (ICOSL) in patients with systemic lupus erythematosus. Lupus **2009**;18(6):501-7 doi 10.1177/0961203308099176.

184. Huang J, Wu Z, Lu S, Shen J, Kong X, Shen Y. Soluble B7-H2 as a novel marker in early evaluation of the severity of acute pancreatitis. Lab Med **2015**;46(2):109-17 doi 10.1309/LMFSRH0V82HFXPPI.

185. Wong SB, Bos R, Sherman LA. Tumor-specific CD4+ T cells render the tumor environment permissive for infiltration by low-avidity CD8+ T cells. J Immunol **2008**;180(5):3122-31 doi 10.4049/jimmunol.180.5.3122.

186. Yan H, Hou X, Li T, Zhao L, Yuan X, Fu H, *et al.* CD4+ T cell-mediated cytotoxicity eliminates primary tumor cells in metastatic melanoma through high MHC class II expression and can be enhanced by inhibitory receptor blockade. Tumour Biol **2016** doi 10.1007/s13277-016-5456-5.

187. Quezada SA, Simpson TR, Peggs KS, Merghoub T, Vider J, Fan X, *et al.* Tumor-reactive CD4(+) T cells develop cytotoxic activity and eradicate large established melanoma after transfer into lymphopenic hosts. J Exp Med **2010**;207(3):637-50 doi 10.1084/jem.20091918.

188. Hu H, Wu X, Jin W, Chang M, Cheng X, Sun SC. Noncanonical NF-kappaB regulates inducible costimulator (ICOS) ligand expression and T follicular helper cell development. Proc Natl Acad Sci U S A **2011**;108(31):12827-32 doi 10.1073/pnas.1105774108.

189. Lownik JC, Luker AJ, Damle SR, Cooley LF, El Sayed R, Hutloff A, *et al.* ADAM10-Mediated ICOS Ligand Shedding on B Cells Is Necessary for Proper T Cell ICOS Regulation and T Follicular Helper Responses. J Immunol **2017**;199(7):2305-15 doi 10.4049/jimmunol.1700833.

190. Wang R, Ye X, Bhattacharya R, Boulbes DR, Fan F, Xia L, *et al.* A Disintegrin and Metalloproteinase Domain 17 Regulates Colorectal Cancer Stem Cells and Chemosensitivity Via Notch1 Signaling. Stem Cells Transl Med **2016**;5(3):331-8 doi 10.5966/sctm.2015-0168.

191. Moss ML, Rasmussen FH. Fluorescent substrates for the proteinases ADAM17, ADAM10, ADAM8, and ADAM12 useful for high-throughput inhibitor screening. Anal Biochem **2007**;366(2):144-8 doi 10.1016/j.ab.2007.04.043.

192. Kwok BH, Koh B, Ndubuisi MI, Elofsson M, Crews CM. The anti-inflammatory natural product parthenolide from the medicinal herb Feverfew directly binds to and inhibits IkappaB kinase. Chem Biol **2001**;8(8):759-66 doi 10.1016/s1074-5521(01)00049-7.

193. Saadane A, Masters S, DiDonato J, Li J, Berger M. Parthenolide inhibits IkappaB kinase, NF-kappaB activation, and inflammatory response in cystic fibrosis cells and mice. Am J Respir Cell Mol Biol **2007**;36(6):728-36 doi 10.1165/rcmb.2006-0323OC.

194. Shih VF, Davis-Turak J, Macal M, Huang JQ, Ponomarenko J, Kearns JD, *et al.* Control of RelB during dendritic cell activation integrates canonical and noncanonical NF-kappaB pathways. Nat Immunol **2012**;13(12):1162-70 doi 10.1038/ni.2446.

195. Mir MA. Developing costimulatory molecules for immunotherapy of diseases. Chapter 1 - Introduction to Costimulation and Costimulatory Molecules. Amsterdam: Elsevier/Academic Press,; 2015. p 1-43.

196. Fujita S, Seino K, Sato K, Sato Y, Eizumi K, Yamashita N, *et al.* Regulatory dendritic cells act as regulators of acute lethal systemic inflammatory response. Blood **2006**;107(9):3656-64 doi 10.1182/blood-2005-10-4190.

197. Wculek SK, Khouili SC, Priego E, Heras-Murillo I, Sancho D. Metabolic Control of Dendritic Cell Functions: Digesting Information. Front Immunol **2019**;10:775 doi 10.3389/fimmu.2019.00775.

198. Londhe P, Yu PY, Ijiri Y, Ladner KJ, Fenger JM, London C, *et al.* Classical NF-κB Metabolically Reprograms Sarcoma Cells Through Regulation of Hexokinase 2. Frontiers in Oncology **2018**;8(104) doi 10.3389/fonc.2018.00104.

199. Tan H-Y, Wang N, Lam W, Guo W, Feng Y, Cheng Y-C. Targeting tumour microenvironment by tyrosine kinase inhibitor. Molecular Cancer **2018**;17(1):43 doi 10.1186/s12943-018-0800-6.

200. Williamson J, Whitfield D, Sidhu H, Salazar S, Vandewalker K. Analytical validation of the Oncomine Immune Response Research Assay (OIRRA) in a CLIA and CAP regulated laboratory for formalin fixed, paraffin embedded (FFPE) solid tumor specimens. Journal of Clinical Oncology **2018**;36(15_suppl):e24200-e doi 10.1200/JCO.2018.36.15_suppl.e24200.

201. Looney TJ, Topacio-Hall D, Lowman G, Conroy J, Morrison C, Oh D, *et al.* TCR Convergence in Individuals Treated With Immune Checkpoint Inhibition for Cancer. Front Immunol **2019**;10:2985 doi 10.3389/fimmu.2019.02985.

202. Tieri P, Termanini A, Bellavista E, Salvioli S, Capri M, Franceschi C. Charting the NF-kappaB pathway interactome map. PLoS One **2012**;7(3):e32678 doi 10.1371/journal.pone.0032678.

203. Fourcade J, Sun Z, Chauvin JM, Ka M, Davar D, Pagliano O, *et al.* CD226 opposes TIGIT to disrupt Tregs in melanoma. JCI Insight **2018**;3(14) doi 10.1172/jci.insight.121157.

204. Allen F, Bobanga ID, Rauhe P, Barkauskas D, Teich N, Tong C, *et al.* CCL3 augments tumor rejection and enhances CD8(+) T cell infiltration through NK and CD103(+) dendritic cell recruitment via IFNgamma. Oncoimmunology **2018**;7(3):e1393598 doi 10.1080/2162402X.2017.1393598.

205. Fend L, Rusakiewicz S, Adam J, Bastien B, Caignard A, Messaoudene M, *et al.* Prognostic impact of the expression of NCR1 and NCR3 NK cell receptors and PD-L1 on advanced non-small cell lung cancer. Oncoimmunology **2017**;6(1):e1163456 doi 10.1080/2162402X.2016.1163456.

206. Chen B, Li L, Li M, Wang X. HIF1A expression correlates with increased tumor immune and stromal signatures and aggressive phenotypes in human cancers. Cell Oncol (Dordr) **2020** doi 10.1007/s13402-020-00534-4.

207. Zuo C, Sheng X, Ma M, Xia M, Ouyang L. ISG15 in the tumorigenesis and treatment of cancer: An emerging role in malignancies of the digestive system. Oncotarget **2016**;7(45):74393-409 doi 10.18632/oncotarget.11911.

208. Zhou T, Wang Y, Qian D, Liang Q, Wang B. Over-expression of TOP2A as a prognostic biomarker in patients with glioma. Int J Clin Exp Pathol **2018**;11(3):1228-37.

209. Sunkara KP, Gupta G, Hansbro PM, Dua K, Bebawy M. Functional relevance of SATB1 in immune regulation and tumorigenesis. Biomed Pharmacother **2018**;104:87-93 doi 10.1016/j.biopha.2018.05.045.

210. Dajon M, Iribarren K, Petitprez F, Marmier S, Lupo A, Gillard M, *et al.* Toll like receptor 7 expressed by malignant cells promotes tumor progression and metastasis through the recruitment of myeloid derived suppressor cells. Oncoimmunology **2019**;8(1):e1505174 doi 10.1080/2162402X.2018.1505174.

211. Kim R, Emi M, Tanabe K. Functional roles of immature dendritic cells in impaired immunity of solid tumour and their targeted strategies for provoking tumour immunity. Clin Exp Immunol **2006**;146(2):189-96 doi 10.1111/j.1365-2249.2006.03215.x.

212. Kalinski P. Regulation of immune responses by prostaglandin E2. J Immunol **2012**;188(1):21-8 doi 10.4049/jimmunol.1101029.

213. Ghiringhelli F, Puig PE, Roux S, Parcellier A, Schmitt E, Solary E, *et al.* Tumor cells convert immature myeloid dendritic cells into TGF-beta-secreting cells inducing CD4+CD25+ regulatory T cell proliferation. J Exp Med **2005**;202(7):919-29 doi 10.1084/jem.20050463.

214. Uto T, Fukaya T, Takagi H, Arimura K, Nakamura T, Kojima N, *et al.* Clec4A4 is a regulatory receptor for dendritic cells that impairs inflammation and T-cell immunity. Nature Communications **2016**;7(1):11273 doi 10.1038/ncomms11273.

215. Salaun B, de Saint-Vis B, Pacheco N, Pacheco Y, Riesler A, Isaac S, *et al.* CD208/dendritic cell-lysosomal associated membrane protein is a marker of normal and transformed type II pneumocytes. Am J Pathol **2004**;164(3):861-71 doi 10.1016/S0002-9440(10)63174-4.

216. Chapoval AI, Smithson G, Brunick L, Mesri M, Boldog FL, Andrew D, *et al.* BTNL8, a butyrophilin-like molecule that costimulates the primary immune response. Mol Immunol **2013**;56(4):819-28 doi 10.1016/j.molimm.2013.08.003.

217. Rescigno M, Martino M, Sutherland CL, Gold MR, Ricciardi-Castagnoli P. Dendritic cell survival and maturation are regulated by different signaling pathways. J Exp Med **1998**;188(11):2175-80 doi 10.1084/jem.188.11.2175.

218. Cheng P, Gabrilovich D. Notch signaling in differentiation and function of dendritic cells. Immunol Res **2008**;41(1):1-14 doi 10.1007/s12026-007-8011-z.

219. Lu J, Chatterjee M, Schmid H, Beck S, Gawaz M. CXCL14 as an emerging immune and inflammatory modulator. J Inflamm (Lond) **2016**;13:1 doi 10.1186/s12950-015-0109-9.